

# Reviews of Geophysics

## REVIEW ARTICLE

10.1029/2017RG000584

### Key Points:

- Soil thermal properties are required in environmental, Earth and planetary sciences, and in engineering applications
- The heat pulse method is a transient method that can be used to estimate soil thermal properties and a variety of other physical and hydraulic parameters
- The development history of 130 years, probe design, construction, calibration, applications, and limitations and perspectives are discussed

### Correspondence to:

H. He and B. Si,  
hailong.he@hotmail.com;  
bing.si@usask.ca

### Citation:

He, H., Dyck, M. F., Horton, R., Ren, T., Bristow, K. L., Lv, J., & Si, B. (2018). Development and application of the heat pulse method for soil physical measurements. *Reviews of Geophysics*, 56, 567–620. <https://doi.org/10.1029/2017RG000584>

Received 10 AUG 2017

Accepted 14 AUG 2018

Accepted article online 26 AUG 2018

Published online 18 OCT 2018

## Development and Application of the Heat Pulse Method for Soil Physical Measurements

**Hailong He<sup>1</sup> , Miles F. Dyck<sup>2</sup>, Robert Horton<sup>3</sup>, Tusheng Ren<sup>4</sup>, Keith L. Bristow<sup>5</sup>, Jialong Lv<sup>1</sup>, and Bingcheng Si<sup>6,7</sup> **

<sup>1</sup>College of Natural Resources and Environment and the Key Laboratory of Plant Nutrition and the Agri-Environment in Northwest China (Ministry of Agriculture), Northwest A&F University, Yangling, Shaanxi, China, <sup>2</sup>Department of Renewable Resources, University of Alberta, Edmonton, Canada, <sup>3</sup>Department of Agronomy, Iowa State University of Science and Technology, Ames, IA, USA, <sup>4</sup>Department of Soil & Water Sciences, China Agricultural University, Beijing, China, <sup>5</sup>CSIRO Agriculture & Food, PMB Aitkenvale, Townsville, QLD, Australia, <sup>6</sup>College of Water Resources and Architectural Engineering, Northwest A&F University, Yangling, Shaanxi, China, <sup>7</sup>Department of Soil Science, University of Saskatchewan, Saskatoon, Saskatchewan, Canada

**Abstract** Accurate and continuous measurements of soil thermal and hydraulic properties are required for environmental, Earth and planetary science, and engineering applications, but they are not practically obtained by steady-state methods. The heat pulse (HP) method is a transient method for determination of soil thermal properties and a wide range of other physical properties in laboratory and field conditions. The HP method is based on the line-heat source solution of the radial heat flow equation. This literature review begins with a discussion of the evolution of the HP method and related applications, followed by the principal theories, data interpretation methods, and their differences. Important factors for HP probe construction are presented. The properties determined in unfrozen and frozen soils are discussed, followed by a discussion of limitations and perspectives for the application of this method. The paper closes with a brief overview of future needs and opportunities for further development and application of the HP method.

### Table of Contents

Development and application of the heat pulse method for soil physical measurements .....	567
Key points: .....	567
Abstract .....	567
1. Introduction .....	568
2. Development and evolution of the HP method .....	570
3. Fundamentals of the HP Method .....	572
3.1 Theory .....	572
3.1.1 Solution to equation (3) for ILHS .....	573
3.1.2 Solution to equation (3) for CLHS .....	573
3.1.3 Solution to equation (3) for SLHS .....	573
3.2 SPHP method .....	573
3.3 Differentiated line heat source (DLHS) method using dual probes .....	574
3.4 DPHP method .....	575
3.4.1 Analysis of the SPM method .....	575
3.4.1.1 SPM Based on ILHS Solution .....	575
3.4.1.2 SPM Based on SLHS Solution .....	575
3.4.2 Analysis of the NMF method .....	576
3.4.3 Numerical simulation .....	577
3.4.4 Semianalytical solutions .....	578
3.5 Comparison of SPHP, DLHS and DPHP methods .....	578
4. Probe Design and Construction .....	579

©2018. The Authors.

This is an open access article under the terms of the Creative Commons Attribution-NonCommercial-NoDerivs License, which permits use and distribution in any medium, provided the original work is properly cited, the use is non-commercial and no modifications or adaptations are made.

4.1 Probe geometry (length, diameter and separation/spacing) .....	579
4.1.1 SPHP sensors .....	579
4.1.2 DPHP sensors .....	582
4.1.3 Thermo-TDR sensors .....	582
4.2 Heater .....	583
4.3 Temperature sensing element, data interpretation, and circuit .....	585
4.4 Probe design with numerical simulation .....	586
4.5 Probe construction .....	587
5. Application of the HP method in unfrozen and frozen soils.....	588
5.1 Overview of the HP method in soil science .....	588
5.2 Physical measurements of unfrozen soils .....	589
5.2.1 Soil thermal properties .....	589
5.2.2 Water content, air filled porosity and bulk density .....	590
5.2.3 Evaporation/transpiration .....	591
5.2.4 Soil water flux density .....	592
5.2.5 Soil heat flux density .....	594
5.3 Physical measurements of frozen soils .....	595
5.3.1 Frozen soil thermal properties .....	595
5.3.2 Unfrozen water/ice content and soil freezing characteristics .....	596
5.3.3 Water flow and heat flux in frozen soils .....	598
5.4 New applications with fiber optics based distributed temperature sensing .....	598
5.5 Thermal conductivity models .....	600
6. Limitations and perspectives of the HP method .....	600
6.1 Accuracy and sources of error .....	601
6.2 Probe dimension/geometry/deflection .....	602
6.3 Contact resistance and probe material .....	603
6.4 Soil heterogeneity .....	604
6.5 Energy input/output .....	605
6.6 Sample volume/outer boundary .....	605
6.7 Thermal instability at close proximity to the surface (soil-air interface) .....	606
6.8 Convection and phase change .....	607
7. Summary .....	608
Abbreviations: .....	609
List of symbols .....	610
Acknowledgements .....	611
References .....	611

## 1. Introduction

Soil thermal properties are a must for the accurate estimation and simulation of the surface energy balance (Brutsaert, 1982; Peters-Lidard et al., 1998; Wilson et al., 2002; Zheng et al., 2015), which affects the soil temperature regime and temperature-dependent soil processes such as decomposition of organic matter by microbes (Hillel, 1998), soil nitrification, or denitrification and the production and release of greenhouse gases from soil (Davidson et al., 1998), plant and crop growth rates (Nagai & Makino, 2011), the geographic distribution of bulk plant sensitivity to global warming (Lapen et al., 2014), seed germination and plant phenology, and biotic components of the ecosystem (Pedersen et al., 2015). They are also an important consideration in managing soil and water in irrigated agriculture (Noborio et al., 1996a). Further, soil thermal properties are important for understanding and predicting temperature-driven changes in hydraulic properties such as soil water retention and unsaturated hydraulic conductivity (Hopmans & Dane, 1986), and hydrological processes such as timing and rate of snowmelt (Lynch et al., 1998), and soil water vapor flow in coupled water and heat transport (Bittelli et al., 2008; Nassar & Horton, 1992); as a result, they are required in many hydrometeorological models at the local (Barr et al., 2012), basin (Endrizzi et al., 2014; Ranzi et al., 2010), and global scales or community land surface models (Liang

et al., 1994; Massey et al., 2014; Niu et al., 2011; Wild et al., 2014). Because of the range in scale, knowing thermal properties at different scales is a necessity.

In addition to energy balance applications, the thermal properties of soils are also used in a large number of geotechnical and geo-environmental applications, including geothermal energy resources (T. Saito et al., 2014; White, 1973; Yoon et al., 2014), radioactive waste disposal (D. Li et al., 2012), geological CO<sub>2</sub> sequestration, and recovery of natural methane gas hydrates (Cortes et al., 2009). These geotechnical applications may require measurements of thermal properties at depth and in weathered or unweathered rocks. In cold regions, the challenges of geotechnical engineering have always relied on an understanding of how civil infrastructure interacts with frozen ground (i.e., permafrost; Brown, 1970). However, these engineering challenges are being exacerbated by the accelerated rate at which climate change is affecting permafrost degradation (Harris et al., 2009). Understanding of the dynamics of permafrost requires accurate partitioning of surface energy balance, which relies on accurate measurements of thermal properties of the partially frozen surface and subsurface materials. Specific challenges include resource and transportation development (Prowse et al., 2009) and mine closure (Mend, 2012) in northern regions.

Furthermore, the measurement of thermal properties are important for estimating heat released from the interior of an extraterrestrial body in order to understand the body's internal structure, composition, and origin (Nagihara et al., 2014). Consequently, measurement of thermal properties were implemented in Apollo 15 and 17 missions to the Moon, NASA's Phoenix lander (Zent et al., 2009, 2010) and InSight missions to the Mars (Nagihara et al., 2014), and ESA's Rosetta spacecraft bound to Comet 67P (Marczewski et al., 2004; Nagihara et al., 2014). For these extraterrestrial applications, rapid, portable, and low energy consumption soil thermal property measurement methods are required.

There are three interrelated soil thermal properties: (1) the soil thermal conductivity ( $\lambda$  or  $K$ ) that describes the soil's ability to transmit heat and is defined as the heat flux conducted under unit temperature gradient (the reciprocal of thermal conductivity is called thermal resistivity); (2) the soil volumetric heat capacity ( $C_v$  or  $\rho c$ ) that defines the change in soil heat storage required to cause a unit rise in temperature; and (3) the soil thermal diffusivity ( $\kappa$  or  $\alpha$ ), which is the ratio of  $\lambda$  to  $C_v$ , describes the transmission rate of temperature changes within the soil or the ability to transmit heat over the ability to store heat.

So far, methods for measuring soil thermal properties generally fall into two categories: the steady-state/stationary and the transient/nonstationary methods. The steady-state method is based on the theory of steady flow of heat, which requires maintenance of a constant temperature gradient (usually one-dimensional) across a soil sample (Woodside & Messmer, 1961a). Steady-state methods (e.g., guarded hot plate, heat flux meter, and divided bar method) require thermal insulation to minimize edge or end effects, and a relatively long time is required to attain thermal equilibrium (Woodside & Messmer, 1961a). For partially saturated soil, this method can alter the thermal properties being measured (Bristow, White, et al., 1994; Farouki, 1981; Moench & Evans, 1970), because heat transport in unsaturated soil is usually accompanied by appreciable moisture migration induced by the temperature gradient, evaporation or distillation of water vapor (de Vries, 1952; de Vries & Peck, 1958a; Farouki, 1981; Heitman, Horton, Ren et al., 2008; Moench & Evans, 1970; Nassar & Horton, 1989, 1992, 1997; Nassar et al., 1992, 1997). In addition, it can also dry the soil adjacent to the heat source (Moench & Evans, 1970). The reader is referred to Sass et al. (1984) and Presley and Christensen (1997) for more information pertaining to the steady-state methods.

Transient methods measure the temperature response of the soil to a heat pulse (HP) from a heat source (e.g., point, line, plane, cylindrical, or spherical surface sources) inserted into soil. The transient method, widely used in the recent literature, is referred to as the HP method, also called cylindrical-probe transient flow method, transient hot-wire method, probe/needle method, or hot/thermal probe method. The HP method is based on the analogies of radial heat flow from a line-source, and to measure temperature change as a function of time,  $T(t)$ . The thermal properties are obtained by fitting analytical/numerical solutions of the heat conduction equation to measured  $T(t)$  (Carslaw & Jaeger, 1959). The duration of applied heat for HP method is much shorter compared to that in steady-state methods. Compared to the steady-state method, the transient method is less likely to induce soil water redistribution (de Vries, 1952; Farouki, 1981; Shiozawa & Campbell, 1990). It has an advantage over the steady-state method with respect to measurement time, cost, and portability for lab and field applications. Because the transient method is generally more amenable to measuring soil thermal properties, the HP method will be the focus of this review.

In this paper, we review the theory on which the HP method is based, together with its development and application. We focus on

1. History and evolution of the HP method;
2. The theory of the HP method. Differences between instantaneous and short duration HP theories, single-probe HP (SPHP) and dual-probe HP (DPHP) methods, and single point method (SPM) and nonlinear model fit (NMF) are compared in order to provide enough information for researchers to choose the most appropriate method to meet their needs;
3. The design, construction, and calibration of HP probes. We also comment on the effects of different probe spacing, and heating strategies on estimated soil thermal properties are simulated and evaluated. We also comment on probe performances and sources of error of the HP method;
4. Application of the HP method and its combination with time domain reflectometry, the thermo-TDR probe. This includes uses of HP and thermo-TDR probes for determination of soil thermal properties, water content, bulk density, water flux, heat flux, and subsurface evaporation. The recent applications of actively heated fiber optics based distributed temperature sensing (AHFO-DTS) for measurement of soil physical properties at intermediate scale (e.g., meters to 10s of kilometers) are also presented and discussed;
5. Limitations of the HP method and perspectives.

The aim of this review is to provide information to the novice and expert alike to guide them on the advantages, limitations, development, and the applications of the HP method.

## 2. Development and Evolution of the HP Method

The advent of the HP method can be traced back to Schleiermacher (1888), who suggested this method for measurements of heat in gas, and this method was then used by Niven (1905) and Niven and Geddes (1912). However, the empirical approximation of the line-heat source method was first given by Stalhane and Pyk (1931). This empirical formula for the solution to the heat conduction equation was mathematically deduced by van der Held (1932). The HP method was then used to determine the  $\lambda$  of liquids by Weishaupt (1940) and by Van der Held and Van Drunen (1949) and of soils by Van Dorssen (1949) and Hooper and Lepper (1950). The HP method has subsequently been applied to a wide range of materials such as gas (e.g., Kolyshkin et al., 1990), liquid (e.g., Horrocks & McLaughlin, 1963; Nagasaka & Nagashima, 1981; H. Zhang et al., 2005), porosint (e.g., insulation material), tree sap flow (e.g., Green et al., 2003; Marshall, 1958; Swanson, 1994), biological tissues (e.g., Balasubramaniam & Bowman, 1977; Liang et al., 1991; Valvano et al., 1984; Xie & Cheng, 2001), and snow (e.g., G. Liu & Si, 2008; Riche & Schneebeli, 2010) under a wide range of temperatures (from  $-35$  to  $90$  °C; e.g., G. S. Campbell et al., 1994; He et al., 2015; Hiraiwa & Kasubuchi, 2000; Olmanson & Ochsner, 2006) and pressures (from vacuum to  $10^9$  Pa; e.g., Andersson & Bäckström, 1976; Merrill, 1968; Wechsler & Glaser, 1965). Detailed descriptions of the historical evolution of the HP method are provided by de Wilde et al. (2008) and Assael et al. (2010). For this review, we only focus on the application of the HP method in soil studies under atmospheric pressure for ambient temperatures between  $-30$  and  $60$  °C.

Advances in the HP method over the past few decades have been accompanied by evolution of probe design/construction, development of data logging equipment, development of mathematical analysis and interpretation techniques, and improvement in computing ability resulting in improved soil thermal property determination. For example, its development can be divided into two eras based on probe geometries and theories: the first era is represented by the SPHP method and the second era is represented by the DPHP method. Both SPHP and DPHP consist of a line heat source (hereafter heater) and at least one temperature sensing device (hereafter temperature sensor) mounted together (SPHP) or separately (DPHP) with heater. The heater is supplied with a constant electrical current for a specified period of time, and the temperature sensor (s) records the temperature change. For the SPHP method, the heater is generally embedded in a small diameter stainless steel tube, and the temperature sensor is generally placed in the same tube (midlength position) next to the heater to ensure excellent thermal contact between the two. A relatively long duration pulse (e.g.,  $\geq 1$  min) of heat is applied in the SPHP (de Vries, 1952; Penner, 1970; Woodside & Messmer, 1961a, 1961b). Instead of having heater and temperature sensor mounted together, the DPHP probe has heater and temperature sensors in separated needles and a

short duration HP (e.g., 8–15 s) is used in the DPHP method (G. S. Campbell et al., 1991; Heitman, Horton, Ren, et al., 2008; Heitman, Horton, Sauer, et al., 2008; Heitman, Xiao, et al., 2008; Mori et al., 2003, 2005).

The cylindrical probe, developed by de Vries (1952) to measure  $\lambda$ , is among the first SPHP probe prototypes. The device could be introduced into soil without markedly disturbing the soil's natural structure, but the probe suffered from durability problems and lack of accuracy (de Vries, 1952). Plotting the temperature rise (the difference between measured temperatures during heating and initial temperature) against  $\log(t)$  (where  $t$  is time) gives a straight line from which  $\lambda$  is estimated. Sometimes the data for the subsequent cooling period were also used for estimating  $\lambda$  (de Vries, 1952; de Vries & Peck, 1958a). The possibility to extract  $\kappa$  was also presented under the condition that the contact resistance was known or negligibly small, but the accuracy was expected to be poor (de Vries & Peck, 1958a). Blackwell (1954) and Bruijn et al. (1983) developed a theory to simultaneously estimate  $\kappa$  and  $C_v$  by explicitly accounting for contact resistance between the soil and the probe. Their experimental results demonstrated 1% accuracy in the determination of  $\lambda$ , but only 10% to 20% accuracy in the determination of  $C_v$  (Van Haneghem et al., 1983). G. S. Campbell et al. (1991) used a DPHP with a new design (temperature sensor and heating element in two parallel hypodermic needles, ~6 mm apart) to measure  $C_v$ . A renewed interest in the HP method in soil science based on the DPHP sensor of G. S. Campbell et al. (1991) is apparent in the literature over the last 20+ years. The DPHP sensor, which allows detection of temperature changes some distance (e.g., 6 mm) from a heater, is now the most widely used design for measuring soil thermal properties (G. S. Campbell et al., 1991; Heitman, Horton, Ren, et al., 2008; Heitman, Horton, Sauer, et al., 2008; Heitman, Xiao, et al., 2008; G. Liu & Si, 2008; Mori et al., 2003, 2005; Ochsner & Baker, 2008; Ren et al., 1999, 2000; Ren, Horton, et al., 2003; Ren, Ochsner, et al., 2003; Y. Zhang et al., 2011; X. Zhang et al., 2012, 2014).

G. S. Campbell et al. (1991) estimated  $C_v$  and presented a potential way to estimate soil water content ( $\theta_v$ ; Bristow, 1998; Bristow et al., 1993; Song et al., 1998; Tarara & Ham, 1997) based on the analytical solution to the heat equation with an instantaneous HP boundary condition. However, Kluitenberg et al. (1993) found that the assumption of an instantaneous HP caused overestimation of  $C_v$ , and they explored the use of a finite, short duration HP assumption described by Carslaw and Jaeger (1959) to overcome this problem. Bristow, Kluitenberg, et al. (1994) and J. H. Knight and Kluitenberg (2004) presented the SPM that uses the maximum temperature rise and the corresponding time to simultaneously estimate  $C_v$ ,  $\kappa$ , and  $\lambda$ . Later a NMF method for data interpretation was presented and compared to the SPM method (Bristow et al., 1995; Welch et al., 1996). Cobos and Baker (2003) demonstrated that a 3-needle HP probe (i.e., one heater and two temperature sensors/needles) could be used to accurately measure soil heat flux, which is the product of measured soil thermal conductivity and the temperature gradient derived from the temperature sensors. These studies together with others served as the basis for many subsequent developments and applications of the HP method. Error analysis of these methods and probe designs were performed and documented (Kluitenberg et al., 1993, 1995, 2010; J. H. Knight et al., 2012; G. Liu et al., 2008; G. Liu & Si, 2010). It should be noted that HP measurements are based on the assumption of local thermal equilibrium within the duration of the measurements (Roshan et al., 2014). Under field conditions, local thermal nonequilibrium is common and should be corrected (Bristow et al., 1993; Jury & Bellantuoni, 1976; Presley & Christensen, 1997; Roshan et al., 2014; Young et al., 2008; X. Zhang et al., 2014). Readers are referred to Wechsler (1966) and Shiozawa and Campbell (1990) for additional papers published before 1990.

Besides measurement of soil thermal properties, recent developments of the HP method in combination with TDR have led to the simultaneous measurement of a range of other properties. Baker and Goodrich (1984, 1987) combined the SPHP and TDR methods to simultaneously measure water content and  $\lambda$ . Noborio et al. (1996b) enclosed a thermocouple junction into the outer electrodes of a 3-pronged TDR probe and a heater into the center in order to combine these two methods. Ren et al. (1999) improved the design of the Noborio et al. (1996b) method and developed the thermo-TDR sensor, which integrated the TDR and HP sensors into a single unit (3-needle probe, one needle serves as heater and center TDR electrode and two other needles function as temperature sensors and TDR ground electrodes). Ren et al. (1999) and Ren, Horton, et al. (2003) used these sensors to make various vadose zone measurements (e.g., soil water content, bulk electrical conductivity [EC], thermal properties, and liquid water flux). The thermo-TDR sensor is ideal for comparing water content measurements between HP and TDR methods, because the probe makes both measurements on similar soil volumes (Ren et al., 2005; Ren, Horton, et al., 2003). The TDR part of the

thermo-TDR, however, is still subject to errors in soils with high EC, large organic matter fraction, and high clay contents largely due to the short physical length of the probe compared to many regular TDR probes (e.g., 2.8–4 versus 15–30 cm). The readers may consult Noborio (2001) and Robinson et al. (2003) for more information about TDR and TDR methods. HP probes with or without TDR can also be used to measure other properties in unfrozen soils such as EC (e.g., Bristow et al., 2001; Mori et al., 2003; Ren et al., 1999), soil water content (e.g., Kamai, 2013; Kamai et al., 2015; Ochsner et al., 2003; Ren, Horton, et al., 2003; Ren, Ochsner, et al., 2003), water flux and pore water velocity (e.g., Kamai et al., 2008; Kamai, 2013; Kluitenberg et al., 2007; Mori et al., 2005; Mortensen et al., 2006; Rau et al., 2014; Ren et al., 2000; Q. Wang et al., 2002), soil bulk density (e.g., X. Liu et al., 2008, 2014; Y. Lu et al., 2016, 2017; Ochsner et al., 2001b; Ren, Horton, et al., 2003; Tian et al., 2018), evaporation (e.g., Deol et al., 2012, 2014; Heitman, Horton, Sauer, et al., 2008; Heitman, Xiao, et al., 2008; Trautz et al., 2014; Xiao et al., 2011, 2014; X. Zhang et al., 2012); and evapotranspiration (X. J. Wang et al., 2015).

Properties of unfrozen soil can be determined reliably by the HP method as noted above. There are, however, only a few reports pertaining to applications of the HP in frozen soil. Available examples include the measurement of thermal properties (e.g., Baker & Goodrich, 1984; Goodrich, 1986; He et al., 2015; Ochsner & Baker, 2008; Putkonen, 2003), unfrozen water and/or ice content (e.g., Kojima, 2015; Kojima et al., 2013, 2014, 2016; G. Liu & Si, 2011b; Tian et al., 2015; Y. Zhang et al., 2011), water and heat flux (e.g., Ochsner & Baker, 2008; Tokumoto et al., 2010), and snow density (e.g., G. Liu & Si, 2008). This limited use of the HP method in frozen soils may be because the HP method can induce a phase change of ice during the application of heat. This phase change and the latent heat fluxes can limit the accurate measurement of thermal properties using solutions to the heat equation assuming only conductive heat flux. Therefore, most applications of the HP method in frozen soils assume negligible ice melting (e.g., Tokumoto et al., 2010), embed the latent heat flux into the thermal properties (e.g., apparent thermal properties; He et al., 2015; Ochsner & Baker, 2008), or take advantage of numerical models (e.g., Kojima, 2015; Kojima et al., 2013, 2014; G. Liu & Si, 2011b; Overduin et al., 2006; Putkonen, 2003; Y. Zhang et al., 2011).

### 3. Fundamentals of the HP Method

#### 3.1. Theory

Conduction of heat in soil with a soil water flux,  $J$ , can be described as (Carslaw & Jaeger, 1959)

$$C_v \frac{\partial T}{\partial t} = \frac{\partial}{\partial x} \left( \lambda_x \frac{\partial T}{\partial x} \right) + \frac{\partial}{\partial y} \left( \lambda_y \frac{\partial T}{\partial y} \right) + \frac{\partial}{\partial z} \left( \lambda_z \frac{\partial T}{\partial z} \right) - \left( V_x \frac{\partial T}{\partial x} + V_y \frac{\partial T}{\partial y} + V_z \frac{\partial T}{\partial z} \right), \quad (1)$$

where  $T$  is temperature ( $^{\circ}\text{C}$ );  $t$  is time (s);  $x$ ,  $y$ , and  $z$  are directions in the Cartesian coordinate system (m);  $C_v$  is the volumetric heat capacity ( $\text{J} \cdot \text{m}^{-3} \cdot ^{\circ}\text{C}^{-1}$ );  $C_v = \rho c$ , where  $\rho$  is density ( $\text{kg}/\text{m}^3$ ) and  $c$  is the specific heat capacity of the medium ( $\text{J} \cdot \text{kg}^{-1} \cdot ^{\circ}\text{C}^{-1}$ );  $\lambda$  is the thermal conductivity ( $\text{J} \cdot \text{s}^{-1} \cdot \text{m}^{-1} \cdot ^{\circ}\text{C}^{-1}$  or  $\text{W} \cdot \text{m}^{-1} \cdot ^{\circ}\text{C}^{-1}$ ); and  $V_x$ ,  $V_y$ , and  $V_z$  are the HP velocity (m/s) along the directions  $x$ ,  $y$ , and  $z$ , respectively. Note that the HP velocity at a direction is related to soil water flux in that direction. For example,  $V_x = J_x \frac{(\rho c)_w}{\rho c}$ , where  $J_x$  (m/s) is the soil water flux along  $x$ ,  $(\rho c)_w$  is the volumetric heat capacity of water, and  $\rho c$  is the volumetric heat capacity of soil (Ren et al., 2000).

In semi-infinite, homogenous, and isotropic media without water flow, provided  $\lambda$  is constant with space and time,  $\lambda$  in equation (1) may be taken out of the derivative and combined with  $C_v$  to give the differential equation of radial heat conduction in a cylindrical coordinate system (Carslaw & Jaeger, 1959; Farouki, 1981):

$$\frac{\partial T}{\partial t} = \kappa \left\{ \frac{\partial^2 T}{\partial r^2} + \frac{1}{r} \frac{\partial T}{\partial r} + \frac{1}{r^2} \frac{\partial^2 T}{\partial A^2} + \frac{\partial^2 T}{\partial z^2} \right\}, \quad (2)$$

where  $\kappa$  is thermal diffusivity ( $\text{m}^2/\text{s}$ ),  $r$  represents radial distance from the center of the coordinate system or the line source/heater (m), and  $A$  is the azimuth ( $^{\circ}$ ). For radial heat flow, equation (2) can be simplified as

$$\frac{\partial T}{\partial t} = \kappa \left( \frac{\partial^2 T}{\partial r^2} + \frac{1}{r} \frac{\partial T}{\partial r} \right). \quad (3)$$

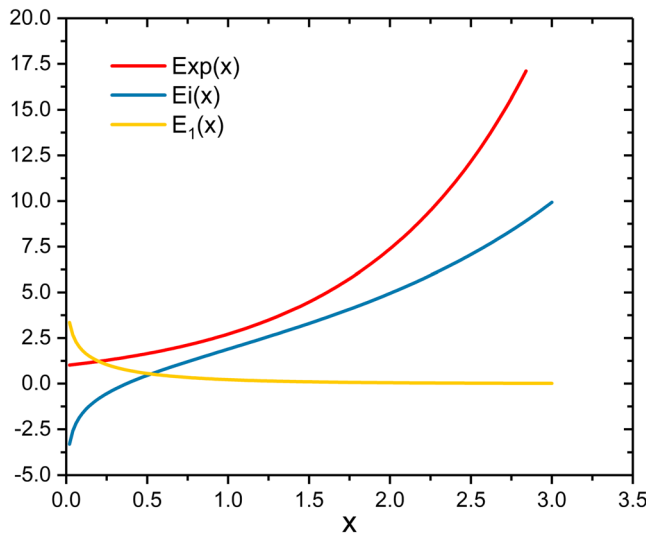


**Figure 1.** Diagram of  $y = E_1(x)$ ,  $y = Ei(x)$ , and  $y = \text{Exp}(x)$  adapted from Abramowitz and Stegun (1972).  $E_1(x) = \int_x^{\infty} \frac{e^{-n}}{n} dn$ , ( $|\arg x| < \pi$ ) and  $Ei(x) = \int_{-\infty}^x \frac{e^{-n}}{n} dn$ , ( $x > 0$ ).

Joule's law (see section 4.2) and is the quantity of heat produced per unit time and unit length of the line source ( $\text{W/m}$  or  $\text{J}\cdot\text{m}^{-1}\cdot\text{s}^{-1}$ ), the solution to equation (3) is (Carslaw & Jaeger, 1959; de Vries, 1952; Merrill, 1968; Presley, 1995)

$$\Delta T(r, t) = \frac{-q'}{4\pi\kappa} Ei\left(\frac{-r^2}{4\kappa t}\right) = \frac{q'}{4\pi\kappa} E_1\left(\frac{r^2}{4\kappa t}\right), \quad (5)$$

where  $Q'$  is heat source strength per unit time ( $\text{m}^2\cdot\text{C}^{-1}\cdot\text{s}^{-1}$ ),  $Q' = q'/pc$ . The exponential integral functions,  $E_1(x)$  and  $Ei(x)$ , are symbolic functions, and their analytical solution can be described as (Cody & Thacher, 1968; de Vries, 1952; Shiozawa & Campbell, 1990)

$$E_1(x) = -Ei(-x) = \int_x^{\infty} \frac{\exp(-n)}{n} dn = -\gamma - \ln(x) - \sum_{n=1}^{\infty} \frac{(-x)^n}{n \cdot n!}, \quad (6)$$

where  $\gamma$  is the Euler-Mascheroni constant ( $0.57721\dots$ ),  $x = r^2/(4\kappa t)$ , and  $n$  is a variable of integration. Figure 1 shows the difference between  $E_1(x)$ ,  $Ei(-x)$ , and  $\text{exp}(x)$ .

### 3.1.3. Solution to Equation (3) for SLHS

Equation (5) is a solution to equation (3) for the heating period, similarly, the cooling period can also be used to determine soil thermal properties. The solutions for heating and cooling periods are (Bristow, Kluitenberg, et al., 1994; de Vries, 1952; Kluitenberg et al., 1993)

$$\Delta T(r, t) = \begin{cases} \frac{q'}{4\pi\kappa} E_1\left(\frac{r^2}{4\kappa t}\right) & 0 < t \leq t_0 \quad (\text{a}) \\ \frac{q'}{4\pi\kappa} \left[ E_1\left(\frac{r^2}{4\kappa t}\right) - E_1\left(\frac{r^2}{4\kappa(t-t_0)}\right) \right] & t > t_0 \quad (\text{b}) \end{cases} \quad (7)$$

where  $t_0$  is the HP duration (s). Equation (7) describes the temperature change at distance  $r$  during a HP, beginning at  $t = 0$  and terminating at  $t = t_0$ , and for the post HP duration period,  $t > t_0$ . The different approaches for deriving soil thermal properties with equation (7) are the essential differences for the SPHP and DPHP methods.

## 3.2. SPHP Method

The SPHP method generally records the temperature rise of the heater probe, half way along its length, and at this location,  $r$  is approximately equal to the radius of the heating wire ( $r_0$ ), where a perfect contact is required between the heater and the temperature sensor and the magnitude of  $r_0$  should be considered

The solutions to equation (3) for an instantaneous line heat source (ILHS), continuous line heat source (CLHS), and line heat source of finite duration (or short-duration line heat source, SLHS) are most commonly used for the HP method.

### 3.1.1. Solution to Equation (3) for ILHS

For an instantaneous heat-pulse applied to an infinite line source in a homogeneous and isotropic medium at a uniform initial temperature, the solution to equation (3) is (Carslaw & Jaeger, 1959)

$$\Delta T(r, t) = \frac{Q}{4\pi\kappa t} \exp\left(\frac{-r^2}{4\kappa t}\right), \quad (4)$$

where  $\Delta T(r, t)$  is the temperature change (i.e., difference between measured temperature and background temperature) at a radial distance  $r$  away from the line heater at time  $t$ ;  $Q$  is the finite quantity of heat liberated by the line source ( $\text{m}^2/\text{C}$ ),  $Q = q/\rho c$  with  $q$  the quantity of heat liberated per unit length of heater ( $\text{J/m}$ ).

### 3.1.2. Solution to Equation (3) for CLHS

For boundary and initial conditions:  $T = 0$  (thermal equilibrium) for  $t = 0$  and  $r \geq 0$ ;  $T = 0$  (no heat flow far from the heat source) for  $t > 0$  and  $r \rightarrow \infty$ ;  $-2\pi r\lambda \frac{dT}{dr} = q'$  for  $t > 0$  and  $r \rightarrow 0$ ,  $q'$  can be calculated using

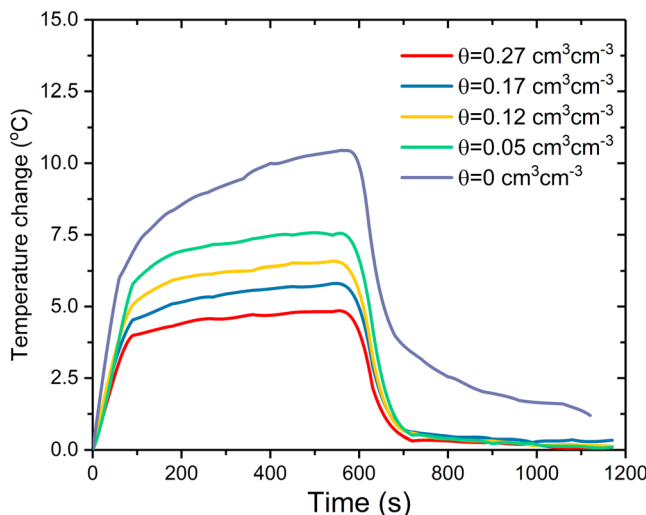


**Figure 2.** Measured temperature of single probe heat pulse method imbedded in a sand ( $<1$  mm, bulk density  $1.5$  g/ $\text{cm}^3$ ) with soil water contents at  $0.27$ ,  $0.17$ ,  $0.12$ , and  $0.05$   $\text{cm}^3/\text{cm}^3$ , and oven dry. The heating duration is  $600$  s and heating strength is  $5.77$  W/ $\text{m}$ .

requires a sufficiently long period of HP to offset the abovementioned errors, because the sources of error have a great influence on the first  $5\text{--}10$  s of recorded data (Bristow, White, et al., 1994).

Subsequent refinements of this method have been given by Blackwell (1953, 1954), Jaeger (1956), de Vries and Peck (1958a, 1958b), Carslaw and Jaeger (1959), Kristiansen (1982), Waite et al. (2006), and G. Liu and Si (2011a). These theoretical interpretations investigate the effects of the finite diameter of the probe, probe heat capacity, nonradial (axial) heat flow, and thermal contact resistance between the probe and samples under test. They can be used to increase the accuracy and precision for the estimates of thermal properties. The simplified equation with *lumped* effects for both the heating and cooling periods can be alternatively expressed by (de Vries, 1952; Shiozawa & Campbell, 1990)

$$\Delta T = \begin{cases} \frac{q'}{4\pi\lambda_h} \ln(t + t_c) + m & t \leq t_0 \\ \frac{q'}{4\pi\lambda_c} [\ln(t + t'_c) - \ln(t + t'_c - t_0) + m'] & t > t_0 \end{cases} \quad [9]$$

where  $t_0$  is the HP duration;  $\lambda_h$  and  $\lambda_c$  are the thermal conductivity values during the heating period and the cooling period, respectively;  $m$  and  $m'$  are constants; and  $t_c$  and  $t'_c$  are time correction terms,  $m$  and  $t_c$  may differ from  $m'$  and  $t'_c$ . Shiozawa and Campbell (1990) suggested to use the mean of  $\lambda_h$  and  $\lambda_c$  to provide the best estimate of thermal conductivity. Figure 2 is an example of a measured heating and cooling curve of the SPHP method at different water contents.

Although SPHP method is primarily used to obtain thermal conductivity, attempts to retrieve thermal diffusivity were made by Blackwell (1954) and Jaeger (1956). But the accuracy of the thermal diffusivity was observed to be poor (Al Nakshabandi & Kohnke, 1965). Interested readers are referred to Wechsler (1966) for more details about the pertinent theoretical developments about SPHP method. Horton and Wierenga (1984) provided practical advice on application of the SPHP method.

### 3.3. DLHS Method Using Dual Probes

Merrill (1968) developed the differentiated line heat source (DLHS) method with two wires (similar to dual probes) for measuring thermal conductivity of powders under vacuum conditions. Based on the CLHS solution as presented in equation (5), the DLHS method is a widely used method in the geophysics community. The probe of DLHS method consists of two linear and parallel needles, one as a heater and the other as a temperature sensor to record the time derivative  $dT/dt$ .  $dT/dt$  is the differentiation of equation (5) with respect to time, which is expressed as (Merrill, 1968; Morabito, 1989)

for imperfect contact (Van der Held & Van Drunen, 1949). If  $t$  is sufficiently large or  $r$  is very small (e.g.,  $r^2/4\kappa\lambda \ll 1$ ) in equation (6),  $T(t)$  at  $r = r_0$  can be approximated as  $T(t) \sim \frac{q'}{4\pi\lambda} \ln(t) + B$ , where  $B$  can be treated as a constant (Blackwell, 1954; G. Liu & Si, 2011a). Then, the temperature values  $T_1$  and  $T_2$  at the heater at respective time  $t_1$  and  $t_2$  can be expressed as (Van der Held, 1953; Van der Held & Van Drunen, 1949)

$$T_2 - T_1 = \frac{q'}{4\pi\lambda} \ln \frac{t_2 + t_c}{t_1 + t_c}, \quad [8]$$

where  $t_c$  is a time correction term that accounts for a few sources of error including (1) dropping the higher terms in the equation (6); (2) deviation of the temperature rise (i.e., initial lag error at short experimental times) in the heater with regard to the ideal rise given that  $r = r_0$ ; (3) influence of the finite diameter of the probe (e.g., thermal capacity of the probe) and finite dimension of samples; (4) axial heat flow error (i.e., nonradial heat flow in the probe and sample at long experimental times); and (5) contact resistance (or heat transfer coefficient) between the probe and the sample (Presley & Christensen, 1997; Wechsler, 1966). Use of equation (8) generally results in a linear relationship between temperature rise and  $\ln(t + t_c)$  with  $q'/4\pi\lambda$  as the slope. With known  $q'$ ,  $\lambda$  can be calculated. But this method

$$\frac{dT(r,t)}{dt} = \frac{q}{4\pi\lambda t} \exp\left(\frac{-r^2}{4\kappa t}\right), \quad (10)$$

where  $dT(r,t)/dt$  can be treated as the first derivative of the temperature change compared to the initial temperature of the tested media with respect to time at some distance ( $r$ ) from the heater. Note that the right hand of equation (10) is identical to that of the equation (4) because  $T(r,t)$  in equation (10) is the temperature for CLHS, and  $T(r,t)$  in equation (4) is for an ILHS. The  $dT(r,t)/dt$  as a function of time shows a bell-shaped curve with the front behaving as  $\exp(-r^2/(4\kappa t))$  and the back behaving as  $1/t$ . The peak of the  $dT(r,t)/dt$  curve is the maximum temperature rise ( $dT(r,t)/dt)_m$ , which occurs at  $d(dT(r,t)/dt)/dt = 0$ . Rearrangement results in (Merrill, 1968)

$$\left(\frac{dT(r,t)}{dt}\right)_m = \frac{q}{4\pi e \lambda t_m}, \quad (11)$$

where  $t_m$  is the time corresponding to the maximum temperature rise ( $dT(r,t)/dt)_m$ . By considering the maximum value of the  $dT/dt$  data,  $(dT/dt)_m$ , and the corresponding time,  $t_m$ , the thermal conductivity and thermal diffusivity can be calculated by (Merrill, 1968; Morabito, 1989)

$$\lambda = \frac{q}{4\pi e (dT/dt)_m t_m}, \quad \kappa = \frac{r^2}{4t_m}. \quad (12)$$

Therefore, the DLHS method is a dual probe method, but is different from DPHP method (section 3.4) in that DLHS measures the time when the maximum temperature change rate ( $dT/dt)_m$  occurs at the sensor probe under a CLHS.

### 3.4. DPHP Method

Different from SPHP method, but similar to DLHS, the DPHP method monitors the temperature change some distance (a few mm) away from the heater. Lubimova et al. (1961) applied this method to estimate the thermal properties of rocks. G. S. Campbell et al. (1991) developed a DPHP sensor and a new data interpretation method for estimating soil heat capacity. The work of G. S. Campbell et al. (1991) marks the start of the second era of the HP method for measuring soil thermal properties. A series of subsequent studies have been performed contributing to the further development of this method. A significant aspect of this development includes the data interpretation methods such as the SPM and NMF method that will be discussed below.

#### 3.4.1. Analysis of the SPM Method

Determining soil thermal properties with the SPM can be divided into two parts: the first is based on the ILHS solution as presented in section 3.1.1, while the second is based on the SLHS theory as presented in section 3.1.3.

##### 3.4.1.1. SPM Based on ILHS Solution

Equation (4) shows temperature change as a function of time. Therefore, by differentiating equation (4) with respect to time and setting the derivative equal to zero, we can obtain the maximum temperature rise ( $\Delta T_m$ ,  $t_m$ ), at a fixed distance,  $r_m$ , from the heater (G. S. Campbell et al., 1991; Lubimova et al., 1961). This gives  $t_m = r_m^2/4\kappa$ . Substituting  $t_m$  into equation (4) gives the maximum temperature change  $\Delta T_m = \frac{Q}{e\pi r_m^2}$  (G. S. Campbell et al., 1991). Including the definition of  $Q = q/C_v$  and solving for the heat capacity gives (G. S. Campbell et al., 1991)

$$C_v = \frac{q}{e\pi r_m^2 \Delta T_m}. \quad (13)$$

Since  $\lambda = \kappa \cdot C_v$ , combining  $\kappa$  of equations (12) and (13) gives

$$\lambda = \frac{q}{4\pi e \Delta T_m t_m}. \quad (14)$$

##### 3.4.1.2. SPM Based on SLHS Solution

Equations (13)–(14) are based on the ILHS solution that assumes instantaneous release of heat to an infinite porous medium (homogeneous, isotropic, and isothermal) by an infinite line source (Bristow, Kluitenberg,

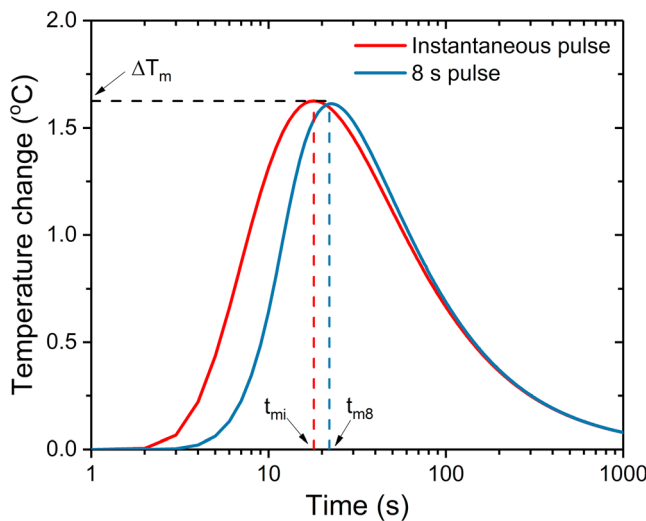


**Figure 3.** Simulated temperature change for instantaneous and short duration line source heat pulse model. Values used for the simulation were: probe spacing  $r = 0.006$  m, heat pulse duration  $t_0 = 8$  s, energy input  $q = 62.5$  W/m, heat capacity  $C_v = 1 \times 10^6$  J·m $^{-3}$ ·°C $^{-1}$ , and thermal diffusivity  $\kappa = 5 \times 10^{-7}$  m $^2$ /s.  $t_{mi}$  and  $t_{m8}$  are time to get maximum temperature for instantaneous and for 8 s pulse, respectively (data from Bristow, Kluitenberg, et al., 1994).

et al., 1994; G. S. Campbell et al., 1991; Carslaw & Jaeger, 1959). In practice, it is not possible to meet the requirements of ILHS theory with a heat source of finite length and a SLHS.

Figure 3 presents an example of the difference between the ILHS and SLHS solutions. The SLHS causes a significant delay in  $t_m$ , but has very little effect on  $\Delta T_m$  (Bristow, Kluitenberg, et al., 1994; Kluitenberg et al., 1993). Many previous studies (Bristow et al., 1993; G. S. Campbell et al., 1991; Lubimova et al., 1961) have concluded that it is possible to obtain accurate  $C_v$  using equation (14) with HP of a short duration. However,  $C_v$  calculated using the ILHS solution is slightly larger than that calculated with the SLHS solution (Kluitenberg et al., 1993).

Kluitenberg et al. (1993) and Bristow, Kluitenberg, et al. (1994) differentiated equation (7)b with respect to time and derived the following expression for  $\kappa$  at the maximum temperature rise:

$$\kappa = \frac{r^2}{4t_m} \left( \frac{t_0}{t_m - t_0} \right) \left[ \ln \left( \frac{t_m}{t_m - t_0} \right) \right]^{-1}. \quad (15)$$

For time  $t > t_0$ , rearrangement of equation (7)b yields the volumetric heat capacity with  $\kappa$  obtained from equation (15).

$$C_v = \frac{q'}{4\pi\kappa\Delta T_m} \left[ E_1 \left( \frac{r^2}{4\kappa t_m} \right) - E_1 \left( \frac{r^2}{4\kappa(t_m - t_0)} \right) \right]. \quad (16)$$

Determination of  $C_v$  in this way requires quantifying  $q'$  and  $\Delta T_m$  in addition to the probe spacing  $r$ ,  $t_m$ , and  $t_0$ . Equation (16) consists of the exponential integral function that is not available in most computer spreadsheet software packages or data logger function libraries. J. H. Knight and Kluitenberg (2004) derived a simplified approximation to equation (16) using the first five terms of a Taylor series expansion to give

$$C_v = \frac{q'}{\varepsilon\pi r^2 \Delta T_m} \left( 1 - \frac{\varepsilon^2}{8} \left\{ \frac{1}{3} + \varepsilon \left[ \frac{1}{3} + \frac{\varepsilon}{8} \left( \frac{5}{2} + \frac{7\varepsilon}{3} \right) \right] \right\} \right), \quad (17)$$

where  $\varepsilon = t_0/t_m$ . J. H. Knight and Kluitenberg (2004) found that  $C_v$  obtained from equation (17) is more accurate than that obtained from equation (14). J. H. Knight and Kluitenberg (2015) later reported a new, accurate calculation method for determining  $C_v$ , even for relatively short probe spacing and long heating times.

Equations (15) and (16) or (17) can therefore be used to obtain the thermal conductivity,  $\lambda$  (W·m $^{-1}$ ·°C $^{-1}$ ), given that  $\lambda = \kappa C_v$ . Combining equations (15) and (16) gives (Noborio et al., 1996b)

$$\lambda = \frac{q}{4\pi\Delta T_m t_0} \left( E_1 \left\{ \frac{\ln[t_m/(t_m - t_0)]}{t_0/(t_m - t_0)} \right\} - E_1 \left\{ \frac{\ln[t_m/(t_m - t_0)]}{t_0/t_m} \right\} \right). \quad (18)$$

The SPM, which is based on the single point values of  $r$ ,  $\Delta T_m$ , and  $t_m$  estimated from the  $\Delta T(t)$  curve, is easy to apply. However,  $C_v$  and  $\lambda$  are sensitive to errors in  $\Delta T_m$ , and  $\kappa$  and  $\lambda$  are extremely sensitive to errors in  $t_m$  due to uncertainty in probe spacing (Kluitenberg et al., 1995, 2010). Because the SPM requires accurate and precise identification of the peak ( $\Delta T_m$  and  $t_m$ ), the method does not work well with broad, flat peaks and sparse, noisy data.

### 3.4.2. Analysis of the NMF Method

To deal with the limitations of the SPM, Bristow et al. (1995) introduced a NMF method for determining  $\kappa$  and  $C_v$  by fitting the measured  $\Delta T(t)$  data with equation (7) through a nonlinear regression by minimizing the sum of squared errors objective function (Bristow et al., 1995). Welch et al. (1996) provided a computer code, HPC, and Yang and Jones (2009) presented another code, INV-WATFLX, for fitting  $\Delta T(t)$  data. Hopmans et al. (2002) and Mori et al. (2005) proposed a nonlinear optimization approach to minimize the residuals between the measured and optimized  $\Delta T(t)$  curves

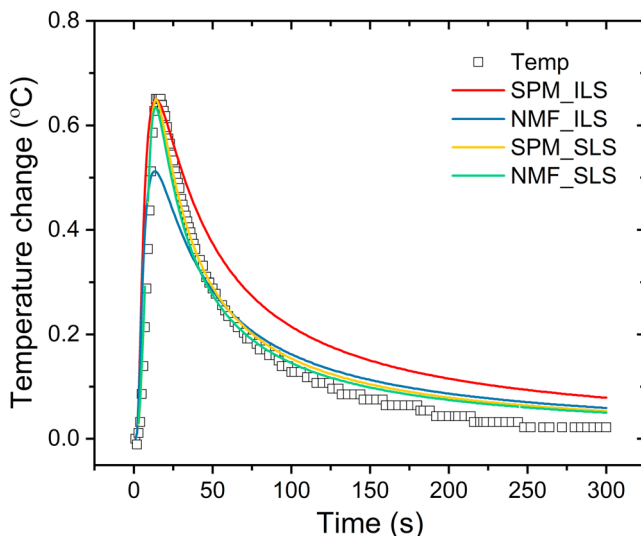


**Figure 4.** Example of the SPM and NMF methods used to determine the soil thermal properties using dual-probe heat-pulse sensors. Energy input  $q = 11.5 \text{ W/m}$ , heat pulse duration  $t_0 = 8 \text{ s}$ , and probe spacing  $r = 0.0068 \text{ m}$ . SPM = single point method; NMF = nonlinear model fitting; ILS = instantaneous line source theory; SLS = short duration line source theory.

weighted NMF method—use of NMF to fit a subset of the  $\Delta T(t)$  data  $>0.75 \Delta T_m$  only to better represent the infinite line-heat source model. The effects of finite probe properties on soil thermal property estimates have been demonstrated in both modeling and experimental studies (Ham & Benson, 2004; Hopmans et al., 2002). J. H. Knight et al. (2012) treated the HP probes as identical-cylindrical-perfect-conductors (ICPC) with finite probe heat capacity and finite probe radius. They demonstrated that finite probe properties could significantly alter the shape of the HP signals, especially at early times. Y. Lu et al. (2013) showed that at least in some cases using late-time data improved the accuracy of the HP method for determining soil thermal properties.

### 3.4.3. Numerical Simulation

Due to ease of use, the analytical solutions have gained wide acceptance for HP data analysis. Generally, reasonably accurate results can be achieved with analytical solutions, which also provide physical insights into the system. Numerical modeling, on the other hand, provides unique opportunities for estimating soil thermal properties as well as soil water contents when the boundary and initial conditions become too complicated for analytical solutions to be used for accurate determination of these properties (J. H. Knight et al., 2012; Sakai et al., 2011; Y. Zhang et al., 2011). The commonly used numerical approaches are finite difference and finite element methods. Initial and boundary conditions need to be carefully set, and the choice for discrete time and space steps are critical. Examples for estimating soil thermal properties with numerical estimation are provided by Papadakis et al. (1990) for SPHP method. Examples on the use of numerical methods to estimate soil thermal properties and a wide range of other properties are provided by Hopmans et al. (2002), Mortensen et al. (2006), Overduin et al. (2006), Kamai (2013), Sakai et al. (2011), and Y. Zhang et al. (2011).

An advantage of using a numerical approach to analyze data collected with the HP method is the elimination of constraints on needle geometry and boundary and initial conditions as imposed by most analytical solutions (Papadakis et al., 1990; H. Saito et al., 2007). Hopmans et al. (2002) took full advantage of numerical solutions (HYDRUS 2D finite element) and inverse modeling to examine the effect of probe geometry on soil thermal properties and water flux estimation using the 3-needle HP probe of Ren et al. (2000). Mortensen et al. (2006) used a similar approach (inverse modeling, HYDRUS 2D) to analyze multifunctional HP (Figure 5) measurements combined with a soil column experiment. They found that the sensor was able to estimate thermal, hydraulic, and solute transport properties in soils. H. Saito et al. (2007) examined the effect of probe geometry, heater probe-induced evaporation, and vapor flow

$$OF_I = \sum_{i=1}^N [\Delta T^M(t_i) - \Delta T^O(t_i, P_i)]^2, \quad (19)$$

where  $OF_I$  is the objective function;  $N$  is the number of measurement points at time  $t_i$ ; superscripts  $M$  and  $O$  refer to the measured and optimized temperatures, respectively. Equation (7b) is fitted by minimizing equation (19) to determine the parameters (e.g., thermal properties) contained in the vector  $P_i$ .

Such fitting can now be achieved in many mathematical software programs such as Excel, Matlab, Maple, and Mathematica.

The NMF method copes better than the SPM with broad, flat peaks and sparse, noisy data. Soil thermal properties obtained using either the SPM or the NMF method should be checked by comparing the fitted model with the measured  $\Delta T(t)$  data. This can quickly determine the validity of the results (Bristow et al., 1995). In fact, SPM also provides good initial guess values for NMF. Figure 4 gives an example of the SPM and the NMF methods used in analyzing  $\Delta T(t)$  data.

The algorithm used for fitting the model to the  $\Delta T(t)$  data minimizes the sum of squares error for the entire data set to obtain the best fit results, together with errors from deviations between solutions for the finite and infinite line source at long times. For example, NMF-estimates could underestimate the  $\Delta T(t)$  at the peak and overestimate it at longer times.

To improve the accuracy of estimates, Bristow et al. (1995) suggested the

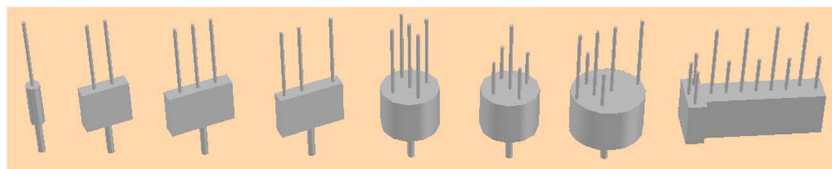


**Figure 5.** Schematic diagram of selected HP probe designs discussed in recent literature (not to scale): (1) single-probe heat-pulse; (2) 2-needle DPHP (G. S. Campbell et al., 1991; J. H. Knight et al., 2007); (3) 3-needle DPHP, three needles are equally spaced (Ren et al., 2000; Ren, Horton, et al., 2003) and with temperature sensors shorter than the heater (Kamai, 2013; Kamai et al., 2008); (4) 3-needle DPHP, two needles 6 mm apart and one reference probe 20 mm apart; (5) 5/penta-needle DPHP (Endo & Hara, 2003; He et al., 2015), all needles are of equal length; (6) 6-needle DPHP (multifunctional heat pulse probe consists of six needles: One heater needle, four temperature sensor needles, and one background temperature sensor needle (Mori et al., 2003, 2005; Mortensen et al., 2006); and (8) 11-needle DPHP (X. Zhang et al., 2012), the 2- to 6-needle heat pulse probes can be converted to thermo-TDR if the heater needle also serves as the center TDR electrode and the temperature sensor needles function as TDR ground electrodes. DPHP = dual-probe heat-pulse; TDR = time domain reflectometry.

in unsaturated soils on thermal properties and soil water flux estimation using HYDRUS 2D. They found that a stronger HP combined with a larger probe diameter could improve liquid water flux estimation, provided vapor transport is considered. Their study convincingly showed the flexibility of a numerical approach to obtain thermal properties of soil from experiments involving coupled liquid water, vapor and heat transport, and finite dimensions of heater needles, which would be impossible to address with analytical solutions. The numerical approach may be adapted to the measurement of soil thermal properties using HP methods with transient water flow in unfrozen and partially frozen soils.

#### 3.4.4. Semianalytical Solutions

As alluded to above, analytical solutions are widely used, but they cannot account for the effects of probe characteristics (e.g., probe radius, probe heat capacity, probe thermal conductivity and contact resistance between probe and soil). Numerical simulations can take such probe characteristics into consideration, but they are relatively complicated. Semianalytical solutions are good alternatives for accurate estimations with moderate complexity. J. H. Knight et al. (2012) developed an ICPC model (semianalytical solution) that accounted for effects of probe heat capacity and probe dimensions to improve the accuracy of soil water estimation. The approach of J. H. Knight et al. (2012) to account for effects of probe heat capacity work equally well with the spatial weighting function theory presented by J. H. Knight et al. (2007) and the correction method by J. Knight and Kluitenberg (2013) for instantaneous heating scenarios. Recently, J. H. Knight et al. (2016) improved the work of J. H. Knight et al. (2012) by deriving a semianalytical solution that accounts for the finite radius and finite conductivity of the DPHP probes and contact resistance between probe and soil. This solution can improve the estimation of thermal properties. These semianalytical approaches remarkably advance the theory and application of HP methods in soil science.

#### 3.5. Comparison of SPHP, DLHS, and DPHP Methods

As stated above, the SPHP and DLHS methods are based on the CLHS theory, while the DPHP method is based on the short-duration line-heat source theory. The DLHS method uses the time derivative  $dT/dt$  data while the SPHP and DPHP method use the  $\Delta T(t)$  data. They also differ in probe design, HP duration, and interpretation. For instance, the DPHP method uses a relatively short heating duration (e.g., 8 to 15 s), while the heating duration of the SPHP and DLHS methods is much longer (e.g., 60 to 600 s). For the DPHP method, the length to spacing (LS) ratio (ratio of the length of the line source and distance between heater and temperature sensor) is much smaller than that for the DLHS method. For example, the sensor of G. S. Campbell et al. (1991) had a LS ratio of roughly 4.6. By contrast, the apparatus described in Figure 3 of Merrill (1968) had a LS ratio of 250. A much larger LS ratio is required by the DLHS method because the heating duration is much longer than that in the DPHP method. All three thermal properties can be determined from DPHP measurements, while only the thermal conductivity can be determined accurately with the SPHP method traditionally. G. Liu and Si (2011a) tested the SPHP and DPHP methods with different data interpretation models on three air-dry soils, and their results showed that both methods yielded similar  $\lambda$  with a relative deviation  $<6.1\%$ . The DPHP method overestimated the  $C_v$  compared to the measurement made by differential scanning calorimetry method, their result

showed SPHP method can be used to well estimate  $C_v$  using a perfect conductor model proposed by Blackwell (1954).

Advances in the design of HP probes enable both SPHP and DPHP measurements to be made using one sensor on the same soil sample. This reduces potential errors associated with any differences in soil samples when comparing the accuracy of these two methods. A good example is the study of Bristow, White, et al. (1994) who included a temperature sensor in the heater of a DPHP probe, so it could be used to make both SPHP and DPHP measurements. They found that the DPHP and SPHP methods yielded similar  $\lambda$  of air-dry sand, and the DPHP measurements of  $C_v$  agreed well with the  $C_v$  calculated using the weighted volume fraction method. However, one possible defect of this two-purpose DPHP probe is that the SPHP and DPHP methods differ in the requirement of energy input per unit time (Bristow, White, et al., 1994), thus the design may not always be optimal for both methods especially for use in moist soil where water migration may occur. For instance, Noborio et al. (2002) demonstrated that at the same energy input (53 W/m), the SPHP gave a smaller  $\lambda$  than the DPHP in the midrange water content. How DPHP and SPHP probes are designed and constructed and how to solve the problem of energy input for a two-purpose DPHP probe are discussed below.

#### 4. Probe Design and Construction

Considerable work has gone into developing HP probes. An early prototype design of the SPHP probe that was with a glass capillary sheath was developed by Van der Held and Van Drunen (1949) for measuring thermal conductivity of liquids, which was adopted by de Vries (1952) for soil measurements. The prototype design of a DPHP probe consisted of two bare wires, one acted as a heater and the other as temperature sensor, for measuring the thermal conductivity of a powder under vacuum. G. S. Campbell et al. (1991) put the heater and the temperature sensors in two hypodermic needles with epoxy filling and used the probe for measuring soil heat capacity. These early efforts served as the foundation for further development in HP probe design.

In most cases a thin electric resistance wire is used as the heater and a temperature sensor is housed at the midlength of the probe either together with the heater or in a separate sheath or *needle* (e.g., a hypodermic needle or a tube made of stainless steel, glass tube, or brass). Sheaths are used to increase the strength/durability of the probe. Thermally conductive epoxy, cement, or resin (with a thermal conductivity  $>4 \text{ W}\cdot\text{m}^{-1}\cdot\text{C}^{-1}$ ) is used to hold the heater/temperature sensor in place within the sheath and to provide electrical insulation and water resistance. Probes of various designs have been developed during the past few decades. Figure 5 displays some examples of the basic designs of several recent probes. The materials and criteria used for making HP probes and their performances have been investigated by many researchers (e.g., Ham & Benson, 2004; G. Liu et al., 2008; X. Liu et al., 2008; H. Saito et al., 2007; Wechsler, 1966; X. Zhang et al., 2012). This section focuses on probe geometries, heaters, temperature sensors, circuits, integration of HP with TDR, and probe performances. Probe geometry will be discussed separately for the SPHP and DPHP probes according to the sources of errors. A summary of selected studies that have used HP probes are given in Table 1.

##### 4.1. Probe Geometry (Length, Diameter, and Separation/Spacing)

###### 4.1.1. SPHP Sensors

Early studies determined thermal conductivity based on the linear relationship between SPHP-measured temperature rise ( $\Delta T$ ) and the logarithm of time,  $\log(t)$  (section 3.2). However, the deviation of linearity in a  $\Delta T - \log(t)$  plot appeared at the early heating stage, which was termed the *initial lag effect* or *initial error* (Wechsler, 1966). At late heating stages, this nonlinearity was termed *axial loss error* (Wechsler, 1966). The initial lag effect may be attributed to the effects of finite probe dimensions (e.g., diameters),  $\lambda$  and  $C_v$  of the probe, and contact resistance between the probe and test material or internal temperature sensor, while the axial loss error is from axial heat loss resulting from the limited length of the SPHP probe. Blackwell (1954) and Nix et al. (1967) showed that inaccuracies arising from the series approximation to equation (6) could be reduced to  $<1\%$  only after sufficient time had elapsed:

$$\left( \frac{(d/2)^2}{\kappa \cdot t} \right)^2 < 0.01. \quad (20)$$

**Table 1**  
*Selected Applications of Heat Pulse Methods, Including SPHP, DPHP, and Thermo-TDR*

Reference	Method	Probe geometry				Experimental application				Properties studied
		Rods	Diameter (mm)	Length (mm)	Spacing (mm) <sup>c</sup>	Heater resistance (Ω)	Heat duration (s)	Heat strength ( $\text{W m}^{-1}$ )	Experimental conditions	
Van der Held and Van Drunen (1949)	SPHP	1	N/A	N/A	-	N/A	Various	N/A	Lab, various liquids	Thermal conductivity
de Vries (1952)	SPHP	1	1.4	100	-	6.31 <sup>a</sup>	180	0.0631 <sup>a</sup>	Field, different depths	Thermal properties
Woodside and Messmer (1961a, 1961b)	SPHP	1	1.651	152.4	-	1600	180	N/A	Lab, vacuum and low pressure, sands, glass beads, sandstones	Thermal conductivity
Wechsler (1966) <sup>b</sup>	SPHP	1	0.508-6.35	75-610	-	N/A	1,200	N/A	Lab, dry and wet soils, insulation, snow, ice, etc.	Thermal conductivity of soil and insulation, probe design
Merrill (1968)	SPHP/DPHP	2	0.00254	150	0.6	N/A	60	N/A	Lab, different temperatures	Thermal conductivity
Panner (1970) <sup>e</sup>	SPHP	1	0.51	102	-	885	600	0.87 <sup>a</sup>	Lab, frozen soil	Thermal conductivity
Kasubuchi (1977)	SPHP	2	1	50	-	N/A	40	N/A	Lab, soil with different water contents, and 1% agar, ethyl alcohol	Thermal conductivity of soil
Baker and Goodrich (1984, 1987)	SPHP+TDR	2	3.2	500	50	N/A	N/A	N/A	Lab and field	Thermal conductivity and water content
Goodrich (1986) <sup>b</sup>	SPHP	1	3, 0.5	500, 210	-	N/A	N/A	N/A	Field, frozen soil	Thermal conductivity
Morabito (1989)	SPHP/DPHP	2	1, 4	70, 300	N/A	N/A	400-1,000	N/A	Lab, dry soil and construction materials	Thermal conductivity and diffusivity
Shiozawa and Campbell (1990)	SPHP	1	1.27	150	-	17.2	100	1-2	Lab and field	Thermal conductivity
G. S. Campbell et al. (1991)	DPHP	2	0.813	28	6	38	1-8	87.5-700	Lab, different soils and water contents	Water content
Bristow et al. (1993)	DPHP	3	0.813	28	6, 20	31.9 <sup>a</sup>	8	75	Lab, multiple depths during soil drying	Water content
Bristol, White, et al. (1994) <sup>b</sup>	SPHP+DPHP	2, 3	0.813	28	5.3, 7, 6, 8.4	31.95 <sup>a</sup>	50, 2-20	4-11, ~55	Lab, dry soil with various initial temperatures and temperature gradients	Water content
Noborio et al. (1996b)	DPHP+TDR	3	0.813	75	10	N/A	13	53	Lab, different water contents	Thermal properties of soils
Ren et al. (1999, 2000) and Ren, Ochsner, et al. (2003)	Thermo-TDR	3	1.3	40	6	45.64	15	9-26, ~50	Lab, soil of different water contents and solute concentration	Thermal properties and water content
Bristow et al. (2001)	DPHP	4	1	28	5/6	31.95	8	N/A	Lab, soils of different water contents and solute concentration	Water content, electric conductivity, thermal properties
Mori et al. (2003, 2005) and Mortensen et al. (2006)	Thermo-TDR/ MFHHP	6	1.27	26	6	21.3 <sup>a</sup>	8	N/A	Lab, water flow	Water flux, soil water content, electric conductivity
Heitman, Horton, Ren, et al. (2008), Heitman, Horton, Sauer, et al. (2008), and Heitman, Xiao, et al. (2008)	DPHP	3	1.3	40	6	N/A	8	3.75	Field, at multiple depths, bare soil surface	Soil evaporation

**Table 1** (continued)

Reference	Method	Rods	Probe geometry				Experimental application			Properties studied
			Diameter (mm)	Length (mm)	Spacing (mm) <sup>c</sup>	Heater resistance (Ω)	Heat duration (s)	Heat strength (w m <sup>-1</sup> )		
G. Liu and Si (2008)	DPHP	5	1.27	28	6	34	60	2–16	Lab, ice and snow samples	Density and thermal properties of snow
Ochsner and Baker (2008)	DPHP	3	1.3	40	~6	21.3 <sup>a</sup>	8	~85	Field, frozen soil at multiple depths and water contents during freezing-thawing	Apparent thermal properties and heat flux
Morin et al. (2010)	SPHP	1	1.5	~100	–	N/A	100	0.4	Field, multiple depths of snowpack	Thermal conductivity of snow
Sayde et al. (2010, 2014)	AHFO-DTS	1	3.8	30000–25000	–	N/A	60–120	11–20	Lab, Field	Soil water content
Steele-Dunne et al. (2010)	PFO									soil thermal properties and soil moisture content
Y. Zhang et al. (2011)	Thermo-TDR	3	1.27	40	6	17.76 <sup>a</sup>	8–60	12.5–33.3 <sup>a</sup>	Lab, frozen soils, different water contents, and temperatures	Total water content
Benitez-Buelga et al. (2014, 2016)	AHFO/PFO-DTS	1,2	1–3.8	15000	5.3–8.2	N/A	40–45	32–40	Lab, unfrozen soils, different FO, and spacings	Heat capacity
X. Zhang et al. (2012, 2014)	DPHP	11	1.3	20,40 <sup>d</sup>	6	N/A	8–12	3.5	Field, multiple depths	Evaporation
Wen et al. (2015) <sup>b</sup>	DPHP	2	1.27	40,50	6.1–6.5	N/A	15	~40,70	Lab, dry and saturated soils, various probe deflections	Deflection

Note: Hyphen means spacing is not necessary because it has only one probe. SPHP = single-probe heat-pulse; DPHP = dual-probe heat-pulse; TDR = time domain reflectometry.

<sup>a</sup>Values are calculated according to the description in the article. <sup>b</sup>Two or more probe designs were used. <sup>c</sup>Distance between the heater and the reference needle. <sup>d</sup>20 and 40 mm are lengths for temperature sensors and heaters, respectively. <sup>e</sup>Hollow probe.

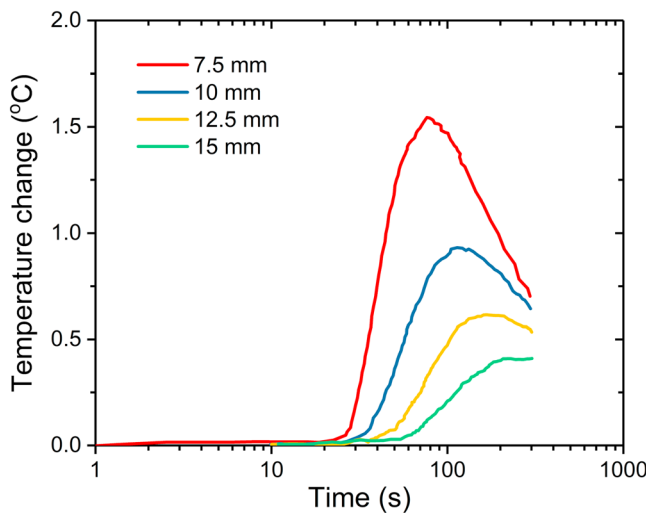


**Figure 6.** Measured temperature change in Sandfly Creek sand (bulk density = 1.5 Mg/m<sup>3</sup>) at sensor probe for various heater-temperature sensor spacing ( $r$  = 7.5–15 mm), energy input  $q' = 123$  W/m for heat pulse duration  $t_0 = 8$  s (data from Bristow, Kluitenberg, et al., 1994).

Baker & Goodrich, 1984; de Vries, 1952; Merrill, 1968; Penner, 1970; Pilkington & Grove, 2012; Shiozawa & Campbell, 1990; Woodside & Messmer, 1961a, 1961b).

#### 4.1.2. DPHP Sensors

In recent literature, the prevalent design of DPHP consists of 2 to 11 parallel needles typically 1–3 mm in diameter, 28–40 mm in length, and 6 mm apart. HP probes of smaller needle diameters make it possible to introduce them into the soil without markedly disturbing the natural structure of soil (de Vries, 1952), but they could affect the accuracy and precision of the measurements due to the sensitivity to probe spacing and deflection (Bristow, Kluitenberg, et al., 1994; G. S. Campbell et al., 1991; Kluitenberg et al., 2010; G. Liu et al., 2012; Noborio et al., 1996b; Ren, Horton, et al., 2003; Wen et al., 2015). The  $C_v$  and  $\kappa$  are sensitive to the probe spacing,  $r$ . For instance, a 2% error in  $r$  results in a 4% error in  $C_v$  (G. S. Campbell et al., 1991), whereas  $r$  does not considerably affect  $\lambda$  estimates (Kluitenberg et al., 2010; Noborio et al., 1996b).

Energy input to the heater and the maximum temperature rise at the temperature sensor are additional issues that need to be considered. With increasing  $r$ , more heating power is required to obtain a particular temperature rise at the sensor probe, which could result in convective heat transfer at the proximity of the heater. With a fixed energy input, larger needle spacing results in lower maximum temperature rise at the sensor needle (see Figure 6). In order to increase the accuracy of thermal property estimates, G. S. Campbell et al. (1991) introduced the approach of calibrating  $r$  in agar-stabilized water. Increasing  $d$  or decreasing  $L$  will improve the durability and rigidity of the probe (Kamai et al., 2015; Kamai & Hopmans, 2007; Kamai, 2013; Kluitenberg et al., 1993). However, a larger  $d$  implies a larger probe that acts as a heat sink. The finite probe length may violate the assumption of infinite line-heat source theory due to axial heat loss, but long probes may lead to uncertainty in the probe spacing (Noborio et al., 1996b). Therefore, the selection of  $r$ ,  $d$ , and  $L$  should be considered together. The optimum LD ratio of SPHP probes may be applicable to DPHP probes. More details of DPHP design will be discussed with the thermo-TDR sensors that combine the functions of DPHP and TDR sensors (sections 4.1.3 and 4.5).

#### 4.1.3. Thermo-TDR Sensors

Considering the similarities in probe geometry, it is possible to combine the TDR and DPHP probes into a single unit, which is referred as thermo-TDR sensor. Similar to a DPHP probe, the thermo-TDR probe also consists of two or more parallel needles. The center needle houses a resistance heater and also serves as the center TDR electrode. The other needles each house a thermistor or thermocouple and act as ground electrodes of a TDR sensor.

The design of a thermo-TDR probe has to satisfy the requirements of both TDR and HP theories. Topp et al. (1984) and Dalton and Van Genuchten (1986) suggested an  $L$  of >0.1 m for TDR probes. Heimovaara (1993)

Rearranging equation (20) gives

$$t \gg 2.5d^2/\kappa \text{ or } d \ll \sqrt{0.4\kappa \cdot t}, \quad (21)$$

where  $d$  is the external diameter (m) of the probe needle. Jones (1988) recommended  $t \gg 12.5d^2/\kappa$  or  $d \ll \sqrt{2\kappa t}$ . To satisfy equation (20), temperature sensors have to be placed very close to the heater or the HP duration needs to be relatively long.

In addition, inaccuracies are a result of the assumptions of a line heat source of infinite length and infinitesimal thickness. In reality, the finite dimension of the probe significantly deviates from this and results in errors such as axial heat loss. To reduce the effects of the finite probe, Blackwell (1954) suggested that the length to diameter (LD) ratio should satisfy

$$\frac{L}{d} > \frac{1}{2} \sqrt{\frac{\kappa \cdot t}{0.0158q^2}}, \quad (22)$$

where  $L$  is the probe length (m). Blackwell (1956) further showed that the influence of the finite probe dimensions could be reduced to be less than 1% if the LD ratio > 25. Typical designs of SPHP probes can be found in Table 1. In general, the lengths of the probes are greater than 10 cm (e.g.,

found that triple TDR sensors with a length  $L < 0.10$  m may result in a mingling of the first and second reflections when the dielectric permittivity was low. Robinson et al. (2003) suggested a sensor length between 0.15 and 0.30 m to provide adequate travel time. A small spacing  $r$  in DPHP probes results in a small representative sampling volume for TDR measurement (J. H. Knight, 1992), while a large  $r$  affects the propagated TDR signal (Zegelin et al., 1992). J. H. Knight (1992) suggested that the diameter  $d$  of the rods in TDR probes should be as large as possible given that it does not cause considerable local disturbance or compaction since an increase in  $d$  likely improved the reflected TDR signal and the durability and rigidity of the probe while introducing it into soil. J. H. Knight (1992) recommended that the ratio of  $r$  to  $d$  should be  $< 10$ .

Based on the error analysis of Kluitenberg et al. (1993, 1995) and others (Bristow, Kluitenberg, et al., 1994; G. S. Campbell et al., 1991), Ren et al. (1999) proposed a design criteria for the HP probe:

$$3.85d < r < 0.23L. \quad (23)$$

Ren et al. (1999) also suggested that the minimum length of a TDR sensor in dry soils was 23 mm. They used 40, 1.3, and 6 mm for  $L$ ,  $d$ , and  $r$  for their thermo-TDR probes. There are reports that an  $L$  of 40 mm may affect the accuracy and precision of water content estimates (He et al., 2015; Olmanson & Ochsner, 2008), but the underlying reasons remain unknown. To address the problem, a new TDR calibration equation, which was similar to the Topp et al. (1980) but with different constants, was suggested for estimating soil water contents with the thermo-TDR sensor (Ren, Horton, et al., 2003). New TDR waveform analysis techniques and the use of thermo-frequency domain reflectometry (thermo-FDR) may provide solutions to this problem. For instance, Z. Wang et al. (2014, 2016) obtained promising soil water contents by combining the tangent line methods and the second-order bounded mean oscillation method to determine the reflection points of thermo-TDR waveforms. The potential to address the problem of the short physical length of thermo-TDR probes using thermo-FDR will be discussed in section 6.2.

#### 4.2. Heater

The heater of a HP probe (both SPHP and DPHP) is commonly made from loops of heating wire of known resistance, which is pulled into the heater needle, and which is then filled with high thermal conductivity epoxy glue to provide water resistant and electrically insulated probes. In some cases, a temperature sensor is also mounted into and centered in the heater needle. Heaters should give a constant/time-invariant heat output (Batty et al., 1984; Presley & Christensen, 1997; Shiozawa & Campbell, 1990; Van der Held & Van Drunen, 1949). Because the fact that the resistance of a heating wire changes with temperature, an inconsistent power output is expected if a constant current is applied. To keep a nearly constant power output: (1) the applied voltage across the heater circuit should be adjusted accordingly; (2) the thermal coefficient (i.e., change of resistivity per unit temperature) of the heating wire should be extremely small; and (3) a feedback mechanism that can be implemented in the electrical circuit to maintain constant power supply. The second approach has been widely used.

Commonly used materials for heating wire are constantan ( $10^{-5} \Omega/\text{C}$ , e.g., de Vries, 1952; Goodrich, 1986; Jones, 1988; Van der Held, 1952, 1953; Verma et al., 1993; Wechsler, 1966; Wechsler & Glaser, 1965), Karma ( $2 \times 10^{-5} \Omega/\text{C}$ , e.g., Morabito, 1989; Woodside & Messmer, 1961a), Manganine ( $2 \times 10^{-5} \Omega/\text{C}$ , e.g., Van der Held & Van Drunen, 1949), and enameled Evanohm wire or Nichrome enameled resistance wire (e.g., Bristow, Kluitenberg, et al., 1994; Bristow, White, et al., 1994; G. S. Campbell et al., 1991; Ham & Benson, 2004; Tarara & Ham, 1997; Y. Zhang et al., 2011). The heating wire may be held straight (e.g., Van der Held & Van Drunen, 1949), folded into a loop or two loops (e.g., de Vries, 1952; Goodrich, 1986; G. Liu et al., 2012; X. Liu et al., 2008; Verma et al., 1993), or coiled (e.g., Baker & Goodrich, 1984; Penner, 1970; Wechsler & Glaser, 1965). More details about heater elements are listed in Table 1, and an example of probe construction is presented in section 4.5.

The magnitude of energy output due to the HP depends on the resistance of the heater, the voltage ( $V$ ) applied across the heater circuit, and the HP duration. A HP is generated by applying a voltage (e.g.,  $\sim 12$  V) from a direct current power supply to the heater for a fixed period. Before 1980s, a potentiometer (Wechsler, 1966; Woodside & Messmer, 1961a), multimeter, or voltmeter (e.g., Kasubuchi, 1977; Penner, 1970) is commonly used to monitor the voltage across the heater circuit and thermocouple prior to the appearance of dataloggers. Since the late 1980s, dataloggers have been used to control and supply the

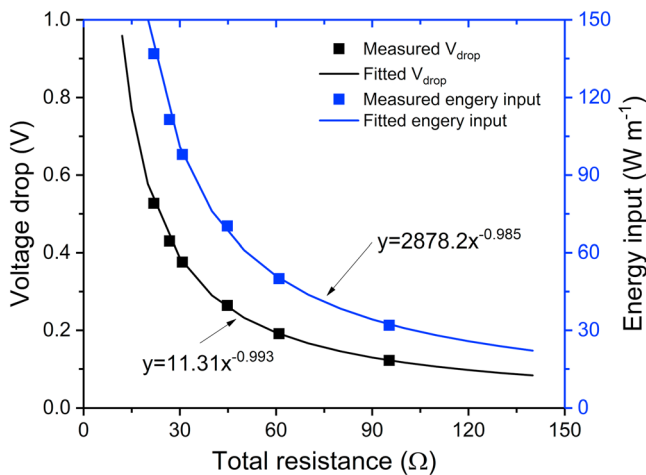


**Figure 7.** Relationship between the energy input, voltage drop, and the total resistance, reference resistor  $R_{ref} = 1 \Omega$ , voltage applied  $V = 12 \text{ V}$ , heater resistance  $R_{heater} = 0.9R_{total}$  (heater is composed of looped 37/40 N80 heavy ML enamel heating wire), probe length  $L = 0.04 \text{ m}$ , heat pulse duration  $t_0 = 8 \text{ s}$ . Data points are from authors' probe design test,  $R^2$  for both fitted line are 1.

voltage to the heating circuit automatically and to continuously monitor the voltage drop or current across the heater circuit and temperature responses of the thermocouple/thermistors sensors (e.g., Shiozawa & Campbell, 1990). More details about temperature sensors can be found in section 4.3. Direct voltage measurement of the heater circuit is impossible with dataloggers (e.g., Campbell Scientific models) that only accept voltage input of  $\sim 5 \text{ V}$  or below because the power source is commonly greater than or equal to  $12 \text{ V}$ . In order to calculate the heat input, a precision resistor (e.g.,  $\sim 1 \Omega$  reference resistor) is usually used in the heater circuit to measure the voltage drop,  $V_{drop}$ , which can be used to determine the current flow through the heater. One can also determine the heat output by directly measuring the current,  $I$ , through the use of a power shunt (e.g., Ochsner & Baker, 2008). The heat source strength can then be calculated according to the Joule's law:

$$q' = I^2 \frac{R_{heater}}{L} = \left( \frac{V}{R_{total}} \right)^2 \frac{R_{heater}}{L} \quad (24)$$

or

$$q' = \left( \frac{V_{drop}}{R_{ref}} \right)^2 \frac{R_{heater}}{L}, \quad (25)$$

where  $R_{total}$  is the total resistance of the heater circuit ( $\Omega$ ),  $R_{heater} = n R_{wire}$  is the total resistance of the heating wire in the probe only ( $\Omega$ ),  $n$  is the number of heating wire loops used in the heater, and  $R_{wire}$  is the resistance per loop of heating wire ( $\Omega$ ).

Accurate determination of  $q'$ , critical for determining thermal conductivity, can be made by inspection of equation (25): (a) accurate resistance of the heating wire ( $R_{heater}$ ) and (b) accurate determination of the electrical circuit ( $=V_{drop}/R_{ref}$ ) by installing a small resistor with precisely known resistance ( $R_{ref} = 1 \Omega$ ) in the circuit, plus precision measurement of voltage ( $V_{drop}$ ) due to the reference resistor in the circuit (Tarara & Ham, 1997). Note that the magnitude of  $q'$  is determined by the values of  $R_{total}$ : the greater the  $R_{total}$ , the smaller the  $q'$  value, when the other conditions are the same (see Figure 7). This means that larger  $R_{heater}$  values are desirable for the SPHP method in order to suppress the overall temperature rise given the long time heating required for the determination of  $\lambda$ , while smaller  $R_{heater}$  values are useful for the DPHP method. In the case that a heater probe is shared by SPHP and DPHP probes, one can either modify the voltage applied across the heater circuit or add an external adjustable reference resistor to the heater circuit. Note that although high power input to the SPHP affects  $\lambda$  estimates, there is little influence on the DPHP data (Bilskie, 1994; Noborio et al., 2002).

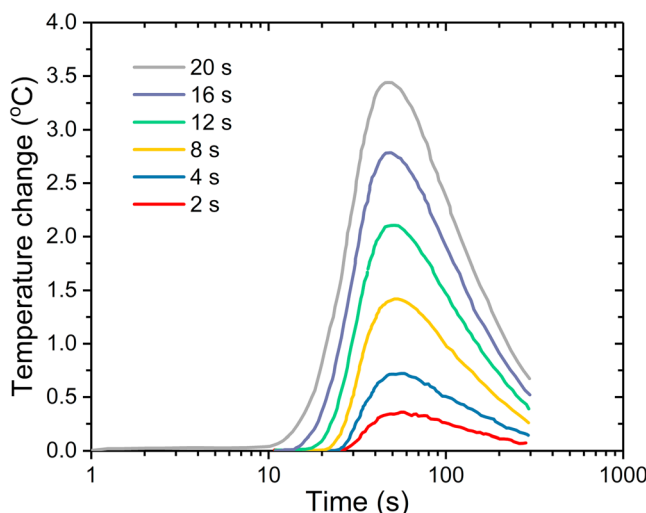


**Figure 8.** Measured temperature change at  $r = 0.0053 \text{ m}$  following application of heat pulses of different durations ( $t_0 = 2\text{--}20 \text{ s}$ ) at constant energy input ( $q' = 55 \text{ W/m}$ ) on an air-dry Clayton sand (bulk density =  $1.5 \text{ Mg/m}^3$ ) in a constant temperature laboratory (after Bristow, Kluitenberg, et al., 1994).

Figures 8 and 9 provide examples on how HP duration and energy input affect temperature changes at  $r = 6 \text{ mm}$ . The maximum temperature change increases with HP duration and energy input, and longer tails of  $\Delta T(t)$  are associated with longer HP duration and greater energy input. Figure 10 shows the temperature change at the heater for probes with the same HP duration and strength but different heater resistances.

To simulate an instantaneous HP, a larger heat input per unit length per unit time with shorter HP duration is required. This is possible for air-dry soils but may not be feasible for soils with intermediate to high water contents due to the possibility of induced convective water flow around the heater. A low heating energy at given heating duration and voltage/current may be facilitated by a greater heater resistance. Thus, appropriate heater resistance and HP duration must be used to optimize the temperature rise, as well as to minimize convective heat flow and

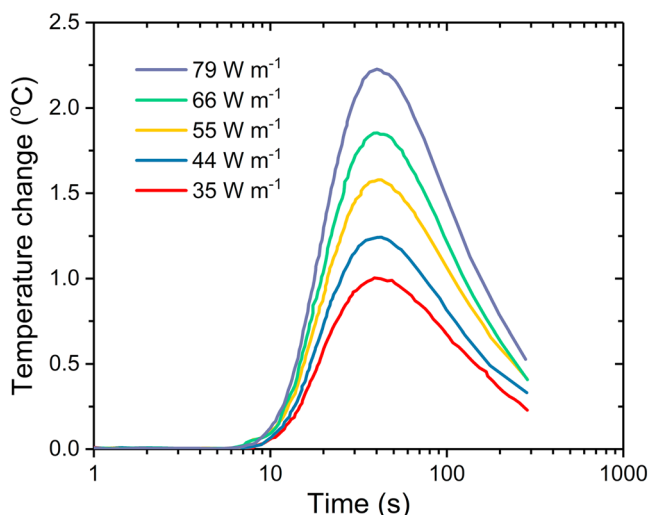


**Figure 9.** Measured temperature change at  $r = 0.0053$  m following various energy inputs ( $q' = 35\text{--}79 \text{ W/m}$ ) on air-dry Sandfly Creek sand (bulk density =  $1.5 \text{ Mg/m}^3$ ) in a constant temperature laboratory (after Bristow, White, et al., 1994).

axial heat flow. The two most commonly used temperature sensors are thermistors and thermocouples. Thermistors are made from metal oxides whose resistance decreases with increasing temperature; referred to as negative temperature coefficient sensors. A thermocouple usually consists of two different metal wires (sometimes metal alloys, e.g., the Type T thermocouple is made of copper and constantan) that produce a voltage proportional to the temperature difference between the junctions of the metal pairs. The relationships between resistance and temperature (the  $R(T)$  curve) for a thermistor, and voltage and temperature (the  $V(T)$  curve) for the thermocouples, form the basis for application of temperature sensors (Figure 11). The  $R(T)$  curve of thermistors is usually provided by the manufacturer, but the calibration curve should be confirmed prior to use (Bittelli et al., 2003).

A relatively small change in temperature can cause a relatively large change in the thermistor resistances, and, therefore, thermistors provide more sensitive measuring system than thermocouple-based systems for temperatures ranging from  $-90$  to  $130^\circ\text{C}$  (Bull, 2008; Goodrich, 1986). For example, a signal of  $35 \text{ MV}^\circ\text{C}$  difference is typical for thermistors, nearly 1,000 times greater than that generated by a thermocouple (e.g., Seebeck coefficient =  $40 \mu\text{V}^\circ\text{C}$  for a Type T thermocouple). The high resistivity of the thermistors allows a typical error of  $<0.05^\circ\text{C}$  (Agilent Technologies, 2000; Bittelli et al., 2003).

Compared to thermistors, thermocouples have a higher upper temperature limit, up to several thousand degrees Celsius. Thermistors have less long-term stability and experience more drift over time (e.g., a few 10s of a degree of change after 1 year), but provide more rapid response to temperature change than thermocouples (Ham & Benson, 2004). The fast response is particularly important for the transient methods used to determine soil thermal properties. Furthermore, thermocouple measurements need a reference temperature sensor, and temperature differences between the reference sensors and the thermocouples can also be problematic. In addition, thermistors are available in very small sizes with fast responses and low thermal masses. Therefore, for HP method applications, thermistors are often preferable to thermocouples, especially for measuring temperature changes in response to heat inputs. However, thermocouples are often used in view of their low cost and the comparatively simple electronic circuitry required. Thermocouples are preferred for ambient temperature measurements because they have less overtime

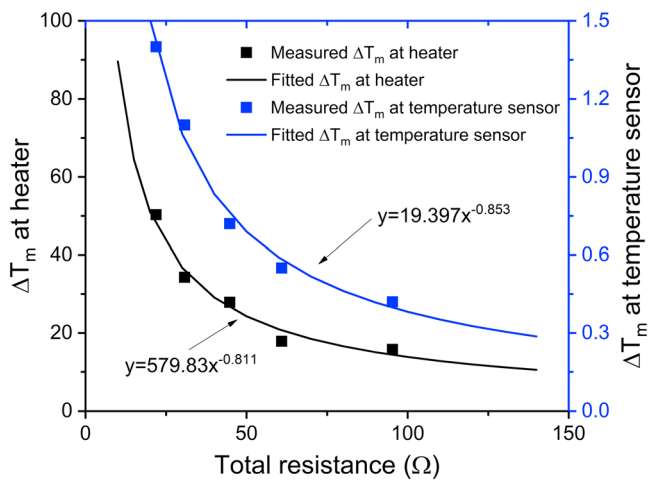


**Figure 10.** Maximum temperature change at the heater ( $R^2 = 0.96$ ) and the temperature sensor ( $R^2 = 0.99$ ,  $r = 6 \text{ mm}$ ) for different resistances when tested in agar-stabilized water. The applied power =  $12 \text{ V}$ , heat pulse duration =  $8 \text{ s}$ .

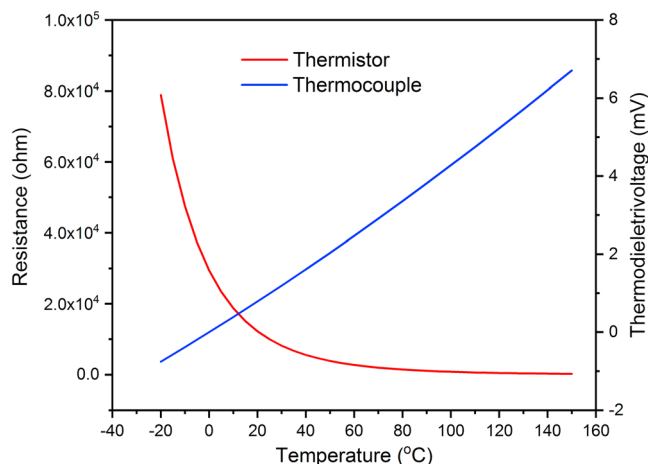


**Figure 11.** Resistance-temperature curve for the thermistor (red) and voltage-temperature curve for a type T thermocouple (blue) with a reference temperature = 0 °C.

be specified for each device (e.g.,  $SH_1$ ,  $SH_2$ , and  $SH_3$  are  $1.1292 \times 10^{-3}$ ,  $2.3411 \times 10^{-4}$ , and  $8.7755 \times 10^{-8}$ , respectively, for the BetaTherm 10KMC1 thermistors).  $T$  is the temperature in Kelvin and  $R$  is the resistance in ohms. Rather than directly calculating the exponentials for the  $R$  ( $T$ ) curve, a data acquisition system can be programmed to use the nested polynomial equation to save execution time.

When using a datalogger (e.g., Campbell Scientific Inc., Logan, Utah, United States, dataloggers) for temperature recording, differential wiring (e.g., copper to high channel, and constantan to low channel for type T thermocouple) is usually used for thermocouples, and a bridge electrical circuit (e.g., half- and full-bridge electrical circuit) is used for thermistors. The most frequently used connection methods for thermistors are 2- or 4-wire-half-bridges. The 2-wire-half-bridge occupies two input channels for each thermistor and allows simultaneous control of more probes, while the 4-wire-half-bridge occupies four channels for each thermistor, with a higher accuracy. Figure 12 shows the wiring of 2- and 4-wire-half-bridges (modified from the CR1000 manual, Campbell Scientific Inc.).

A circuit board, which helps to wire the circuit together and making the connection on a datalogger or on multiplexer panels, is useful when making measurements with multiple probes. Reference resistors can be taken out of the circuit board or excluded from the probe handle of the customized HP probe to reduce costs, which also allow easy switching among different measurement methods (half bridge, and 2- and 4-wire-half-bridges).

#### 4.4. Probe Design With Numerical Simulation

An appropriate design of a HP probe can be labor intensive and time consuming, because one must consider various issues (e.g., probe materials, geometry, needle to needle spacing) and heating strategies (e.g., heating duration and strength; Ham & Benson, 2004; Wechsler, 1966). Any changes to the boundary conditions and/or introduction of new processes (e.g., phase changes) may preclude the use of analytical solutions. Thus, numerical solutions are required (Kamai & Hopmans, 2007; H. Saito et al., 2007). In fact, numerical simulation can be a more efficient design approach than to physically make a number of prototype sensors, because numerical simulations can take into account the effects of probe materials, diameter/length, spacing, contact resistance, phase change, and even probe distribution on soil or water flow, and the optimized design can be selected from simulated scenarios (Kamai & Hopmans, 2007; G. Liu et al., 2007; Mortensen et al., 2006; H. Saito et al., 2007).

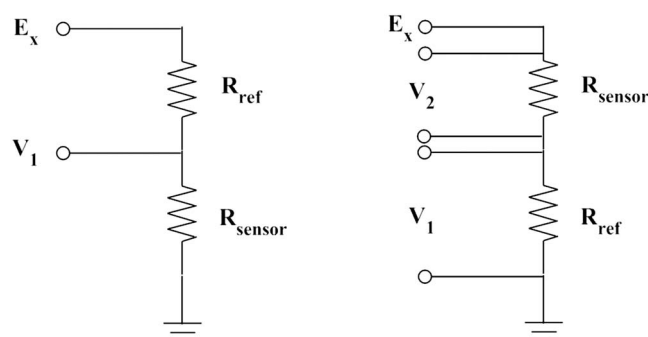


**Figure 12.** Schematic showing a 2- and 4-wire half-bridges circuit for thermistors to measure temperature changes when using single-probe heat-pulse and dual-probe heat-pulse sensors.  $E_x$  is the excitation,  $V_1$  and  $V_2$  are used to measure the voltage drop,  $R_{sensor}$  and  $R_{ref}$  are single-probe heat-pulse/dual-probe heat-pulse sensors and reference resistor, respectively.

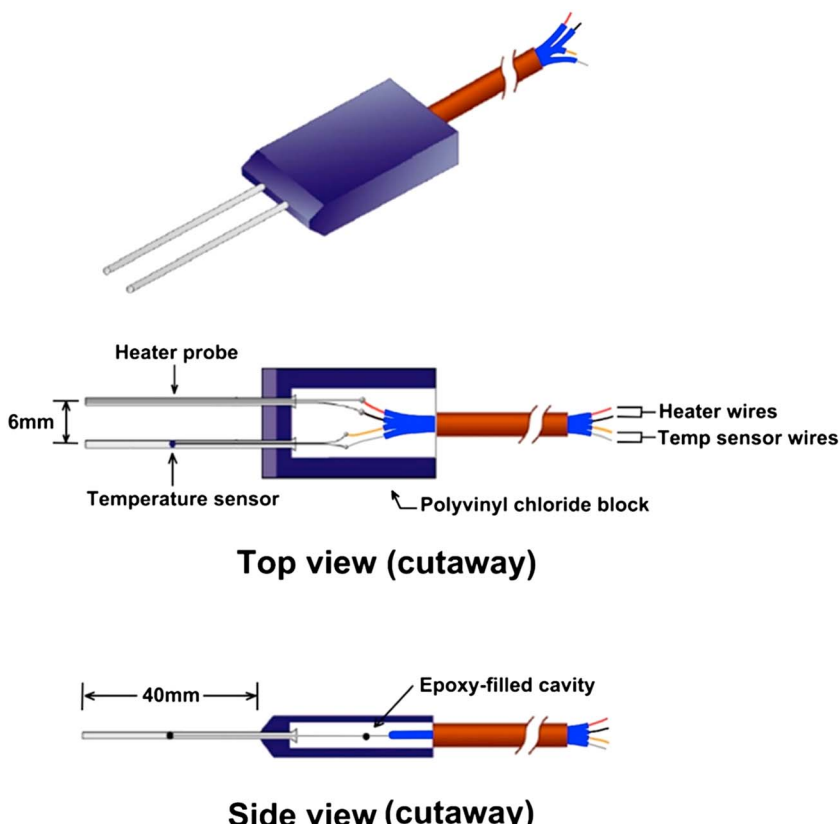


**Figure 13.** Example of dual-probe heat-pulse probe construction (after Heitman et al., 2003).

For example, H. Saito et al. (2007) employed the HYDRUS code to evaluate the effects of HP sensor location and body material, heater diameter, heat strength, and vapor flow. They found that only temperature measurements near the middle length of heater satisfied the assumption of infinite line heat source. For a rigid probe, the length of the temperature sensor needle can be much shorter than the heater needle. The larger the heater diameter (e.g., 2 or 4 mm), the greater the heat input, and the higher the sensitivity to water flux measurements. These findings can be used to improve the capabilities of HP probe to measure small water flux densities, compared to the traditional HP probe design (Kamai & Hopmans, 2007; H. Saito et al., 2007), which can only measure soil water flux density  $>2.4$  cm/day (Mori et al., 2005; Ochsner et al., 2005). Kamai et al. (2008) developed a HP probe with a heater needle of 4 mm in diameter. The improved design successfully extended the measurement range of water flux density to 1 cm day, which is suitable for many vadose zone flux measurements.

#### 4.5. Probe Construction

Probe design depends on and must enable achievement of the objectives of a particular study. The factors to be considered include but are not limited to the number of needles, probe length, diameter, spacing, heater resistance estimated from the desired maximum temperature rise and HP duration, loops of heating wire based on the desired heater resistance, number of conductors of extension cable, and the cable length. All these parameters should be documented before and during the design and construction for later reference. We present an example of the procedure to construct a 2-needle DPHP probe.

**DPHP probe:** 2 needles, 40 mm long, 6 mm spacing (Figure 13).

**Materials and tools:** hollow stainless steel tubing (~50 mm long, 1.03 mm outer diameter, O.D.), heater (e.g., Evan ohm resistance wire, one loop, ~120 mm long), temperature sensor (e.g., 10KMCD1 thermistor), and 10 K reference resistor (preventing short circuit and form half bridge circuit), thermally conductive epoxy (for filling of needle), thermally nonconductive epoxy for probe handle, extension wire, solder

(e.g., 7% silver), mold for probe handle construction, release agent/oil (a film between the probe handle and the mold for easy probe removal), syringe and flexible tube (for injection of epoxy), and wire cutter/stripper.

#### Procedures:

1. Strand the heating wire loop into a hollow stainless steel tubing and fill the tubing with thermally conductive epoxy through a flexible tube using a syringe once the heating wire is in place (keep at the axis of the heater needle) and let it dry when completed.
2. Place the thermistor axially at 20 mm from one tip of the temperature sensor needle. Fill the sensor needle with epoxy and let it dry.
3. Strip the ends of the heating wires and splice them to two stripped conductors of the extension cable and solder the splices.
4. Strip the ends of the thermistor and splice each end to two stripped conductors. Put one 10 K resistor between one thermistor end and the connecting wire. Sometimes the 10 K resistor is taken out of the handle so both the 2- and 4-wire-half-bridges can be used for measurement.
5. Clamp the completed heater- and temperature-needle assemblies into a mold or jig that holds the needles 6 mm apart, extend the needles 40 mm out of the mold. Spray release agent/oil on the mold before casting with thermally nonconductive epoxy (mixture of resin and hardener).
6. Check probe connection, carry out calibration to determine effective probe spacing ( $r$ ), and test probe performance before using the probe. The connections can be checked simply with a multimeter, and the spacing calibration can be done with agar stabilized water (to prevent free convection) as G. S. Campbell et al. (1991). The probe performance should then be calibrated by comparing the experimentally determined thermal properties of standard materials (e.g., dry Ottawa sand, Pyrex 7740, Fused Silica, Pryoceram 9606, glycerine/glycerol, paraffin wax, or agar-stabilized water) to their known values. For more details on calibration see ASTM D5334-14 *Standard Test Method for Determination of Thermal Conductivity of Soil and Soft Rock by Thermal Needle Probe Procedure* and IEEE Std 442-2017 *IEEE Draft Guide for Thermal Resistivity Measurements of Soils and Backfill Materials*.

The SPHP probe, which includes both heating wire and temperature sensor in a long probe, can be constructed using similar procedures. For more details on the construction and operation of a DPHP sensor see Benson (2004) and Schubert and Schumacher (2005). For construction of the TDR part of a thermo-TDR, please refer to Evett (2000). Construction of HP probes needs to consider mechanical strength and durability to withstand handling and the stresses of repeated insertions into and removals from the test media (e.g., different soils). Making a measurement requires additional instruments and tools. These include a laptop computer with appropriate software connecting it to a datalogger (e.g., Campbell Scientific dataloggers), power supply (e.g., 12 V DC), screw driver (e.g., for cable connection), and multimeter (e.g., to check circuit connections).

While the SPHP, DPHP, and thermo-TDR are mostly homemade, certain probes are available from the manufacturers (e.g., KD2 Pro from Decagon Devices, Hukseflux thermal sensors TPO1/02/08 heated-needle probes, ISOMET 2114 from the Applied Precision Ltd., TPA2000 from GeothermUSA, TK04 from TeKa, Quickline 30 from Anter Corporation, and STP-1 from A.R.P.). Customized probes can be made in workshops (e.g., Yang Scientific or East 30 Sensors). The 3-D printing technology may be adopted to fabricate the HP probe or thermo-TDR to reduce labor and cost of probe construction. It should be noted that the list of companies is not complete, and it does not imply any company endorsement. Readers may contact the authors for advice on probes and/or associated programs for data analysis.

## 5. Application of the HP Method in Unfrozen and Frozen Soils

### 5.1. Overview of the HP Method in Soil Science

Although numerous applications of the HP method have been used to measure thermal properties of liquids, gases, biomaterials, and construction materials, the HP applications related to Earth and environmental sciences is the focus of this review. We performed an extensive literature review to summarize the current state and future directions of the HP method in Earth and environmental sciences. We include mainly peer reviewed journal articles, books, and theses/dissertations to have wide coverage. Only English-language

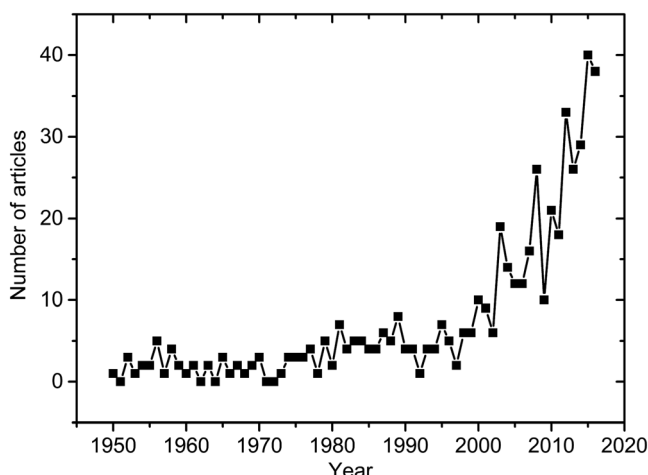


**Figure 14.** Number of publications using heat pulse probes by year.

literature is presented. The academic engines and databases we used are Scopus, EBSCOhost, ScienceDirect, Web of Science, ProQuest Dissertations and Theses, IEEE Xplore, and Google Scholar.

The terms that most frequently appeared in titles and abstracts were chosen as descriptors for the search. The main terms were *heat pulse probe*, *dual probe heat pulse*, *single probe heat pulse*, *thermo-time domain reflectometry*, *KD2 pro*, *thermal probe*, *thermal needle*, *needle probe*, *cylindrical probe*, *hot wire method*, *line heat source*, *distributed temperature sensing/DTS*, *soil thermal properties*, *thermal conductivity*, *thermal resistivity*, *soil water content*, *soil ice content*, *evaporation*, *nonstationary/nonsteady-state*, and *transient method*. In addition, we also worked backward by reviewing other papers written by the identified authors as well as citations in the papers identified from the databases. The search serves as a framework for gaining an understanding of the HP method. Every article retrieved through the search process was carefully reviewed to ensure its relevance, and a total of 490 articles were identified for the period of 1950 to 2016 (Figure 14). The number of articles published increased significantly since the 1990s, and there were averages of 20 papers per year since 2000, and 30 papers per year from 2010. We also summarized the most frequently published journals for these articles (Table 2). The Soil Science Society of America Journal, Vadose Zone Journal, and Water Resources Research are the three more utilized journals for publication of HP method related articles.

The 490 articles were divided into different categories based on measurement theories (e.g., SPHP/DPHP/thermo-TDR/DTS, analytical, or numerical methods), experimental conditions (e.g., unfrozen soil or frozen soil, laboratory, or field), and properties measured (e.g., soil thermal properties, water content, water flux, heat flux, and evaporation). The classification is somewhat arbitrary because multiple properties were measured in recent articles, or both laboratory and field studies were performed, thus, making the sum of each category >490 (Figure 15). We will continue our discussion based on the categories described.

The prominent research groups using the HP method for soil physical measurements are mainly led by Gaylon S. Campbell (former professor at Washington State University, now with METER Group, Inc., United States), Gerard J. Kluitenberg at Kansas State University (United States), Jan W. Hopmans at University of California at Davis (United States), Robert Horton at Iowa State University (United States), Scott B. Jones at Utah State University (United States), Keith Bristow at CSIRO (Australia), Kosuke Noborio at Meiji University (Japan), John H. Knight at University of Sydney (Australia), Tusheng Ren and Gang Liu at China Agriculture University (China), Tyson Ochsner at Oklahoma State University (United States), Joshua L. Heitman at North Carolina State University (United States), Bing C. Si at the University of Saskatchewan (Canada), Tamir Kamai at Agricultural Research organization, Volcanic Center (Israel), and Yuki Kojima at Gifu University (Japan).

## 5.2. Physical Measurements of Unfrozen Soils

### 5.2.1. Soil Thermal Properties

All studies with the HP method have been used to estimate one or more soil thermal properties. By reviewing the 490 studies, we found that soil thermal properties largely vary with texture and water content. For example,

thermal conductivity of air-dry soils generally ranges from about 0.17 for clayey soils to 0.32  $\text{J}\cdot\text{m}^{-1}\cdot\text{s}^{-1}\cdot\text{C}^{-1}$  for sandy soils, volumetric heat capacity from 0.89 to 1.33  $\text{J}\cdot\text{m}^{-3}\cdot\text{C}^{-1}$ , and thermal diffusivity from 1.70 to 2.66  $\text{m}^2/\text{s}$  based on the soil thermal conductivity database we are developing.

Soil thermal inertia ( $\rho = \sqrt{\lambda C_v}$ ) is another thermal property that characterizes soil resistance to surrounding temperature change and has been used in remote sensing for soil moisture estimation (Price, 1977; Verstraeten et al., 2006). This property can also be validated with the HP method (Maltese et al., 2010; Minacapilli et al., 2012). S. Lu et al. (2009) and Y. Lu, Horton, Zhang, et al. (2018) reported soil water content from values of soil thermal inertia determined with remote sensing methods.

**Table 2**

Most Utilized Journals for Publication of Heat Pulse Related Studies

Journal	Number of articles
Soil Science Society of America Journal	64
Vadose Zone Journal	26
Water Resources Research	15
Soil Science	11
Agricultural and forest meteorology	9
Journal of Geophysical Research	8
Geotechnical Testing Journal	8
Canadian Geotechnical Journal	5

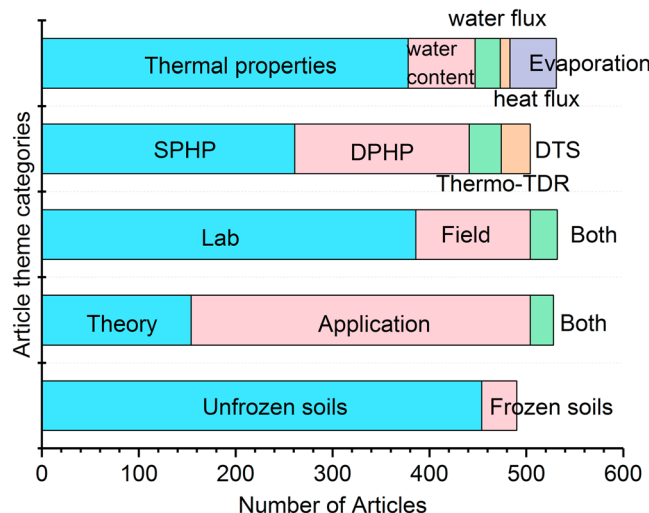


**Figure 15.** Distribution of articles using heat pulse probes according to topics. SPHP = single-probe heat-pulse; DPHP = dual-probe heat-pulse; DTS = distributed temperature sensing; Thermo-TDR = thermo-time domain reflectometry.

### 5.2.2. Water Content, Air Filled Porosity, and Bulk Density

Indirect measurements of soil water content are based on DPHP-estimated  $C_v$ , and air-filled porosity and bulk density are based in part on DPHP-estimated  $C_v$  or  $\lambda$ . As is well known, volumetric heat capacity of a soil can be expressed as the sum of the heat capacities of soil components (de Vries, 1963; Ochsner et al., 2001b)

$$C_v = \theta_v \rho_l c_l + f \rho_g c_g + (1 - \Phi) \rho_s c_s, \quad (27)$$

where  $\theta_v$ ,  $f$ , and  $\Phi$  are volumetric fraction of water, air filled pores, and total porosity ( $m^3/m^3$ ), respectively; subscripts  $l$ ,  $s$ , and  $g$  indicate liquid water, solid, and air, respectively;  $\rho$  is density ( $kg/m^3$ );  $c$  is the specific heat capacity ( $J \cdot kg^{-1} \cdot ^\circ C^{-1}$ ). The second term on the right-hand side in equation (27) is much smaller relative to the other terms, thus, it is usually neglected. Additionally,

$$(1 - \Phi) \rho_s = \rho_b. \quad (28)$$

Inserting equation (28) into equation (27) gives (G. S. Campbell et al., 1991)

$$C_v = \theta_v \rho_l c_l + \rho_b c_s. \quad (29)$$

By rearranging equation (29), the soil water content can be determined by (G. S. Campbell et al., 1991; Ochsner et al., 2001b; Ren et al., 1999; Ren, Horton, et al., 2003)

$$\theta_v = \frac{C_v - \rho_b c_s}{\rho_l c_l}. \quad (30)$$

G. S. Campbell et al. (1991) reported a 0.5% accuracy of  $\theta_v$  for soil of various textures and water contents. Tarara and Ham (1997) noted that a real strength of the DPHP method is to measure changes in  $\theta_v$ . Since the bulk density or organic matter content rarely changes very much between two sampling times, the accuracy of  $\theta_v$  differences are generally within 1%. DPHP can also monitor water depletion in the root zone at a fine scale (e.g., every 2 cm; Song et al., 1999) and hydraulic lift (roots extracting water from deep wet subsoil and releasing it in upper dry soil; Song et al., 2000). D. I. Campbell et al. (2002) applied this method on peat soils and found that the DPHP-estimated water contents agreed well with gravimetric values, and the measurements were more sensitive in peat soil than in mineral soils.

Bulk density can be determined by the gravimetric method, and  $c_s$  can be measured on dry soil, estimated from published values, or measured by using differential scanning calorimetry. In saturated soils,  $\theta_v = 1 - \rho_b / \rho_s$ , where  $\rho_s$  is the particle density (about  $2.65 \text{ g/cm}^3$  for mineral soils). Therefore, saturated soil water content and/or soil bulk density can be determined for a two phase system such as saturated soils or suspensions as shown by M. Li et al. (2015). For a three-phase system such as unsaturated soils, either the volumetric soil water content or bulk density must be known before the other could be determined with a HP measurement. For example, if  $\theta_v$  is known or can be measured (i.e., by gravimetric method or TDR), then arrangement of equation (29) gives (M. Li et al., 2015; X. Liu et al., 2008, 2014; Ochsner et al., 2001b; Ren, Horton, & Ochsner, 2003)

$$\rho_b = \frac{C_v - \theta_v \rho_l c_l}{c_s}. \quad (31)$$

In a recent article, Y. Lu, Horton, and Ren (2018) reported that a DPHP measurement can, for wet soils, be used to estimate water content and bulk density simultaneously. The theory behind is that soil heat capacity and thermal conductivity vary with water content and bulk density, and simultaneous determination of heat capacity and thermal conductivity provide the opportunity to estimate both water content and bulk density. Y. Lu et al. (2016, 2017) also proposed a way to obtain  $\rho_b$  by relating it to  $\lambda$  and  $\theta_v$  determined with thermo-TDR sensors using an empirical  $\lambda$  model (S. Lu et al., 2007). Although no explicit expression for calculating  $\rho_b$

was given, their results showed that this approach could be used to accurately estimate  $\rho_b$  and in laboratory soils and in situ with RMSE < 0.17 g/cm<sup>3</sup> when soil texture was available. Y. Lu et al. (2016) stated that the  $\lambda$ -based method performed better than the  $C_v$ -based method for estimating  $\rho_b$ , because  $C_v$  was more sensitive to the probe deflection than  $\lambda$ . This  $\lambda$ -based approach, being empirical, is promising, but requires further verification. This is because the reliability of the  $\rho_b$  estimates (similar to  $\theta_v$ ) may largely depend on the reliability of the selected thermal conductivity model.

Ochsner et al. (2001b) used a thermo-TDR probe for simultaneous measurement of soil water content, air filled porosity, and bulk density. The results, however, indicated fairly large deviations between thermo-TDR estimates and gravimetric measurement of bulk density. By using an improved thermo-TDR sensor, X. Liu et al., (2008, 2014) found that bulk density results from thermo-TDR sensors had relative errors generally within 5% under laboratory conditions and within 10% under field conditions.

### 5.2.3. Evaporation/Transpiration

A sensible heat balance (SHB) concept was initially proposed by Gardner and Hanks (1966). Heitman, Horton, Sauer, et al. (2008); Heitman, Xiao, et al. (2008); and Heitman et al. (2017) developed the HP based SHB method (HP-SHB) for direct measurement of subsurface soil evaporation with HP-measured  $C_v$ ,  $\lambda$ , and temperature, while Kojima (2015) and Kojima et al. (2013, 2014, 2016) applied this method to determine soil freezing/thawing rate and ice content:

$$\Delta G - \frac{\Delta S}{\Delta t} = \begin{cases} L_e \rho_{water} E_{vap} & T > 0^\circ C \quad (a) \\ -L_f \rho_i \frac{\theta_{ice}}{\Delta t} \Delta z & T < 0^\circ C \quad (b) \end{cases} \quad (32)$$

where,

$$\Delta G = G_u - G_d = \left( -\lambda_u \frac{\Delta T_u}{\Delta Z} \right) - \left( -\lambda_{lower} \frac{\Delta T_d}{\Delta Z} \right), \quad (33)$$

$$\frac{\Delta S}{\Delta t} = \frac{C_u + C_d}{2} \frac{\Delta T_{avg}}{\Delta t} \Delta Z, \quad (34)$$

$$L_e = 2.49463 \times 10^9 - 2.247 \times 10^6 T_{avg}, \quad (35)$$

where  $G_u$  and  $G_d$  are soil sensible heat fluxes at upper and lower depths of a measured soil layer, respectively (W/m<sup>2</sup>),  $\Delta T_u$  and  $\Delta T_d$  are the temperature differences over  $\Delta Z$  at the upper and lower sensor needles (with the heater needle in the center), respectively.  $\Delta S/\Delta t$  is the change of sensible heat storage (W/m<sup>2</sup>) between the three needles over the time interval  $\Delta t$  (Heitman et al., 2007; Heitman, Horton, Ren, et al., 2008; Heitman, Horton, Sauer, et al., 2008; Heitman, Xiao, et al., 2008);  $L_e$  is the latent heat of evaporation (J/m<sup>3</sup>), which can be calculated according to equation (35) (Forsythe, 1964);  $T_{avg}$  is the average soil temperature (°C) over the three needles at a given time step;  $E_{vap}$  is the rate of evaporation (m/s); and  $L_f$  is the latent heat of fusion (J/kg). By placing HP sensors at various depths and applying the above calculation sequence to each sensor, the evaporation rates can be determined for subsurface soil layers at various depths.

The HP-SHB method has been applied to measure subsurface evaporation in the laboratory (Deol et al., 2012; Trautz et al., 2014), at bare soil sites (Deol et al., 2014; Heitman, Horton, Ren, et al., 2008; Heitman, Horton, Sauer, et al., 2008; Y. Wang et al., 2017; Xiao et al., 2011), and vegetated fields (Xiao et al., 2014). This method provides an alternative and complementing approach for long-term measurement of evaporation, especially in vegetated sites where root water uptake alters soil water distribution (Agam et al., 2012), and the existence of vegetation changes the micro-climate (e.g., decrease in temperature and increase in humidity; Holland et al., 2014) through wind speed reduction (Cammalleri et al., 2010; Heilman et al., 1994) and shading (Colaizzi et al., 2010; Ham & Kluitenberg, 1993; Horton, 1989; Horton et al., 1984; Pieri, 2010). Previous studies have used the HP-SHB method to determine the magnitude of evaporation, and the results of SHB agreed well with Bowen ratio and a water-balance based methods. Laboratory sand field studies, along with numerical simulations (Deol et al., 2012, 2014; Heitman, Horton, Ren, et al., 2008; Heitman, Horton, Sauer, et al., 2008; Sakai et al., 2011; Trautz et al., 2014; Xiao et al., 2011; X. Zhang et al., 2012) have shown that evaporation mostly took place in the 0–5 cm soil layer, and this leads to a deep understanding of the time/depth dynamics of soil water evaporation.

The other applications of HP method include the combination of HP-SHB-measured soil evaporation and HP-measured sap flow to estimate the rates of evapotranspiration (X. J. Wang et al., 2015). The HP-SHB is also capable to partition evapotranspiration into evaporation and transpiration in ecosystems. Note that soil water evaporation is often characterized by two distinct periods—an initially high and relatively constant rate termed Stage I evaporation, followed by a lower and gradually dropping evaporation rate (Stage II) reflecting a transition to diffusion-limited vapor transport. The HP-SHB method can only measure stage II subsurface evaporation rates. It is unfeasible to measure stage I evaporation rates when evaporation occurs at the soil surface. Therefore, the method is most suited to monitor evaporation rates over long drying periods (Kool et al., 2014). Numerical evaluation of the HP-SHB method showed that a smaller temperature sensor spacing near the surface minimized the underestimation of subsurface evaporation close to the soil surface and improved the accuracy of estimated total subsurface evaporation rate (Sakai et al., 2011).

#### 5.2.4. Soil Water Flux Density

For a homogeneous, isotropic, infinite medium with water moving at a uniform low velocity in a multiphase incompressible porous medium (e.g., saturated soil) along the  $x$  direction with uniform 3-dimensional heat flow, a low flow rate means that conductive heat transfer can dominate over convective effects, and equation (1) is simplified as (Ren et al., 2000)

$$\frac{\partial T}{\partial t} = \kappa \left( \frac{\partial^2 T}{\partial x^2} + \frac{\partial^2 T}{\partial y^2} + \frac{\partial^2 T}{\partial z^2} \right) - V_h \left( \frac{\partial T}{\partial z} \right), \quad (36)$$

where  $V_h$  is the HP velocity or the thermal front advection velocity (m/s), which is defined as (Kluitenberg et al., 2007; Marshall, 1958; Ren et al., 2000)

$$V_h = \theta_v v_z \frac{(\rho c)_l}{\rho c} = J \frac{C_l}{C_v}, \quad (37)$$

where  $J$  is soil water flux ( $\text{m}^3 \cdot \text{m}^{-2} \cdot \text{s}^{-1}$ ),  $\rho c$  and  $C_v$  are the volumetric heat capacity of soil ( $\text{J} \cdot \text{m}^{-3} \cdot ^\circ\text{C}^{-1}$ ), and  $(\rho c)_l$  or  $C_l$  are the volumetric heat capacity of water ( $\text{J} \cdot \text{m}^{-3} \cdot ^\circ\text{C}^{-1}$ ).

Equation (36) only applies to conduction dominated systems (Ren et al., 2000). This is true even when soil water flows at higher velocities (Quintard & Whitaker, 1995; Roshan et al., 2014). However, the applicability of equation (36) remains poorly understood when preferential water flow dominates.

Byrne et al. (1967, 1968), Byrne (1971), and Cary (1973) were the first to use heat as a tracer (point and line heat source) to measure water fluxes in saturated soils, but their methods relied on empirical calibration curves rather than the heat transport theory and may not be applicable in unsaturated soils (Kamai et al., 2008; Rau et al., 2014). Therefore, the HP method would be a better choice and it has been widely used for measurement of sap flow, 1 m/day or larger, in plant sciences (Burgess et al., 2001; Granier, 1987; Marshall, 1958). The development revolutionized sap flow measurements, but remained empirical. Ren et al. (2000) constructed a 3-needle thermo-TDR: the common plane of the three cylindrical, parallel, and equidistant needles is parallel to the water flow, the center needle is the heater; the other two are temperature sensors, one positioned upstream and one positioned downstream of the heater. Based on this design, Ren et al. (2000) developed an analytical solution of equation (36) for calculating the maximum dimensionless temperature difference (MDTD) between the downstream ( $T_d$ ) and upstream ( $T_u$ ) temperature sensors:

$$\Delta T(t) = \begin{cases} \frac{q'}{4\pi\lambda} [T_d(t) - T_u(t)], & 0 < t \leq t_0 \quad (\text{a}) \\ \frac{q'}{4\pi\lambda} [T_d(t) - T_u(t)], & t > t_0 \quad (\text{b}) \end{cases} \quad (38)$$

where,

$$T_d(t) - T_u(t) = \begin{cases} \int_0^t s^{-1} \left\{ \exp \left[ -\frac{(r_d - V_h \cdot s)^2}{4\kappa \cdot s} \right] - \exp \left[ -\frac{(r_u + V_h \cdot s)^2}{4\kappa \cdot s} \right] \right\} ds, & 0 < t \leq t_0 \quad (\text{a}) \\ \int_{t-t_0}^t s^{-1} \left\{ \exp \left[ -\frac{(r_d - V_h \cdot s)^2}{4\kappa \cdot s} \right] - \exp \left[ -\frac{(r_u + V_h \cdot s)^2}{4\kappa \cdot s} \right] \right\} ds, & t > t_0 \quad (\text{b}) \end{cases} \quad (39)$$

where  $s$  is defined as  $t - t'$  and  $0 < t' \leq t_0$ ;  $r_u$  and  $r_d$  are distances directly upstream and downstream from the heater. The integrals in equation (43) were further simplified by Kluitenberg and Warrick (2001).

The MDTD of upstream and downstream sensors is a function of  $\kappa$  and  $V_h$ , but is insensitive to variations in  $\kappa$ . Thus, HP-determined MDTD can be used to estimate  $V_h$ , which in turn can be used to compute  $J$  with equation (37). Therefore, equation (39) can be used to indirectly estimate the water flux from the MDTD between the downstream and upstream sensors of a 3-needle HP probe, given that the thermal properties of the soil were already known or can be determined separately with a zero-water flux condition. Moreover, the pore water velocity ( $J/\theta_v$ ) can also be obtained because the thermo-TDR can determine  $\theta_v$ .

With the inspirational work of Ren et al. (2000), Q. Wang et al. (2002) simplified the procedure by using the ratio of temperature increases at downstream ( $T_d$ ) and upstream ( $T_u$ ) positions instead of using  $T_d(t) - T_u(t)$  in equation (39),

$$\frac{T_d}{T_u} = \exp\left[\frac{V_h(r_u + r_d)}{2\kappa}\right], t \gg t_0. \quad (40)$$

Equation (40) approaches a constant value as  $t$  becomes larger than the heating period  $t_0$  (Ochsner et al., 2005). Soil water flux density can be calculated by substituting equation (40) into (37)

$$J = \frac{2\lambda}{C_w(r_d + r_u)} \ln\left(\frac{T_d}{T_u}\right). \quad (41)$$

This method results in an asymptotic solution, and it has been applied by Gao et al. (2006), Mori et al. (2003), and Ochsner et al. (2005). Ochsner et al. (2005) confirmed the existence of a time window following a HP application when the temperature ratio remained constant via HP measurements in steady water flow laboratory soil columns. Their measurements also confirmed that soil water flux was proportional to  $\ln(T_d/T_u)$ . However, equation (41) may not apply well for high water flux where thermal dispersion becomes significant (Hopmans et al., 2002). Mori et al. (2003) reported that actual soil water flux was underestimated by equation (41) based on HP measurements. Kluitenberg et al. (2007) attributed the errors to the approximation nature of the Q. Wang et al. (2002) method, and they proposed the following model for  $T_d/T_u$ :

$$\frac{T_d}{T_u} = \exp\left[\frac{(r_u + V_h t)^2}{4\kappa t} - \frac{(r_d - V_h t)^2}{4\kappa t}\right]. \quad (42)$$

Kluitenberg et al. (2007) stated that the use of  $t - t_0/2$  instead of  $t$  would improve the approximation of equation (42), in this case the instantaneous heat input takes place midway between  $t = 0$  and  $t = t_0$ . The water flux can then be calculated by substituting equation (42) into equation (37)

$$J = \frac{2\lambda}{C_w(r_d + r_u)} \ln\left(\frac{T_d}{T_u}\right) + \frac{C_v(r_d - r_u)}{2C_w[t - (t_0/2)]}, \quad t > t_0/2. \quad (43)$$

Compared to equation (41), equation (43) has an additional term that corrects the time dependence of  $T_d/T_u$  at intermediate times. The method of Kluitenberg et al. (2007) improves the accuracy in estimating water flux, but it still retains the simple algebraic form.

The solutions of Q. Wang et al. (2002) and Kluitenberg et al. (2007) are sensitive to variations in probe spacing (Kamai et al., 2008).

Most studies have included water flux density greater than 0.024 m/day (Mori et al., 2005; Ochsner et al., 2005), which do not represent all vadose zone applications, where water flux is usually below 0.01 m/d. Kamai et al. (2008, 2010) developed a new probe design (larger heater needle,  $r_o = 2$  mm, spacing between heater and temperature sensors  $\approx 4$  mm) based on the results of numerical sensitivity analysis. The upstream and downstream temperature rises are defined as

$$\Delta T(t) = \begin{cases} \frac{q'}{4\pi\lambda} \int_A^B \left\{ s^{-1} \exp\left[\frac{(r_u + v_h \cdot s - r_0)^2}{-4\kappa \cdot s}\right] \exp\left[\frac{r_0(r_u + v_h \cdot s)}{-2\kappa \cdot s}\right] I_0\left(\frac{r_0(r_u + v_h \cdot s)}{-2\kappa \cdot s}\right) \right\} ds, & (a) \\ \frac{q'}{4\pi\lambda} \int_A^B \left\{ s^{-1} \exp\left[\frac{(|r_d - v_h \cdot s| - r_0)^2}{-4\kappa \cdot s}\right] \exp\left[\frac{r_0|r_d - v_h \cdot s|}{-2\kappa \cdot s}\right] I_0\left(\frac{r_0|r_d - v_h \cdot s|}{-2\kappa \cdot s}\right) \right\} ds, & (b) \end{cases} \quad (44)$$

where  $I_0$  is the modified Bessel function of the first kind of order zero and the integration limits are

$$A = \begin{cases} 0, & 0 < t \leq t_0 \\ t - t_0, & t > t_0, \end{cases} \quad (a) \quad B = t \quad (b) \quad (45)$$

Kamai et al. (2008, 2010) report that their HP approach can be used to estimate water flux from 0.01 to 10 m/day.

The above approaches for estimating water flux use single point values of temperature. However, Mori et al. (2005) stated that the use of a single point maximum temperature change can lead to errors, so they used a parameter optimization approach (inverse modelling) presented by Hopmans et al. (2002) to obtain parameters with a series of upstream and downstream data to estimate fluxes:

$$OF_{II} = \sum_{i=1}^N [\Delta T_d^M(t_i) - T_d^O(t_i, P_{II})]^2 + \sum_{i=1}^N [\Delta T_u^M(t_i) - T_u^O(t_i, P_{II})]^2, \quad (46)$$

where  $P_{II}$  is the parameter vector containing the unknown  $V_h$ , which can be optimized by minimizing equation (46), and from which the  $J$  can be calculated using equation (37). Thermal diffusivity  $\kappa$  can be estimated simultaneously with the  $J$  if  $C_v$  and  $\theta_v$  are known. The inverse modelling method can be applied to coupled water and heat flow studies to estimate several parameters (e.g., thermal properties, water content, and water fluxes) simultaneously without limitations to the number and type of measurements (Hopmans et al., 2002). The parameter optimization approach has been used by a few investigators (e.g., Kamai et al., 2008; Mortensen et al., 2006). Yang and Jones (2009) developed the INV-WATFLX program (in FORTRAN) based on the inverse method for simultaneous estimation of thermal diffusivity, thermal conductivity, and heat velocity/water flux.

HP methods for measuring water fluxes work well on sandy soils (Ochsner et al., 2005; Ren et al., 2000), but water flux may be underestimated in fine-textured soils (Mori et al., 2003, 2005). The discrepancy may be attributed to a multitude of factors such as errors associated with the simplified solution (Ochsner et al., 2005), the exclusion of thermal dispersion (Hopmans et al., 2002; Ochsner et al., 2005), and effects of physical size of the heater (Hopmans et al., 2002). However, Gao et al. (2006) found that the discrepancy between water flux estimated from HP method and from outflow may result from wall flow, and the magnitude of wall flow was largely determined by soil texture. The errors of water flux estimated by the Q. Wang et al. (2002) approach were reduced to 5% by using amplification factors (1.12 for the sandy loam and 1.24 for the sandy clay loam; Gao et al., 2006).

For coupled water flow and heat conduction, the issue of heat dispersion caused by different flow velocities in different channels has been raised by Hopmans et al. (2002), but remains poorly understood. A systematic overestimation of MDTD by 10% may arise when fluxes is greater than 2.4 m/day (Hopmans et al., 2002; Ren et al., 2000). The error may be attributed to the thermal dispersity and the physical size of the heater cylinder (Hopmans et al., 2002; X. Lu et al., 2009; Ochsner et al., 2005). Taking thermal dispersion into the heat conduction-convection model, water flux estimates can be determined accurately at the range of 1 to 10 m/day (Hopmans et al., 2002). However, Mori et al. (2005) showed that the effects of thermal dispersion are insignificant, and the simulated thermal diffusivity was almost independent of water flux. Rigorous experimental verification of the dispersion effect and establishment of the threshold for it to occur are critically needed for measuring and modelling of coupled water and heat transfer in soil.

### 5.2.5. Soil Heat Flux Density

Soil heat flux is a critical component of the surface energy balance along with net radiation, sensible, and latent heat flux. The traditionally used combination method includes a heat flux plates (Fuchs & Tanner,

1968) which can perturb water/vapor and heat flow in soil. Besides, there is contact resistance between the plate and the soil, and differences in soil and plate thermal conductivity, which together likely cause relatively large measurement errors (Ochsner et al., 2006; Peng et al., 2015; Sauer et al., 2007). Cobos and Baker (2003) and Peng et al. (2017) demonstrated that 3-needle or multineedle HP probes (i.e., heater and temperature sensors positioned in a vertical plane perpendicular to the soil surface) could be used to accurately measure soil heat flux ( $G$ ,  $J \cdot m^{-2} \cdot s^{-1}$  or  $W/m^2$ )

### 5.3. Physical Measurements of Frozen Soils

#### 5.3.1. Frozen Soil Thermal Properties

The HP method has been widely applied in unfrozen soils for water and heat flux measurements as discussed above. Implementation of the HP method in partially frozen and freezing soils, however, has been primarily confounded by the fact that soil ice melts and refreezes due to the application of heat (Kojima, 2015; Kojima et al., 2013, 2014, 2016, 2018; Ochsner & Baker, 2008; Putkonen, 2003; Tian et al., 2015, 2017; Y. Zhang et al., 2011). Melting and refreezing of ice results in a significant amount of the HP energy being directed to phase changes rather than to conduction heat transfer (Putkonen, 2003). Ice melting increases the HP-predicted volumetric heat capacity and decreases the soil thermal diffusivity because the general assumptions of the HP method derived under unfrozen conditions (i.e., no phase change and temperature-invariant thermal properties) do not apply to partially frozen soils. In addition,  $C_v$  and  $\kappa$  show a distinct dependence on the ambient soil temperature in partially frozen soils compared to that in unfrozen soils (Ochsner & Baker, 2008). For example, the HP melts less ice when the soil ambient temperature is very small (e.g., below  $-20$  to  $-2$  °C depending on soil types and heating strategies) and the HP-measured thermal properties approach the real thermal properties (G. Liu & Si, 2011b; Putkonen, 2003; Y. Zhang et al., 2011).

The propagation of heat from the heater to the temperature sensors is described by the heat conduction equation that includes phase change in partially frozen soils, in the radial coordinate system (Ochsner & Baker, 2008; Overduin et al., 2006; Y. Zhang et al., 2011)

$$C_v \frac{\partial T}{\partial t} = \frac{1}{r} \frac{\partial}{\partial r} \left( r \lambda \frac{\partial T}{\partial r} \right) + L_f \rho_I \frac{\partial \theta_I}{\partial t}. \quad (47)$$

There is no analytical solution to equation (47) for realistic soil conditions, and application of the HP method in partially frozen soils is confounded by melting and refreezing of ice induced by the HP. Three approaches can be found in the literature for application of the HP method to partially frozen soil studies:

1. By simply applying the analytical solution used in unfrozen soil by assuming that no phase change occurs (no ice melt results from the HP method; Goodrich, 1986; Overduin et al., 2006; Sun et al., 2016; Tokumoto et al., 2010; B. Zhang et al., 2015).
2. By limiting the ice melting through optimized heat application as investigated by G. Liu and Si (2011b), Y. Zhang et al. (2011), and Tian et al. (2015). However, HP-induced ice melting could only be controlled at temperatures below  $-2$  °C (e.g.,  $<-2$  to  $-20$  °C), and ice melting was large at high subzero temperatures, especially around 0 °C.
3. By accounting for the influence of the ice melting on measured thermal properties. Ochsner and Baker (2008) incorporated the ice melting effects into apparent thermal properties which could be used to estimate lumped conduction and latent heat terms. When both the change of  $\lambda$  with temperature and the HP-induced temperature change are small,  $\lambda$  can be taken out of the partial derivatives in equation (47) and then it may be simplified as (Ochsner & Baker, 2008; Overduin et al., 2006)

$$C_a \frac{\partial T}{\partial t} = \lambda_a \left( \frac{\partial^2 T}{\partial r^2} + \frac{1}{r} \frac{\partial T}{\partial r} \right). \quad (48)$$

Equation (48) effectively lumps convection and latent heat terms into an apparent thermal conductivity ( $\lambda_a$ ) parameter and an apparent volumetric heat capacity parameter ( $C_a$ ). The apparent volumetric heat capacity can be expressed as

$$C_a = C_v + L_f \rho_I \frac{\partial \theta_I}{\partial T}. \quad (49)$$

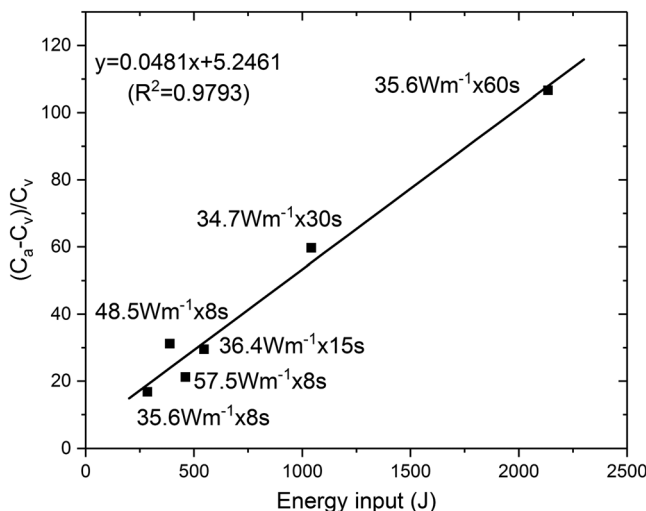


**Figure 16.** Relationship between time domain reflectometry- $C_v$ , heat pulse- $C_a$ , and energy input (after He et al., 2015).

The apparent heat capacity can be explained as the amount of energy required to raise the temperature of a unit volume of partially frozen soil by one degree even while phase change between liquid water and ice occurs due to the HP-induced temperature change (Anderson et al., 1973; Kozlowski, 2012; Ochsner & Baker, 2008; Pusch et al., 1978).  $L_f$  is latent heat of fusion,  $3.34 \times 10^5$  J/kg.

The method of Ochsner and Baker (2008) did not quantify the ice melting or attempt to retrieve the real thermal properties. He et al. (2015) evaluated the TDR method to quantify ice melting and extend the possibility to obtain accurate thermal properties of frozen soil. They combined the approach of Ochsner and Baker (2008) and the composite dielectric mixing models for unfrozen liquid water and ice content (He et al., 2016; He & Dyck, 2013). The TDR-measured liquid water and ice content could be used to calculate  $C_v$  prior to the application of HP according to equation (27). Comparison of the calculated  $C_v$  and the HP-estimated  $C_a$  which is affected by ice melting can be used to estimate the amount of ice melt (He et al., 2015, Figure 16).

He et al. (2015) tested this approach on a sandy soil and found that 0.5% and 2% ice melting had significant impacts on the HP-estimated soil thermal properties, further confirming that the HP method without further corrections was inappropriate for frozen soil thermal property measurements when temperatures were between  $-5$  and  $0$  °C (G. Liu & Si, 2011b; Putkonen, 2003; Y. Zhang et al., 2011). The TDR and HP-estimated heat capacity are hysteretic as are the soil freezing characteristics and soil freezing and thawing curves.

### 5.3.2. Unfrozen Water/Ice Content and Soil Freezing Characteristics

Partitioning liquid and ice water contents in partially frozen soil is a frontier cutting across soil science, hydrology, and engineering. The application of the HP method in recent years advanced the frontier. Two approaches complementing each other have been proposed. The first approach partitions ice and liquid water through their drastically different heat capacities. Y. Zhang et al. (2011) evaluated the HP method for detecting unfrozen water content of sands at various total water contents and temperatures using different heating strategies (ranging from 8 to 60 s and 100 to 2,000 J/m) in combination with one-dimensional finite difference numerical simulations that account for phase change. They suggested that the HP method is applicable for estimating unfrozen water content ( $\pm 0.05$  m<sup>3</sup>/m<sup>3</sup>) when ambient temperatures is below  $-4$  °C and only limited ice melting occurs. G. Liu and Si (2011b) used small heat strength with long heat duration (25 W/m, 60 s) to reduce HP-induced ice melting in sands. In combination with a finite element model, they reported that ice content could only be estimated accurately at temperatures less than about  $-20$  °C.

The second approach is based on the SHB (equation (32)b, Figure 17), as pioneered by Kojima (2015) and Kojima et al. (2013, 2014, 2016) for direct measurement of transient soil ice contents due to freezing and thawing in both laboratory and field studies. The results showed that the SHB method was able to determine dynamic changes in ice contents during initial soil freezing and during thawing for soil temperatures between  $-5$  and  $0$  °C when latent heat values associated with phase change (forming or melting of ice) were relatively large.

Because latent heat fluxes were small and below the sensitivity of the SHB method at soil temperature below  $-5$  °C, this method could not accurately estimate ice content. Instead, soil ice contents during extended freezing periods at temperatures below  $-5$  °C could be estimated from changes in volumetric heat capacity determined with HP probe. Thus, HP measurements used for SHB calculations at temperatures between  $-5$  and  $0$  °C combined with HP probe determined volumetric heat capacity at temperatures below  $-5$  °C covers the range of temperatures at which soil freezes.

The determination of soil freezing characteristics and soil thermal properties is essential for describing and modeling soil thermal and physical processes in partially frozen soils. The SHB method can be used for the determination of soil thermal properties as a function of soil temperature, but it is tedious. As shown by Anderson and Tice (1972), Anderson et al. (1973), and Tokumoto et al. (2010), soil freezing characteristics can be expressed as an algebraic function of soil temperature with two or three soil-specific parameters.

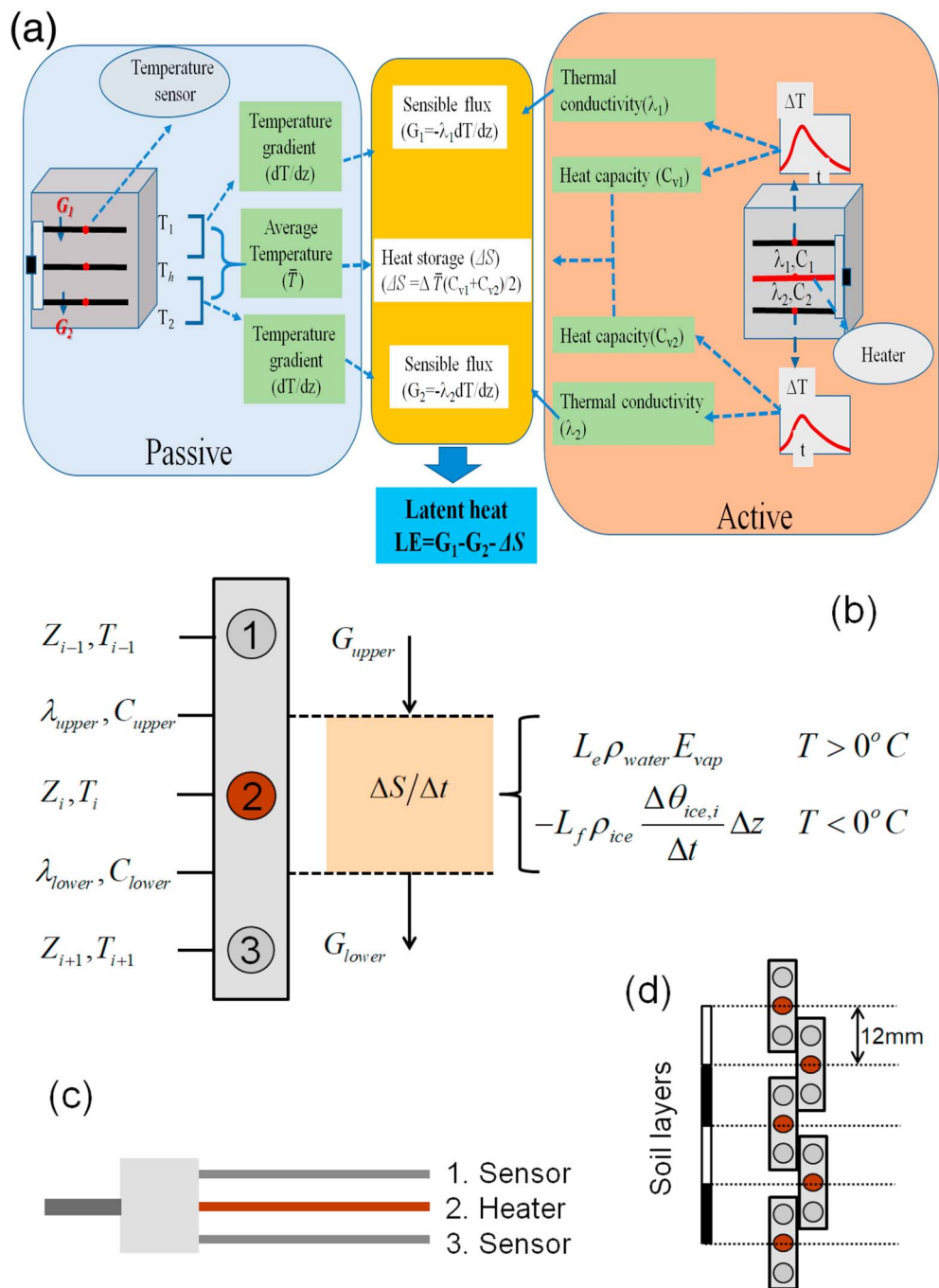


**Figure 17.** Diagram for using combined passive and active needles to determine latent heat fluxes due to evaporation, freezing, and thawing (a), and the sensible heat balance method to determine latent heat associated with evaporation/condensation or soil freezing/thawing (b) using measurements of three-needle heat-pulse sensor with 6 mm needle-to-needle spacing (c), and an example of the basic probe installation for laboratory or field application (d). For the sensible heat balance method, thermal conductivity ( $\lambda$ ) and heat capacity ( $C$ ) are averaged from heat-pulse response curve calculations at needles 1 and 3. Other symbols denote temperature ( $T$ ) at three depths (subscripts 1, 2, 3), heat flux at the upper ( $G_{upper}$ ) and lower ( $G_{lower}$ ) depth of the measured soil layer, change in soil heat storage ( $\Delta S/\Delta t$ ) and latent heat (after Heitman, Horton, Sauer, et al., 2008, and Kojima et al., 2016).

This parametric approach can greatly reduce the number of unknowns. Only a few HP experiments performed at different soil temperatures may be sufficient for obtaining the needed parameters through inverse numerical solution of equation (47). Combining parametric representation of soil thermal

**Table 3**

Comparison Between DTS and SPHP or DPHP Method (after He et al., 2018)

	DTS	SPHP/DPHP
T measurement Frequency	Minutes	$\leq 1$ s
Measurements	Thermal conductivity, water content	Thermal conductivity, water content
Probe length	1 m to $>10$ km	0.1–0.6 m for SPHP, 0.04–0.06 m for DPHP
Probe diameter (mm)	3–5	0.5–2
Hardness	Soft	Rigid
Heater material	Metallic component (e.g., stainless steel) and carbon fiber	Resistance heating wire
Nominal voltage	40/60 12 VDC or 108/120/240VAC	12 V
Heating duration	1–10 min	1–10 min for SPHP, 8–15 s for DPHP
Energy	10–100 W	0.4–2 W/m for SPHP, 2–700 W/m for DPHP
Protective sheath/outer jacket	multiple layer	Stainless steel
Temperature sensor	Optical fiber (temperature sensing at 0.1–1 m spacing)	1 thermistor/thermocouple at the midlength
Temperature resolution ( $^{\circ}$ C)	0.01	0.01
Availability/ease of access	Commercially available	Commercially available or customized
Cost	as low as U. S. \$1 per meter	>U. S. \$200 each
Durability/life span	design life of 30 year+	Various
Long-term stability	Temperature drift	Suffer from temperature drift
Additional major equipment	DTS unit, computer	Datalogger, computer

Note. The values presented in the table only represent the most frequently occurring values in the literature, not all scenarios are included. DTS = distributed temperature sensing; DPHP = dual-probe heat-pulse; SPHP = single-probe heat-pulse.

properties at different soil temperatures with the inverse procedures may require only a few HP experiments, and thus be less time consuming than the SHB method, which consequently may be worthy of further investigation in partially frozen soils. Kojima et al. (2018) provide guidance on a possible path forward on how to use HP measurements to determine soil thermal properties of partially frozen soils. Further work is needed to determine the effectiveness of the suggested approach.

### 5.3.3. Water Flow and Heat Flux in Frozen Soils

In unfrozen soil, heat conduction is the dominant heat transfer mechanism and latent heat is usually important in the 0 to 5 cm layer where evaporation occurs. Ochsner and Baker (2008) took advantage of uniqueness of the HP method in detecting both latent and sensible heat transfer to measure the soil heat flux during freezing and thawing periods. The results showed that the measured heat flux was remarkably greater than the estimated values based on conduction only, and the peak of measured latent heat flux occurred at the spring snowmelt infiltration period. Using thermo-TDR sensors and thermally insulated tensiometers, Tokumoto et al. (2010) also found that water flow toward a frozen zone from the underlying unfrozen layers, and the transition layer between the unfrozen and frozen soil layers decreased sensible heat flux because of latent heat associated with phase change from unfrozen water to ice. These innovative applications of the HP method in determining heat fluxes in partially frozen soil could provide critically needed parameters in constraining the uncertainties in earth system models.

### 5.4. New Applications With Fiber Optics Based DTS

In the last few years, the AHFO-DTS system has been used for *in situ* or laboratory measurements of soil thermal properties and water content  $\theta_v$  (Benítez-Buelga et al., 2016; Ciocca et al., 2012; Sayde et al., 2010; Striegl & Loheide, 2012). A DTS system consisting of a fiber-optic cable (up to 10s of kilometers) and readout equipment like a series of temperature sensors along the fiber-optic cable. The difference is that each temperature measurement from a DTS has a spatial resolution of 10–200 cm, which is much longer than that of DPHP and SPHP sensors (4 cm long for DPHP and about 10 cm for SPHP). Through active heating of an insulated electrical wire or the electrically conductive armor surrounding the fiber-optic cable, the AHFO-DTS can serve as a series of SPHPs. Therefore, AHFO-DTS has the potential to extend thermal property and  $\theta_v$  measurements from a point scale to an intermediate scale. Table 3 and Figure 18 show the comparison among DPHP, SPHP, and AHFO-DTS.

Like SPHPs, the AHFO-DTS can be used to determine soil thermal conductivity. However, determination of other thermal properties and  $\theta_v$  using AHFO-DTS can be more challenging than with a SPHP sensor. As stated above, good contact and low thermal resistance between the probe and soil are essential for accurate measurements from a SPHP. Unfortunately, due to the construction of DTS cables, the contact and thermal resistance between the armored fiber-optic cable and surrounding soil can be worse than that for SPHP. The

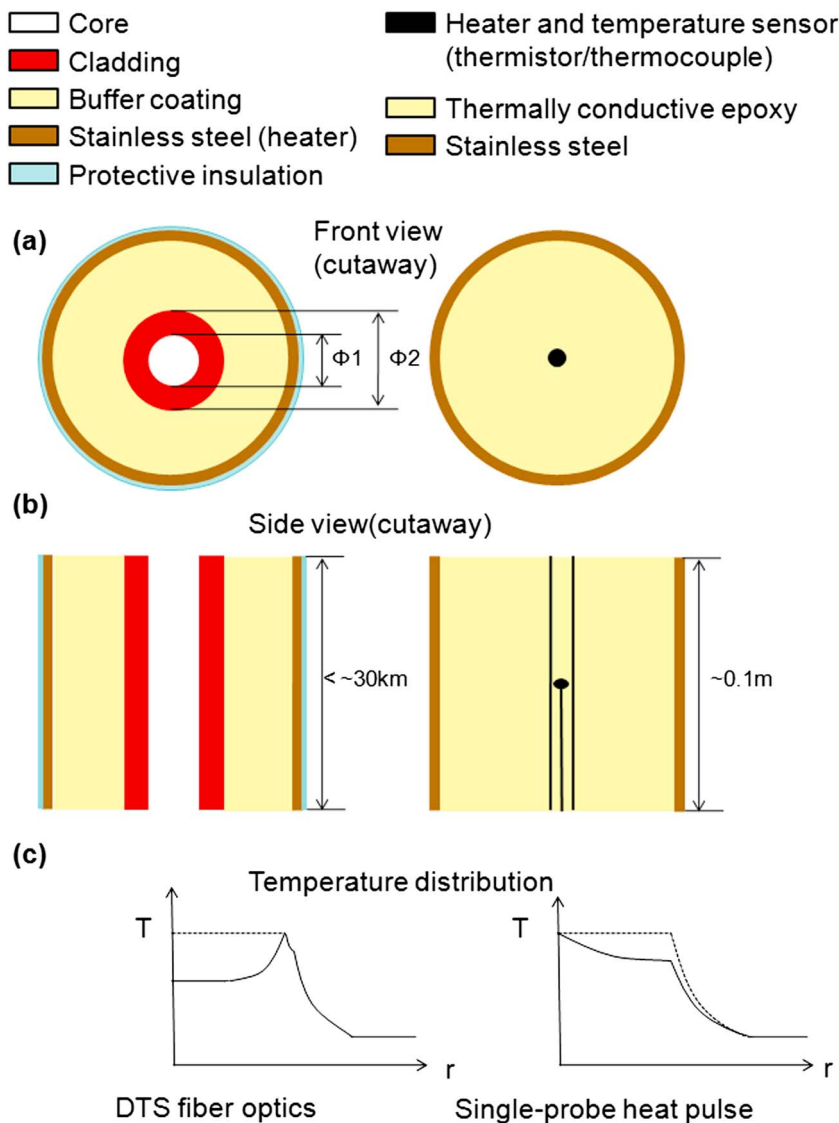


**Figure 18.** Schematics and comparison of fiber optics (left) and single-probe heat pulse (right) system (not to scale). For DTS fiber optics,  $\Phi 1$  and  $\Phi 2$  are the outer diameters of core and cladding, respectively, marked as  $\Phi 1/\Phi 2$ . The common  $\Phi 1/\Phi 2$  size for fiber optics are 62.5/125  $\mu\text{m}$  (multimode), 50/125  $\mu\text{m}$  (multimode), and 8–10/125  $\mu\text{m}$  (single mode). (a) Fiber optic, (b) distributed temperature sensing system, (c) heat pulse probe, and (d) heat pulse connecting system (after He et al., 2018). DTS = distributed temperature sensing.

DHPH approach has also been applied to an AHFO-DTS system (Benítez-Buelga et al., 2014). However, as stated above, the DPHP is very sensitive to the spacing ( $r$ ) between the heat and sensor probes, and keeping two long cables (1 m to 10 km) parallel at an exact fixed distance can be problematic for the AHFO-DTS. Therefore, the AHFO-DTS is currently limited to the measurements of space insensitive  $\lambda$ . In order to use the well-developed theories of HP methods, innovation in fiber-optic cable construction to mimic an infinite line source and good conductor is needed. Therefore, recent applications of DTS to measure soil heat capacity and water contents have focused on the development of methods.

There have been three approaches to infer soil water content from AHFO-DTS measurements: (1)  $\theta_v$  was inferred from the  $\lambda-\theta_v$  relation (Ciocca et al., 2012); (2) from the maximum temperature increase ( $\Delta T_m$ )- $\theta_v$  relation (Striegl & Loehde, 2012); or (3) from the cumulative temperature increase ( $T_{cum}$ ; Sayde et al., 2010). However, the  $\theta_v$  estimation errors were relatively high (more than 0.05  $\text{m}^3/\text{m}^3$ ) at high water contents for all three methods. Error analysis showed that  $\theta_v$  measurements from the  $\Delta T_{cum}$  ( $\theta_v$ ) method were more precise than those from the  $\Delta T_m$  ( $\theta_v$ ) method. The  $\Delta T_{cum}$  ( $\theta_v$ ) method was further applied in the field (Sayde et al.,

2014) and used to measure the wetting patterns of a drip irrigation emitter in a soil column study (Gil-Rodríguez et al., 2013). However, because of their strong dependence on soil bulk density and soil texture, all three methods (i.e.,  $\lambda(\theta_v)$ ,  $\Delta T_m(\theta_v)$ , and  $\Delta T_{cum}(\theta_v)$  method) require site specific calibration to determine thermal diffusivity, heat capacity, and soil water content. Improvements in the methods are needed before wide application of the AHFO-DTS will occur.

Field installation of fiber-optic cables may significantly disturb soil structure, affect the macropore structure, change water movement pathways, and have imperfect contact between soil and the cable. A proper cable installation protocol is required to minimize soil disturbance. The other problems associated with field applications are power supply and the uncertainty in the installation depth. Surface application of fiber optics could result in higher than actual measurements due to heat adsorption by the fiber-optic cables. Thermal instability may become apparent for long-term application of AHFO-DTS. In addition, there are trade-offs between precision in temperature, temporal resolution, and spatial resolution. For example, short measurements are less precise than measurements taken over longer spans in time and space (Selker et al., 2006).

For more information about the principles, limitations, opportunities, and applications of DTS in hydrological and soil physical studies see Weiss (2003), Selker et al. (2006), Tyler et al. (2009), and He et al. (2018).

### 5.5. Thermal Conductivity Models

Although development have occurred for the HP and DTS methods, larger scale applications of these methods are still time consuming, labor intensive, and expensive. Soil thermal conductivity models, on the other hand, can be used for uninstrumented sites and some of them can be incorporated into numerical heat transfer algorithms for wide applications (Becker et al., 1992). For instance, the Kersten (1949) model, Johansen (1975) model, Farouki (1981) model, G. S. Campbell (1985) model, and the Chung and Horton (1987) model have been widely used and have been incorporated into several numerical simulation model, such as the Soil-Vegetation-Atmosphere Transfer Schemes, CLM, and HYDRUS (Simunek et al., 1997). The reader is referred to Progelhof et al. (1976), Khader et al. (1980), Farouki (1981), Tavman (1996), Dong et al. (2015), and He et al. (2017) for more details on the current availability of soil thermal conductivity models in literature, the evolution history of empirical/semiempirical/physical models, their incorporation status in numerical simulation programs, and the evaluation of model performance.

Some thermal conductivity models are based on data obtained by steady-state methods (e.g., G. S. Campbell, 1985; de Vries, 1963; Johansen, 1975; McCumber & Pielke, 1981), which suffer from inaccuracy resulting from errors of water redistribution in the form of water or vapor flow and phase change from water to vapor or ice to water. Poor estimations of soil thermal conductivity are bound to cause large biases in surface energy balance studies and in predicting soil temperature (Peters-Lidard et al., 1998). Therefore, the right choices of soil thermal conductivity models are key for accurate numerical simulations. To better model or predict the soil thermal regime and thermal conductivity, it is necessary to reevaluate the performance of or calibrate currently available models or develop new formula/models that can be easily used experimentally or incorporated into numerical simulation models (e.g., S. Lu et al., 2007; Y. Lu et al., 2014) based on HP data. To achieve these objectives, the HP data should be used because the HP method has long been recognized as accurate measurements of soil thermal conductivity compared to steady-state methods, especially for unsaturated soils and frozen soils. Unfortunately, only a few data sets measured with HP method are available in literature and more measurements on soils of various textures, structures, water contents, bulk densities, and organic matter contents should be performed (S. Lu et al., 2007; Ochsner et al., 2001a). Data sets on frozen soils are especially encouraged.

## 6. Limitations and Perspectives of the HP Method

In this section, we start with a list of attributes desirable for thermal property estimation methods and discuss the HP method performance with respect to these desirable attributes:

1. **Improved accuracy in soil thermal property determinations are needed** for accurate inference of other soil properties such as soil water content and bulk density. For example, an error of 10% in the heat capacity may result in  $>0.01 \text{ cm}^3/\text{cm}^3$  error in soil water content estimates and many factors could make the measurement error in heat capacity greater than 10%. Further, most hydrometeorological models generally use empirical/semiempirical/physical models to estimate soil thermal properties (e.g., G. S.

Campbell, 1985; Chung & Horton, 1987; de Vries, 1963; Farouki, 1981; Johansen, 1975; McCumber & Pielke, 1981). These soil thermal conductivity models vary in complexity and their applicability is limited only to certain soil types under specific conditions and may introduce biases in numerical simulation studies (Becker et al., 1992), and the output results (e.g., surface energy balance and soil temperature regimes) of numerical studies are largely dependent on the choice of these soil thermal conductivity models (Kahan et al., 2006; Y. Lu et al., 2014; Peters-Lidard et al., 1998; Zheng et al., 2015). This highlights the importance of a fundamental understanding of the various factors influencing soil thermal properties and the need for accurate measurements.

2. **Portable measurement devices are needed.** The energy and water balances in the top few centimeters of soil are critical for accurate estimation of soil temperature and evaporation (Or et al., 2013). This requires accurate measurements of thermal conductivity and heat storage (heat capacity) in fine spatial resolution. Thus, it is desirable to have instrumentations of small dimensions and low energy consumption that are portable for measurement of thermal properties at remote locations on Earth and other extraterrestrial bodies (e.g., Moon and Mars).
3. **The thermal properties need to be determined in situ.** Soil thermal properties depend on several factors such as soil texture, bulk density, particle geometry, temperature, and the contents and ratios of the water phase (i.e., ice, liquid water, and vapor; Baker & Goodrich, 1984; Carter, 1993; Ewing & Horton, 2007; Y. Lu et al., 2014; Shiozawa & Campbell, 1990; Wechsler, 1966). Disturbance to soil will likely lead to error-prone measurements, which calls for nondestructive methods.
4. **Rapid data acquisition is desirable.** Thermal properties of soils are strongly affected by rapidly varying soil water content and temperature from minute to day scales, especially those during rapid freezing and thawing (Ochsner & Baker, 2008; Tokumoto et al., 2010). Therefore, rapid measurement is a prerequisite for accurate determination of soil thermal properties for estimating soil temperature and other hydrological processes.
5. **Soil thermal property determination methods need to be adaptable.** First, the accurate partitioning of sensible and latent heat requires determination of soil thermal properties as well as soil water content, matric potential, and osmotic potential in saline soils. Therefore, simultaneous determination of thermal properties and one or more of these hydrological variables in the same soil volume is desirable. This requires that instrumentation for thermal property measurements be easily combined with instrumentation used to measure other soil properties such as TDR used to measure soil water content and EC (Ren et al., 1999; Topp et al., 1980), suction lysimeter (Si et al., 1999), or matric potential sensors (Noborio et al., 1999; Or & Wraith, 1999). Second, because subsurface thermal properties with depth are also important for many geotechnical applications, thermal property profiling is desirable.
6. **There is a potential need/application for scaling up thermal property determinations.** The depth scale of thermal property measurements varies from millimeters to hundreds of millimeters. However, the horizontal scale of applications varies from a few millimeters (such as soil skin temperature in the vertical direction) to 10s of kilometers (a pixel of remote sensing of soil water and temperature by satellites). Therefore, extrapolation of the thermal property measurements to a great depth to a larger domain is needed. To this end, greater progress is desired for coupling the HP method with a fiber-optic cable buried in boreholes or in horizontal trenches.

We will discuss the limitations and perspectives of HP method section based on the abovementioned desirable attributes and accuracy and sources of error.

### 6.1. Accuracy and Sources of Error

The accuracy of HP probes has been reported at  $\pm 10\%$  for  $\lambda > 0.1 \text{ W}\cdot\text{m}^{-1}\cdot\text{C}^{-1}$  (Presley & Christensen, 1997; Wechsler, 1966), but accuracy may be reduced when  $\lambda < 0.1 \text{ W}\cdot\text{m}^{-1}\cdot\text{C}^{-1}$  (Nicolas et al., 1993). Some researchers reported satisfactory  $\lambda$  values (Horai, 1981; Woodside, 1958), but others found lower values than with a steady-state method under low atmospheric pressure or under vacuum (Wechsler & Glaser, 1965). Measurements taken under vacuum or low pressure are beyond the scope of this paper and are not discussed further.

Sources of error associated with the HP method and potential for reducing these errors include (1) finite dimensions of the probe such that there is uncertainty in the DPHP probe spacing and violations to the assumption of a perfect line heat source of infinite LD ratio for both the DPHP and SPHP methods. Errors

resulting from line heat source violations can be minimized (<1%) by using a LD ratio  $\geq 25$  (Blackwell, 1954, 1956); (2) finite thermal properties of the probe and contact resistance between the probe and the surrounding sample due to the imperfect contact between them, different conductivities, and the potential of air entrapment during probe insertion (Sepaskhah & Boersma, 1979); (3) inappropriate selections of the heating wire material and total resistance, varying power output due to resistance of the heater wire changing with temperature can be reduced by using heater wire with a low temperature coefficient of resistance; (4) sample of infinite extent, which may be practically accommodated by limiting the time interval/energy input to complete the measurements before the input heat reaches any external boundary of the sample, and the finite sample does not violate the infinite size assumption for the finite time of measurement; and (5) thermal instability due to soil heterogeneity and nonisothermal boundary conditions near the soil surface that may significantly affect the accuracy of estimated thermal properties.

## 6.2. Probe Dimension/Geometry/Deflection

Thermal properties obtained using the DPHP are sensitive to probe spacing ( $r$ ) between the heater and sensor needles, and it is necessary to calibrate  $r$  using materials with known heat capacity. G. S. Campbell et al. (1991) verified the performance of the HP probe using agar-immobilized water (e.g., 2 g/L). The small amount of agar was assumed to have a negligible effect on  $C_v$  of water ( $4.18 \times 10^6 \text{ J} \cdot \text{m}^{-3} \cdot \text{C}^{-1}$ ), but it was enough to prevent natural convection in the water. This method of probe spacing calibration has been widely used; most researchers use 3 to 6 g/L agar concentrations (G. Liu et al., 2008; X. Liu et al., 2008; Ochsner et al., 2001a, 2001b; Ren et al., 1999). Probe spacing can be calculated either by SPM or NMF methods.

Probe spacing should yield the same value if a sensor is calibrated with different media of different  $C_v$ ; however, studies show that  $r$  increases as media  $C_v$  decreases at lower water contents. This can lead to overestimations of  $C_v$  and soil water content as soil dries (Basinger et al., 2003; Ham & Benson, 2004; Song et al., 1998; Tarara & Ham, 1997). The problem may be from model errors (i.e., solution to the heat conduction equation of  $C_v$ ), instrumentation errors (e.g., inaccurate measurement of  $q$ ,  $\Delta T_m$ , and  $t_m$ ), the reduced heat capacity of bound water, the heat capacity differences between dry soils and the probe (dry soils usually have smaller  $C_v$  than that of the probe materials), and increased probe-soil contact resistance (will be discussed in section 6.3).

Needle deflection may occur upon insertion of a DPHP probes into a soil, or from ice formation during soil freezing, and from frost heave (i.e., distance between the heater and temperature needles), and thus, changing the value of  $r$ . This is an impediment for field application of HP methods. Studies have been carried out to investigate the influence of errors in  $r$  on measured unfrozen soil thermal properties (Bristow, Kluitenberg, et al., 1994; Kluitenberg et al., 1993, 1995, 2010; G. Liu & Si, 2010; G. Liu et al., 2013, 2016; Wechsler, 1966; Wen et al., 2015). Wechsler (1966) found that probe construction had little effect in dry soils, with an accuracy of  $\pm 8\%$ . G. S. Campbell et al. (1991) found that  $C_v$  was most sensitive to errors in  $r$ , as was the water content deduced from  $C_v$  (Bristow et al., 1993; Noborio et al., 1996b). This agrees well with Kluitenberg et al. (1993, 1995, 2010) who showed that  $\kappa$  and  $C_v$  were sensitive to errors in  $r$ , but  $\lambda$  was unaffected by errors in  $r$ . This is because  $\lambda$  calculated from equation (18) is actually independent of  $r$  (no  $r$  appears in the equation), which indicates that the effect of  $r$  is entirely reflected in the magnitudes of  $t_m$  and  $\Delta T_m$ , whose changes with  $r$  compensate for each other and  $\lambda$  remains constant (Noborio et al., 1996b). This has also been experimentally proven by Kluitenberg et al. (2010) who found that inward or outward deflections of a DPHP probes ( $\sim \pm 15\%$  spacing change) resulted in small changes in  $\lambda$  ( $\leq 0.04 \text{ W} \cdot \text{m}^{-1} \cdot \text{C}^{-1}$ ).

G. Liu et al. (2008) derived a 3-D analytical solution to account for influences of inclined heater or sensor needles, and their model yielded good results for deflections between  $-6$  and  $+6^\circ$ . G. Liu et al. (2013, 2016) and Wen et al. (2015) designed a DPHP probe with two or three thermistors in each temperature sensing needle that made it possible to reduce errors associated with probe deflections in DPHP-estimated  $C_v$ . Other approaches, for instance, shorter probes or larger probe diameter (Ham & Benson, 2004; Kamai, 2013; Kamai et al., 2010, 2015, 2008; Mori et al., 2003) and sensors with different geometries (partial cylindrical thermo-TDR: Olmanson & Ochsner, 2008; button-shaped HP probe: Kamai et al., 2009), were also introduced to minimize the deflection effects. For example, Yang et al. (2013) and Kamai et al. (2015) used shorter needles for the temperature sensors (about half the length of the heater needle; Figures 5, 6). Kamai et al. (2015) used thick-walled stainless steel tubes (e.g., 0.97 mm I.D. and 2.38 mm O.D. compared to  $\sim 0.6$  mm I.D. and

~1 mm O.D. for conventional probes) to construct rigid DPHP probes that were more resistant to deflection compared to conventional probes. Their results showed that the rigid DPHP probe in combination with the ICPC model (semianalytical solution) developed by J. H. Knight et al. (2012, 2016) that accounted for effects of probe heat capacity and dimension could improve the accuracy of soil water estimation.

Bristow, Kluitenberg, et al. (1994) found that keeping probe spacing relatively small enabled well-defined  $\Delta T(t)$  data sets and made it relatively easy to identify  $\Delta T_m$  and  $t_m$  values, but if probe spacing was too small, it was difficult to calibrate the probe spacing. Small probe spacing also leads to small sample volumes, which may not well represent the representative elementary volume of the soil. Using a multineedle probe provides multiple estimates of the thermal properties by analyzing the  $\Delta T(t)$  data from each thermistor separately. Sometimes an average of each estimate is used in the case of local heterogeneity. However, the use of multineedle probes may cause changes in the local soil bulk density. Moreover, more needles may introduce additional distortion in the heat field due to the presence of highly thermally conductive materials (stainless steel) and heat storages and the prevalent data analysis model and theory does not account for the finite size and properties of the needles. There are applications, however, where a small sampling volume is desirable. For example, DPHP probes can be used to measure soil physical properties of fine spatial resolution, like water content changes close to soil surface (e.g., ~2 cm) or near to plant roots, which is a limitation for the traditional methods (Bristow et al., 2001; Kirkham, 2014; Song et al., 1998).

The short physical probe length of a thermo-TDR sensor also limits the accuracy of soil water determination. A possible alternative is to use a thermo-FDR (Sheng et al., 2016), because capacitance or impedance sensors (FDR) allow more flexibility in electrode configuration with reduced measurement complexity compared to TDR, in addition to lower costs of the electronics system and minimal postprocessing (Sheng et al., 2016; Xu et al., 2012; Zent et al., 2009, 2010). Sheng et al. (2016) coupled an electromagnetic sensor to determine water content with a penta-needle thermo-FDR, which demonstrated a significant improvement in soil water content determination (with RMSE = 0.012 cm<sup>3</sup>/cm<sup>3</sup> compared to RMSE = 0.042 cm<sup>3</sup>/cm<sup>3</sup> of the HP methods). It should be noted the proper frequency range must be used to obtain accurate soil water determination as well as to reduce effects of temperature and salinity, but the use of FDR has difficulty in soils with high clay content. In addition, FDR measurements at multiple low frequency dielectric spectroscopy (much lower than the TDR bandwidth) have potential to determine ice content and unfrozen water content (Bittelli et al., 2004), which advances its applications in frozen soil studies. Future investigations on a range of soil conditions are required, because results of Bittelli et al. (2004) showed that this method might only be feasible on coarse-textured soils.

### 6.3. Contact Resistance and Probe Material

Early applications of the SPHP method in geophysics estimated the thermal properties of rocks (Clauser & Huenges, 1995; Lubimova et al., 1961). The SPHP probe requires a cylindrical shape so it can be inserted into a diamond-drilled hole. Calculation of thermal properties of test material is based on the known thermal properties of the SPHP probe itself and the rate of temperature change with time according to a suitable theoretical relationship.

The SPHP method is based on the assumption of zero contact resistance; however, there may be imperfect contact between the probe and the external tested media. When heat flows across the interface between two contacting bodies (e.g., probe and soil), a temperature discontinuity occurs at the interface. The discontinuity can be a result of differences in the thermal conductivities due to a change in transport media. The heat flux across the interface is proportional to the temperature difference and the proportionality constant is called thermal contact conductance. Analogous to Ohm's law, the inverse of the thermal contact conductance is the thermal contact resistance. For a stainless steel probe in uniform media such as a liquid or gel, because of the interface, there is small contact resistance, even though the contact is perfect beyond the molecule level. When a probe is inserted into soil, however, in addition to the interface resistance, there are surface roughnesses at the interface due to the mismatch between the cylindrical surface of the probe and the irregular shape of soil particles. There may also be air gaps between soil particle and the probe in unsaturated soils. Therefore, the surface roughness and gaps will further impede heat flow across the interface and increase contact resistance. Therefore, for a probe inserted into soil, thermal contact resistance is the sum of resistance due to the existence of the interface and resistance due to the poor contact between the probe and the media. For example, long drill holes may not be very straight, and the probe must be loosely

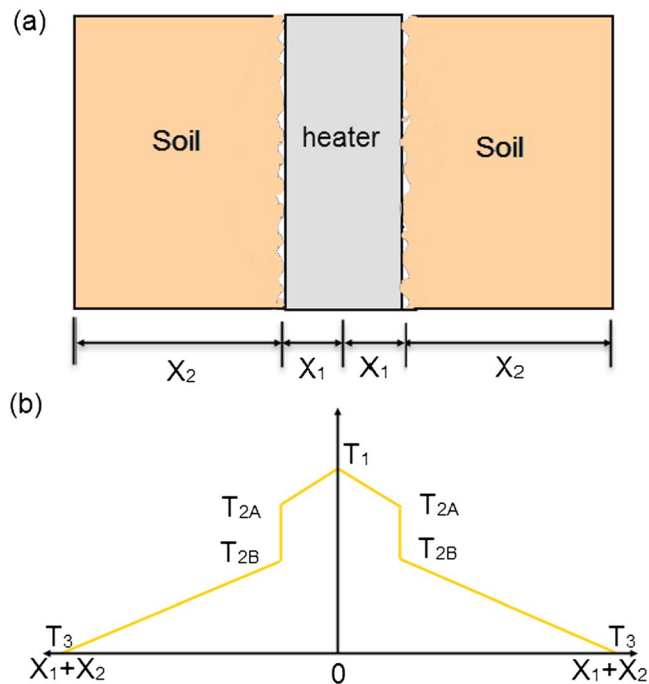


**Figure 19.** Schematic of the interface between heater and the surrounding soils (a) illustrating the discontinuous temperature distribution from probe heater to soil as a result of contact resistance (b).

fitted in the hole; insertion of a HP probe into soils of low density results in local soil disturbance and poor contact between soil and probe while it is hard to insert a HP probe into soils of high density. Sometimes high thermal conductivity grease (with thermal conductivity  $>4 \text{ W}\cdot\text{m}^{-1}\cdot\text{C}^{-1}$ ) is used to reduce poor contact, but this method does not always work for low density soils (Barry-Macaulay et al., 2014). An imperfect thermal contact at the interface between a HP probe and the external medium under test can result in a nonzero thermal contact resistance (e.g., Figure 19), which must be accounted for to obtain accurate thermal property estimates (Blackwell, 1954; G. Liu et al., 2017). A SPHP probe can be either solid with a small radius or hollow with a thin wall to be a relatively good conductor with low heat storage (Blackwell, 1956), so that radial temperature difference within the probe material is negligible, and temperature is uniform over its cross section (Blackwell, 1956; Jaeger, 1955). Air entrapment at the surface of a probe during introduction of probe into wet soil is another issue causing potential errors (Nagpal & Boersma, 1973). In practice, it is hard to separate the interface resistance from the contact resistances. Currently, little is known about the characteristics of the two in soils, and further developments in theory, practice, and verification are needed.

For the SPHP method, data for the first 5 to 100 s, depending on the duration of the HP and the probe dimensions, are affected by the probe characteristics and the contact resistance between the probe and the soil (Bristow, White, et al., 1994; Wechsler, 1966), but data at longer times reflect increasingly more the mean characteristics of the surrounding soil

(Shiozawa & Campbell, 1990). This is also why SPHP can obtain accurate thermal conductivity estimates from large time temperature rise measurements during a long HP. The effects of axial flow and resolution of temperature measurement may increase for the late time data. Therefore, the SPHP method generally applies a relatively long HP duration, but a small heat input per unit time is used to prevent heat-induced water redistribution. DPHP generally uses a relatively short heating duration with relatively large heat input per unit time to approximate the theory of an instantaneous HP, but similar to SPHP, it must avoid causing significant heat convection in the vicinity of the heater. Most analysis methods assume radial heat dissipation occurs in ideal soil that is homogeneous, isotropic, and highly conductive, with negligible contact resistance between the soil and the measurement probes. How soil heterogeneity and energy input affects the thermal property measurements will be discussed in the following sections.

#### 6.4. Soil Heterogeneity

The solutions to the heat conduction equation used to analyze most HP measurements assume the soil thermal properties are isotropic and homogeneous with an initially isothermal temperature distribution within the measurement volume. However, in reality, soils are highly heterogeneous even at small scales. Heterogeneous examples are soils containing rocks or plant roots, layered soils, and soils subject to wetting/drying or freezing/thawing processes. Soil heterogeneity may significantly affect the performance of HP methods.

Philip and Kluitenberg (1999) initiated the investigation of DPHP errors resulting from the spatial variation of soil thermal properties and presented a simplified approximation for a solution to the heat conduction equation in a heterogeneous region based on the instantaneous line source theory. Four different configurations that simulate practical conditions were tested: heater is located at the interface between different soils (effects of layered soils), near or behind a wetting front (the behavior of a DPHP when a sharp wetting front approaches it during infiltration), and near a soil surface (how close can it be installed to the soil surface without surface interface interference). The results showed that errors are small when the distance of the heterogeneity (e.g., soil layer interface and wetting front) to the probe is greater than probe spacing (e.g., 6 mm). The solution allows regions with different  $\lambda$  and  $C_v$  but uniform  $\kappa$ . They later improved the solution to give precise results for probes with four different configurations (the first three scenarios of Philip &

Kluitenberg, 1999, and the case of heater and temperature sensor on different sides of the interface/wetting front; Kluitenberg & Philip, 1999). In an infinite region ( $z < z_1$ ,  $z_1 \geq 0$ ), the thermal conductivity and the volumetric heat capacity are  $\lambda$  and  $C_v$ ; in  $z > z_1$  they are  $\alpha\lambda$  and  $\alpha C_v$ , the thermal diffusivity is assumed to be uniform through  $-\infty < z < \infty$ . Initial conditions of the solution are:  $t = 0$ ,  $-\infty < x < \infty$ ,  $-\infty < z < \infty$ ,  $T = 0$ , heat strength  $q$  released at  $(x, z, t) = (0, 0, 0)$ .

$$\Delta T(x, z, t) = \begin{cases} \frac{q}{4\pi\lambda t} \left[ \exp\left(-\frac{x^2 + z^2}{4\kappa t}\right) + \frac{1 - \alpha}{1 + \alpha} \exp\left(-\frac{x^2 + (2z_1 - z)^2}{4\kappa t}\right) \right] & z \leq z_1 \quad (a) \\ \frac{q}{2\pi(1 + \alpha)\lambda t} \exp\left(-\frac{x^2 + z^2}{4\kappa t}\right) & z \geq z_1 \quad (b) \end{cases} \quad (50)$$

where  $z_1$  is the interface/wetting front and  $\alpha$  is a parameter related to the heterogeneity.

The results of Philip and Kluitenberg (1999) and Kluitenberg and Philip (1999) show that the DPHP gives good estimates of water content near a wetting front interface. But this method is based on the assumption of having uniform  $\kappa$  (two regions may differ much more in thermal conductivity than in diffusivity) and ILHS theory. More studies are required for layered soils with differing  $\kappa$  or when freezing/thawing or wetting/drying front approaches a HP sensor.

### 6.5. Energy Input/Output

A theoretical analysis by de Vries and Peck (1958b) indicated that the temperature gradients resulting from the application of HPs can cause soil water to migrate away from the heater giving rise to lower water contents in the vicinity of the SPHP probe and a slight increase in soil water content at small radial distance from the probe axis. The water redistribution depends on soil physical properties, probe radius, and heating duration. The magnitude of water content decline at the probe surface is approximately inversely proportional to the probe radius, and it increases with increasing duration of heating and with higher temperatures. For most soils, water redistribution and its effects on  $\lambda$  are small at temperatures below about 40 °C (de Vries & Peck, 1958b). Horton and Wierenga (1984) provide practical guidelines for SPHP measurements in unfrozen soils.

Moisture migration is a source of error when probes are used in wet soils at temperatures above freezing (de Vries & Peck, 1958b; Wechsler, 1966). At temperatures below freezing, moisture migration is significantly reduced (Wechsler, 1966), but ice melting can occur (He et al., 2015; G. Liu & Si, 2011b; Ochsner & Baker, 2008; Y. Zhang et al., 2011). G. Liu and Si (2010) found that thermally induced heat flow was negligible when comparing DPHP-measured water contents from sand saturated with water and sand saturated with agar stabilized water. Small heat strength for a long duration reduced overestimation of  $C_v$  compared to short duration with a large heat strength (e.g., 60 s, <6 W/m versus 8 s, >80 W/m) for the DPHP method (G. Liu & Si, 2010). However, a long duration HP requires a large sample volume and could lead to excessive radial and axial heat loss (G. S. Campbell et al., 1991; de Vries & Peck, 1958b; Wechsler, 1966). How the sample volume size influences the measurements of soil thermal properties will be discussed in section 6.6. Therefore, a heater should be properly designed, constructed, and used to minimize water redistribution and convective heat flow around the heater in order to determine thermal properties accurately.

Several applications of HP probe are performed indoors with easy access to a power supply, but solar panels may be required for long-term field studies, weather stations, or remote locations or on Earth and other extra-terrestrial bodies with limited or no power access. The power draw of HP systems vary depending on the probe design (heater resistance), heating scheme (duration of heating cycle), frequency of measurements, and wireless control and communication of data. Therefore, low power consumption of HP probes is an important characteristic required for field applications where power supply is limited. New automated, self-sustained, economic, durable, and wirelessly communicated HP systems should be properly designed for field studies (Jorapur et al., 2015; Palaparthi et al., 2015).

### 6.6. Sample Volume/Outer Boundary

There are two kinds of heat losses that need to be considered during the application of a HP: (1) the radial heat wave released by the heat source may be absorbed by the sample or reflected by the boundaries of the sample and (2) axial heat flow may become significant depending on the sample size and the duration

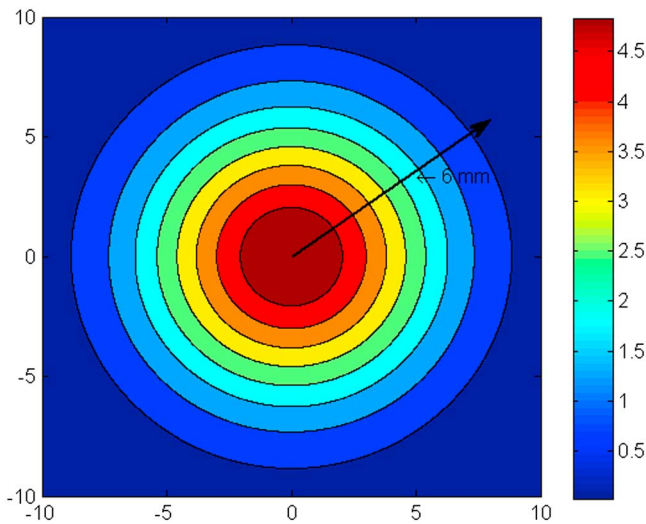


**Figure 20.** A cross section of simulated temperature change distributions in a homogeneous and isotropic soil for the dual-probe heat-pulse method assuming a zero background temperature. Energy input  $q = 500 \text{ J/m}$ , heat pulse duration  $t_0 = 8 \text{ s}$ , time at the maximum temperature change  $t_m = 18 \text{ s}$ , thermal diffusivity  $\kappa = 5 \times 10^{-7} \text{ m}^2/\text{s}$ , and heat capacity  $C_v = 10^6 \text{ J}\cdot\text{m}^{-3}\cdot^\circ\text{C}^{-1}$ .

radius of a heater at time  $t_m$ , as

of heating (Presley & Christensen, 1997). The finite sample size should be properly selected, because it can influence the measured temperature changes. De Vries and Peck (1958a) recommended that the sample size to be expressed as  $R$ , where  $R$ , the radial extent of the material being measured, must satisfy

$$\exp\left(\frac{-R^2}{4\kappa t}\right) \ll 1. \quad (51)$$

This shows that sample size depends on the thermal diffusivity of the material and the duration of heating. Equation (51) provides a conservative estimate of the sample size effect. Errors due to absorption (e.g., isothermal boundary) or reflection (e.g., adiabatic boundary) of the heat wave due to a finite sample size would reduce to  $<1\%$  if

$$t < \frac{0.25R^2}{\kappa} \text{ or } R \gg 2\sqrt{\kappa t}. \quad (52)$$

Deviations from a linear rise in temperature when plotted against  $\log(t)$  tend to be concave upward when the sample size is too small and concave downward when axial heat loss is significant (Wechsler, 1966).

For the DPHP method, G. S. Campbell et al. (1991) estimated the influence

$$r_0 = r_m [1 - \ln(\Delta T_0 / \Delta T_m)]^{1/2}, \quad (53)$$

where  $\Delta T_0$  is the temperature change at any distance  $r_0$  from the heater at time  $t_m$ . If taking  $\Delta T_0 / \Delta T_m = 0.01$  as the outer boundary, then  $r_0 = 2.37 r_m$ . This also indicates that the radius of a soil sample used for measuring soil thermal properties should be greater than  $2.37 r_m$ . Equation (53) could be used as a rule of thumb for the determination of minimum soil sample volumes especially for laboratory tests. Figure 20 provides an example of the area of influence of the heater. Accurate measurements require a large enough sample and a steady boundary condition where temperature change is less than  $\pm 0.1\text{--}0.2 \text{ }^\circ\text{C}$  over the course of the measurement.

J. H. Knight et al. (2007) used a perturbation expansion approach to derive spatial sensitivity functions to test the effective measurement volume of typical DPHP sensors. They found that 99% of the spatial sensitivity was attributed to an ellipse with area of  $168 \text{ mm}^2$  and a major axis of  $15.6 \text{ mm}$  long for a DPHP of  $6 \text{ mm}$  needle-spacing.

## 6.7. Thermal Instability at Close Proximity to the Surface (Soil-Air Interface)

Thermal instabilities or drift is another problem that can cause inaccurate measurements of thermal properties (Bristow et al., 1993; Jury & Bellantuoni, 1976; Presley & Christensen, 1997; Young et al., 2008; X. Zhang et al., 2014). These problems can be minimized by (1) increasing the interval between measurements, so the sample can return to thermal and hydraulic equilibrium; (2) shortening the HP measurement time; or (3) accounting for changes in the background temperature during the measurement period. The first method can be easily applied in laboratory studies, but difficulties can arise in the field environment due to the effects of ambient temperature (e.g., diurnal temperature variations close to the ground surface) for long-term field application (Presley & Christensen, 1997). The second approach is restricted to short-term measurements. Thus, the third approach may be the most appropriate. Field experiments showed that ambient temperature changes had significant impacts on measured  $\Delta T(t)$  data sets and the estimated thermal properties. Measurement accuracy could be improved by accounting for changes in ambient temperature during the measurement period (Bristow et al., 1993). Efforts have been made to account for the impact of abrupt spatial changes in thermal properties, such as near the soil-air interface, on HP measurements. Theory has been presented by Philip and Kluitenberg (1999), Kluitenberg and Philip (1999), G. Liu et al. (2013, 2017), and X. Zhang

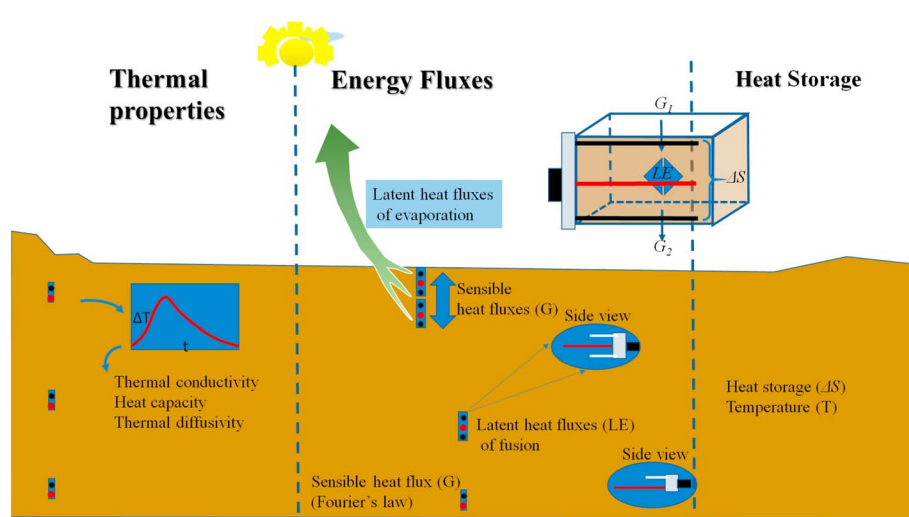


**Figure 21.** Diagram to show the capacities of heat pulse method for determination of soil thermal properties, energy fluxes (latent heat fluxes of evaporation/fusion and sensible heat flux), and heat storage.

et al. (2014, 2017). Xiao et al. (2015) successfully applied the theory to adjust HP thermal properties measured near soil surface interfaces.

### 6.8. Convection and Phase Change

During the measurements, heat convection/water migration in the vicinity of the heater may result from thermal gradients due to the heat input. Heat inputs must be controlled effectively as mentioned in section 6.5. Another issue caused by the HP method is the phase change of water to vapor in unfrozen soils and ice to water in frozen soils because of the release of heat (He et al., 2015). Phase change-associated latent heat is not considered in heat conduction equation solutions for HP methods. Therefore, the resulting thermal properties and other calculated physical property values should be corrected (He et al., 2015), or the results can only be applied to certain scenarios such as soil evaporation measurement (Heitman, Horton, Sauer, et al., 2008; Heitman, Xiao, et al., 2008; Heitman et al., 2017, see section 5.2.3) or frozen soil thermal properties,

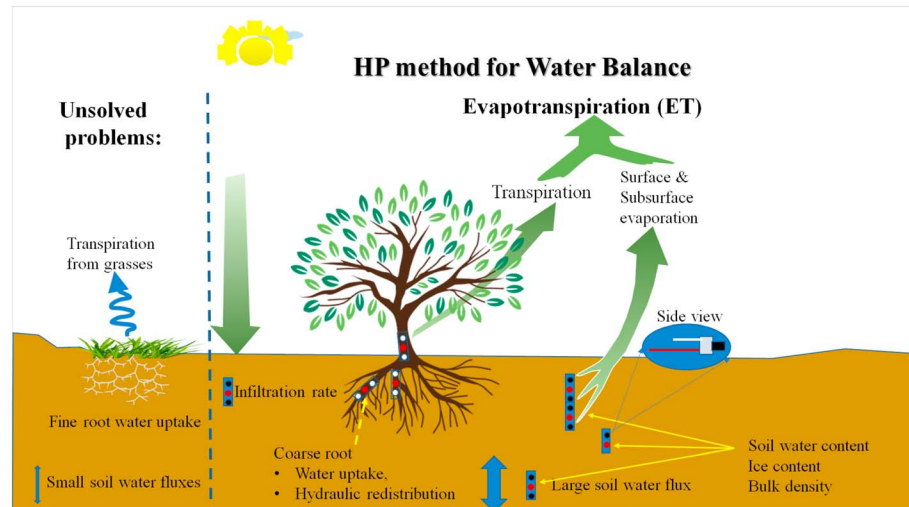


**Figure 22.** The HP method for water balance studies: infiltration, evaporation, soil water content, ice content, bulk density, soil water flux, sap flow/ET, plant water use, and hydraulic redistribution. More study is needed for the determination of small water flux, fine root water uptake, and transpiration from grasses with the HP method. HP = heat pulse.

unfrozen water, and ice content at low subfreezing temperatures (G. Liu & Si, 2010; Y. Zhang et al., 2011, see section 5.3).

## 7. Summary

A comprehensive review of the HP method that applies to the determination of soil thermal properties and a range of other properties in unfrozen and frozen soils is presented. This review covers theories of heat conduction and practical issues such as probe design, construction, and calibration as well as data interpretation methods.

HP probes can be classified into two types: SPHP and DPHP. SPHP can be long or short, and thus can have a range of sampling volume. It is also robust, alleviating the error due to needle deflection. Unfortunately, SPHP can only be used to accurately determine thermal conductivity. To advance SPHP to determine other properties such as heat capacity and soil water content, an improved understanding of thermal contact conductance between soil and probe is needed.

There have been major advances in DPHP in the last 30 years, beginning with G. S. Campbell et al. (1991). It can be used to measure all three thermal properties, soil water contents, and potentially bulk density (Figure 21). It has also been used to measure soil water flux and heat flux, allowing partitioning of evapotranspiration into transpiration through sap flow measurements and to soil water evaporation (Figure 22). Progress has been made in measuring soil ice content and latent and sensible heat fluxes within soil. To date, DPHP has become an important selection in our toolbox for characterizing hydrological processes. Like any other measurement technique, DPHP has its advantages and weaknesses. DPHP has a small sampling volume, and because of that, it is irreplaceable in sap flow measurements and in measuring subsurface evaporation occurring at the 0 to 5 cm of soil, a process that was not possible to determine and to understand with other tools. For other processes, DPHP may be limited by the small measurement volume and its shortcomings for use to describe large areas of soil.

DPHP can be combined with other soil property instrument such as TDR used to measure soil water content and EC, suction lysimeter, and matric potential sensors. Such combinations enable multiple soil properties and processes to be determined for the same soil sampling volume and at the same time.

Some of the weaknesses of SPHP and DPHP can be overcome with advancements in technology. For example, the combination of SPHP or DPHP with fiber-optic cable could potentially revolutionize the application of HP methods in science and engineering and provides much-needed data for ground truthing of remote sensing observation, and for calibration and validation of earth system models.

Future studies should focus on the following aspects:

1. Present probe design limits the representative volume of the soil sample measured. Its extreme sensitivity to needle spacing results in a lack of accuracy, precision, and durability; the short length of thermo-TDR needles may affect the accuracy and precision for water content or water flux estimation. Low energy consumption and wireless communication are among the important properties for field applications (e.g., weather monitoring stations and remote research sites) of HP probes. Moreover, a single HP probe that enables the measurement of spatial variability of soil physical properties will be of interest and significance. New and innovative probes are continually being designed and should continue to contribute to the versatility of the HP method in Earth and environmental sciences and engineering research.
2. Examining probe performance in nonideal field conditions: heterogeneity of soil samples, rock and root contents, initially nonuniform temperature, time varying ambient temperature, and spatiotemporal changes of moisture and bulk density.
3. Improved data interpretation and error analysis modeling warrant attention. The linkage of such an analysis into a computer program could provide a comprehensive and user friendly  $\Delta T(t)$  data analysis package and make the data interpretation procedure as simple as possible. Further, numerical solutions and inverse modeling for estimation of thermal properties should be developed for arbitrary initial and boundary conditions with transient water flow in heterogeneous soil. Such approaches are particularly useful for nonconventional HP applications, such as hotter or colder water injection into subsurface soils with the widespread use of ground source heat pump systems (T. Saito et al., 2014).

4. Efforts to extend the range of HP and AHFO-DTS measurements into partially frozen soils are of substantial interest. However, the possibility of ice melting by the HP confounds the understanding of these processes and restricts its applications in partially frozen soils. New theories, methods, heating strategies, and probe designs for the estimation of soil thermal properties, unfrozen water content, and ice content are in their infancy, but they potentially could greatly improve our understanding of the measurement techniques and the properties of partially frozen porous materials.
5. AHFO-DTS extends the capability of HP methods to field scales and offers new possibilities for multiscale characterization of soil thermal properties and monitoring of soil water dynamics. However, in order to use the well-developed theories of HP methods, innovations in fiber-optic cable construction to mimic an infinite line source with good conductor is needed. Otherwise, new theories/paradigms that are specific to AHFO-DTS are needed before adoption of AHFO-DTS systems will occur for routine monitoring of soil thermal and hydrological processes.
6. Imperfect contact is an issue for HP sensors and for many other methods, such as TDR and neutron moisture meters. To totally avoid it is impossible, but it can be minimized if caution is taken in installing the probes. However, we have, so far, limited knowledge on thermal contact resistance. Microscopically, thermal contact resistance between soil and the probe is affected by the contact area between the two, which is affected by the probe dimensions and geometry, compactness of soil particles, which are in turn affected by bulk density, soil particle size distribution, soil structure, and particle shapes. Displacement of soil air with water also increases the thermal contact, shortens heat conduction pathways, and thus reduces thermal contact resistance. Quantitative descriptions of the relationships between thermal contact conductance (or contact resistance) and bulk density, particle size distribution and particle arrangement, and soil structure and soil water contents are needed for further advancement of SPHP techniques.
7. Soil thermal and hydrological properties and processes in the 0–5 cm soil surface layer are important for understanding critical processes such as evaporation, greenhouse gas emission, and biological activity and for soil management and flood and drought forecasting. Although HP methods have had some successes in these areas, further advancements may require new probe designs and possibly new methodologies.
8. Measurement of the thermal properties of deep subsurface soils is a challenge for the HP method. An alternative HP design to allow a HP probe to be mounted on a direct push-probe is needed. While bore-hole heated DTS systems have been used to measure soil thermal conductivity and soil water content, extension to measurements of other thermal and hydraulic properties is needed.
9. Evaluating and calibrating available thermal conductivity models that are developed from steady-state measurements and developing new models based on the HP measurements are needed. The HP method has been recognized for accurate measurement of soil thermal conductivity, however, some of the existing thermal conductivity models are based on steady-state data that suffer from inaccuracy resulting from errors of temperature gradient driven water migration and phase change from water to vapor or ice to water. To better model or predict soil thermal conductivity, it is necessary to further validate existing models and to develop new models based on HP data. These models can be used to estimate soil thermal properties for a range of soil conditions and be incorporated into sophisticated numerical simulation models for larger scale applications.
10. A standard test method of SPHP (thermal needle probe) for determining thermal conductivity of soil and soft rock has been developed (e.g., ASTM D5334-08, 2008; IEEE, 1981), but there is a lack of standards of DPHP and DTS for measurements of soil heat capacity, thermal diffusivity, and hydraulic properties. Such protocols should be established for the purpose of providing accepted applications of the HP method in both science and engineering.

## Abbreviations

AHFO-DTS	actively heated fiber optic-distributed temperature sensing;
CLHS	continuous line heat source;
DLHS	differentiated line heat source;
DPHP	dual-probe heat-pulse;
EC	electrical conductivity;

FDR	frequency domain reflectometry;
HP	heat pulse;
ICPC	identical-cylindrical-perfect-conductors;
ILHS	instantaneous line heat source;
I.D.	inner diameter;
LD ratio	length to diameter ratio;
LS ratio	Length to spacing ratio;
MDTD	maximum dimensionless temperature difference;
MFHPP	multifunctional heat pulse probe;
NMF	nonlinear model fit;
O.D.	outer diameter;
SFTCs	soil freezing-thawing curves;
SHB	sensible heat balance;
SLS	short-duration line source;
SLHS	short line heat source;
SMRC	soil moisture retention characteristic;
SPHP	single-probe heat-pulse;
SPM	single point method;
Thermo-FDR	heat pulse-frequency domain reflectometry;
Thermo-TDR	heat pulse-time domain reflectometry;
TDR	time domain reflectometry

### List of symbols

$A$	the azimuth, °;
$C_a$	apparent volumetric heat capacity, $\text{J}\cdot\text{m}^{-3}\cdot\text{°C}^{-1}$ ;
$C_v$	volumetric heat capacity, $\text{J}\cdot\text{m}^{-3}\cdot\text{°C}^{-1}$ , $C_v = \rho c$ ;
$E_{vap}$	evaporation rate, m/s;
$G$	soil sensible heat fluxes, W/m <sup>2</sup> ;
$G_{lower}$	soil sensible heat fluxes at lower depth, W/m <sup>2</sup> ;
$I$	current, A;
$I_0$	the modified Bessel function of the first kind of order zero;
$J$	soil water flux, $\text{m}^3\cdot\text{m}^{-2}\cdot\text{s}^{-1}$ or m/s;
$L$	probe length, m;
$L_e$	latent heat of evaporation, J/m <sup>3</sup> ;
$L_f$	latent heat of fusion, J/kg;
$Q$	finite quantity of heat liberated by the heater/line heat source, $\text{m}^2/\text{°C}$ ;
$Q'$	finite quantity of heat liberated by the heater/line heat source per unit time, $\text{m}^2\cdot\text{°C}^{-1}\cdot\text{s}^{-1}$ ;
$R$	resistance, $\Omega$ ;
$SH$	the Steinhart-Hart parameters;
$\Delta S$	change in sensible heat storage, W/m <sup>2</sup> ;
$T$	temperature, °C;
$\Delta T$	temperature differences over $\Delta z$ ;
$V$	the heat pulse velocity, m/s;
$V_h$	the thermal front advection velocity, m/s;
$c$	specific heat capacity of the medium, $\text{J}\cdot\text{kg}^{-1}\cdot\text{°C}^{-1}$ ;
$d$	probe diameter, m;
$d$	subscript d indicates lower soil depth or downstream;
$f$	volumetric fraction air filled pores;
$g$	subscript g indicates air phase;
$i$	subscript i indicates ice phase;
$l$	subscript l indicates liquid water;
$m$	constant parameter for SPHP method during the heating period;

$m'$	constant parameter for SPHP method during the cooling period;
$q$	quantity of heat liberated per unit length of heater, J/m;
$q'$	rate of heat liberated per unit length of heater, $J \cdot m^{-1} \cdot s^{-1}$ or W/m;
$r$	radial distance from the heater, mm;
$s$	subscript $s$ indicates soil solid;
$t$	time, s;
$t_o$	duration of heat pulse, s;
$t_c$	time correction term during the heating period, s;
$t_m$	the time corresponding to the maximum temperature rise, s;
$t'_c$	time correction term during the cooling period, s;
$u$	subscript $u$ indicates upper soil depth or upstream;
$x, y, z$	directions in the Cartesian coordinate system, m;
$\theta_v$	volumetric water content, $m^3/m^3$ ;
$\kappa$	thermal diffusivity, $m^2/s$ ;
$\lambda$	thermal conductivity, $W \cdot m^{-1} \cdot ^\circ C^{-1}$ ;
$\lambda_a$	apparent thermal conductivity, $W \cdot m^{-1} \cdot ^\circ C^{-1}$ ;
$\lambda_h$	thermal conductivity value during the heating period of the SPHP method, $W \cdot m^{-1} \cdot ^\circ C^{-1}$ ;
$\lambda_c$	thermal conductivity value during the cooling period of the SPHP method, $W \cdot m^{-1} \cdot ^\circ C^{-1}$ ;
$\rho$	density, $kg/m^3$ ;
$\rho_b$	dry soil bulk density, $kg/m^3$ ;
$\rho_s$	soil particle density, $kg/m^3$ ;
$\phi$	total porosity, $m^3/m^3$ ;

## Acknowledgments

Data used in this study can be found in the supplementary file. The authors are indebted to Jing Li, Yang Liu, S. Lee Barbour, Jinxin Wang, Min Li, You Hu, Dong He and Ying Zhao for the helpful discussion of the paper. The authors greatly appreciate the valuable and insightful comments by Mark Moldwin, Gregory Okin, Gerard J. Kluitenberg, and four anonymous reviewers. Funding for this research was provided in part by Natural Science Foundation of China (NSFC, Grant Nos. 41501231, 41630860, 41671223), the National Key Research and Development Program of China (No. 2017YFD0200205) the Fundamental Research Funds for the Central Universities at the Northwest A&F University (Nos. 2452015178 and 2452015287), the 111 project (No. B12007), the Strategic Priority Research Program of Chinese Academy of Sciences (No. XDA20040202), Natural Science and Engineering Research Council of Canada (NSERC) discovery for Dr. Miles Dyck and Dr. Bing Si), and the U.S. National Science Foundation (NSF Award 1623806).

## References

- Abramowitz, M., & Stegun, I. A. (1972). *Handbook of mathematical functions with formulas, graphs, and mathematical tables* (228 pp.). U.S. Department of Commerce.
- Agam, N., Evett, S. R., Tolk, J. A., Kustas, W. P., Colaizzi, P. D., Alfieri, J. G., et al. (2012). Evaporative loss from irrigated interrows in a highly advective semi-arid agricultural area. *Advances in Water Resources*, 50(6), 20–30. <https://doi.org/10.1016/j.advwatres.2012.07.010>
- Agilent Technologies (2000). Retrieved from <http://cp.literature.agilent.com/litweb/pdf/5965-7822E.pdf>, accessed on 28 October 2014.
- Al Nakshabandi, G., & Kohnke, H. (1965). Thermal conductivity and diffusivity of soils as related to moisture tension and other physical properties. *Agricultural Meteorology*, 2(4), 271–279. [https://doi.org/10.1016/0002-1571\(65\)90013-0](https://doi.org/10.1016/0002-1571(65)90013-0)
- Anderson, D. M., & Tice, A. R. (1972). Predicting unfrozen water content in frozen soils from surface measurement. *Highway Research Record*, 393, 12–18.
- Anderson, D. M., Tice, A. R., & McKim, H. L. (1973). The unfrozen water and apparent specific heat capacity of frozen soils. In *Proceedings of the 2nd International Conference on Permafrost* (pp. 289–295). Yakutsk, Washington, DC: USSR. National Academy of Sciences.
- Andersson, P., & Bäckström, G. (1976). Thermal conductivity of solids under pressure by the transient hot wire method. *Review of Scientific Instruments*, 47(2), 205–209. <https://doi.org/10.1063/1.1134581>
- Assael, M. J., Antoniadis, K. D., & Wakeham, W. A. (2010). Historical evolution of the transient hot-wire technique. *International Journal of Thermophysics*, 31(6), 1051–1072. <https://doi.org/10.1007/s10765-010-0814-9>
- ASTM D5334-08 (2008). Standard test method for determination of thermal conductivity of soil and soft rock by thermal needle probe procedure.
- Baker, T. H. W., & Goodrich, L. E. (1984). A probe for measuring both thermal conductivity and water content of soils. In *Proceedings Third International Specialty Conference Cold Regions Engineering* (Vol. 2, pp. 835–849). Edmonton, Alberta, Canada: North Resources Development.
- Baker, T. H. W., & Goodrich, L. E. (1987). Measurement of soil water content using the combined time-domain reflectometry-thermal conductivity probe. *Canadian Geotechnical Journal*, 24(1), 160–163. <https://doi.org/10.1139/t87-016>
- Balasubramanian, T., & Bowman, H. (1977). Thermal conductivity and thermal diffusivity of biomaterials: A simultaneous measurement technique. *Journal of Biomechanical Engineering*, 99(3), 148–154. <https://doi.org/10.1115/1.3426282>
- Barr, A. G., van der Kamp, G., Black, T. A., McCaughey, J. H., & Nesic, Z. (2012). Energy balance closure at the BERMS flux towers in relation to the water balance of the White Gull Creek watershed 1999–2009. *Agricultural and Forest Meteorology*, 153, 3–13. <https://doi.org/10.1016/j.agrformet.2011.05.017>
- Barry-Macaulay, D., Bouazza, A., Singh, R., & Wang, B. (2014). Thermal properties of some Melbourne soils and rocks. *Australian Geomechanics*, 49(2), 31–44.
- Basinger, J. M., Barnes, P. L., Kirkham, M. B., Frank, J. M., Klitenberg, G. J., & Ham, J. M. (2003). Laboratory evaluation of the dual-probe heat-pulse method for measuring soil water content. *Vadose Zone Journal*, 2(3), 389–399. <https://doi.org/10.2136/vzj2003.3890>
- Batty, W. J., Probert, S. D., Ball, M., & O'Callaghan, P. W. (1984). Use of the thermal-probe technique for the measurement of the apparent thermal conductivities of moist materials. *Applied Energy*, 18(4), 301–317. [https://doi.org/10.1016/0306-2619\(84\)90011-4](https://doi.org/10.1016/0306-2619(84)90011-4)
- Becker, B. R., Misra, A., & Fricke, B. A. (1992). Development of correlations for soil thermal conductivity. *International Journal of Heat and Mass Transfer*, 35(1), 59–68. [https://doi.org/10.1016/0735-1933\(92\)90064-C](https://doi.org/10.1016/0735-1933(92)90064-C)
- Benítez-Buelga, J., Rodríguez-Sinobas, L., Sánchez-Calvo, R., Gil-Rodríguez, M., Sayde, C., & Selker, J. S. (2016). Calibration of soil moisture sensing with subsurface heated fiber optics using numerical simulation. *Water Resources Research*, 52, 2985–2995. <https://doi.org/10.1002/2015WR017897>

- Benítez-Buelga, J., Sayde, C., Rodríguez-Sinobas, L., & Selker, J. S. (2014). Heated fiber optic distributed temperature sensing for measuring soil volumetric heat capacity and water content: A dual probe heat-pulse approach. *Vadose Zone Journal*, 13(11). <https://doi.org/10.2136/vzj2014.02.0014>
- Benson, E. (2004). A guide for the construction and operation of dual-probe heat-capacity sensors.
- Bilskie, J. R. (1994). Dual-probe methods for determining soil thermal properties: Numerical and laboratory study, (Ph.D. Dissertation). Ames, IA: Iowa State University
- Bittelli, M., Flury, M., & Campbell, G. S. (2003). A thermoelectric analyzer to measure the freezing and moisture characteristic of porous media. *Water Resources Research*, 39(2), 1041. <https://doi.org/10.1029/2001WR000930>
- Bittelli, M., Flury, M., & Roth, K. (2004). Use of dielectric spectroscopy to estimate ice content in frozen porous media. *Water Resources Research*, 40, W04212. <https://doi.org/10.1029/2003WR002343>
- Bittelli, M., Ventura, F., Campbell, G. S., Synder, R. L., Gallegati, F., & Pisa, P. R. (2008). Coupling of heat, water vapor, and liquid water fluxes to compute evaporation in bare soils. *Journal of Hydrology*, 362(3-4), 191–205. <https://doi.org/10.1016/j.jhydrol.2008.08.014>
- Blackwell, J. H. (1953). Radial-axial heat flow in regions bounded internally by circular cylinders. *Canadian Journal of Physics*, 31(4), 472–479. <https://doi.org/10.1139/p53-046>
- Blackwell, J. H. (1954). A transient flow method for determination of thermal constants of insulating materials in bulk part I—Theory. *Journal of Applied Physics*, 25(2), 137–144. <https://doi.org/10.1063/1.1721592>
- Blackwell, J. H. (1956). The axial-flow error in the thermal-conductivity probe. *Canadian Journal of Physics*, 34(4), 412–417. <https://doi.org/10.1139/p56-048>
- Bristow, K. L. (1998). Measurement of thermal properties and water content of unsaturated sandy soil using dual-probe heat-pulse probes. *Agricultural and Forest Meteorology*, 89(2), 75–84. [https://doi.org/10.1016/s0168-1923\(97\)00065-8](https://doi.org/10.1016/s0168-1923(97)00065-8)
- Bristow, K. L., Campbell, G. S., & Calissendorff, K. (1993). Test of a heat-pulse probe for measuring changes in soil water content. *Soil Science Society of America Journal*, 57(4), 930–934. <https://doi.org/10.2136/sssaj1993.03615995005700040008x>
- Bristow, K. L., Horton, R., Kluitenberg, G. J., & Bilskie, J. R. (1995). Comparison of techniques for extracting soil thermal properties from dual-probe heat-pulse data. *Soil Science*, 160(1), 1–7. <https://doi.org/10.1097/00010694-199507000-00001>
- Bristow, K. L., Kluitenberg, G. J., Goding, C. J., & Fitzgerald, T. S. (2001). A small multi-needle probe for measuring soil thermal properties, water content and electrical conductivity. *Computers and Electronics in Agriculture*, 31(3), 265–280. [https://doi.org/10.1016/S0168-1699\(00\)00186-1](https://doi.org/10.1016/S0168-1699(00)00186-1)
- Bristow, K. L., Kluitenberg, G. J., & Horton, R. (1994). Measurement of soil thermal properties with a dual-probe heat-pulse technique. *Soil Science Society of America Journal*, 58(5), 1288–1294. <https://doi.org/10.2136/sssaj1994.03615995005800050002x>
- Bristow, K. L., White, R. D., & Kluitenberg, G. J. (1994). Comparison of single and dual probes for measuring soil thermal properties with transient heating. *Soil Research*, 32(3), 447–464. <https://doi.org/10.1071/SR9940447>
- Brown, R. J. (1970). *Permafrost in Canada: Its influence on northern development*. Toronto, Canada: University of Toronto Press. <https://doi.org/10.3138/9781442632615>
- Bruijn, P. J., van Haneghem, I. A., & Schenk, J. (1983). An improved nonsteady-state probe method for measurements in granular materials. I: Theory. *High Temperatures - High Pressures*, 15(4), 359–366.
- Brutsaert, W. (1982). *Evaporation into the atmosphere: Theory, history, and applications*, (p. 299). Kluwer Boston Dordrecht, Holland; Boston, Hingham, Mass: Reidel. <https://doi.org/10.1007/978-94-017-1497-6>
- Bull, K. (2008). Thermistors and thermocouples: Matching the tool to the task in thermal validation. *Journal of Validation Technology*, 14(2), 73–76.
- Burgess, S. S. O., Adams, M. A., Turner, N. C., Beverly, C. R., Ong, C. K., Khan, A. A. H., & Bleby, T. M. (2001). An improved heat pulse method to measure low and reverse rates of sap flow in woody plants. *Tree Physiology*, 21(9), 589–598. <https://doi.org/10.1093/treephys/21.9.589>
- Byrne, G. F. (1971). An improved soil water flux sensor. *Agricultural Meteorology*, 9, 101–104. [https://doi.org/10.1016/0002-1571\(71\)90010-0](https://doi.org/10.1016/0002-1571(71)90010-0)
- Byrne, G. F., Drummond, J. E., & Rose, C. W. (1967). A sensor for water flux in soil. "Point Source" instrument. *Water Resources Research*, 3(4), 1073–1078. <https://doi.org/10.1029/WR003i004p01073>
- Byrne, G. F., Drummond, J. E., & Rose, C. W. (1968). A sensor for water flux in soil: 2. "Line Source" instrument. *Water Resources Research*, 4(3), 607–611. <https://doi.org/10.1029/WR004i003p0060>
- Cammalleri, C., Anderson, M. C., Ciraolo, G., D'Urso, G., Kustas, W. P., La Loggia, G., & Minacapilli, M. (2010). The impact of in-canopy wind profile formulations on heat flux estimation in an open orchard using the remote sensing-based two source model. *Hydrology and Earth System Sciences*, 14(12), 2643–2659. <https://doi.org/10.5194/hess-14-2643-2010>
- Campbell, G. S. (1985). *Soil physics with BASIC: Transport models for soil-plant systems*, (3rd ed.). New York: Elsevier.
- Campbell, G. S., Calissendorff, C., & Williams, J. H. (1991). Probe for measuring soil specific heat using a heat-pulse method. *Soil Science Society of America Journal*, 55(1), 291–293. <https://doi.org/10.2136/sssaj1991.03615995005500010052x>
- Campbell, G. S., Jungbauer, J. D. Jr., Bidlake, W. R., & Hungerford, R. D. (1994). Predicting the effect of temperature on soil thermal conductivity. *Soil Science*, 158(5), 307–313. <https://doi.org/10.1097/00010694-199411000-00001>
- Campbell, D. I., Laybourne, C. E., & Blair, I. J. (2002). Measuring peat moisture content using the dual-probe heat pulse technique. *Soil Research*, 40(1), 177–190. <https://doi.org/10.1071/SR00108>
- Carlsaw, H. S., & Jaeger, J. C. (1959). *Conduction of heat in solids*, (2nd ed.). London: Oxford University Press.
- Carter, M. R. (1993). *Soil sampling and methods of analysis*. Washington, DC: CRC Press.
- Cary, J. W. (1973). Soil water flowmeters with thermocouple outputs. *Soil Science Society of America Journal*, 37(2), 176–181. <https://doi.org/10.2136/sssaj1973.03615995003700020010x>
- Chung, S. O., & Horton, R. (1987). Soil heat and water flow with a partial surface mulch. *Water Resources Research*, 23(12), 2175–2186. <https://doi.org/10.1029/WR023i012p02175>
- Cioccia, F., Lunati, I., van de Giesen, N., & Parlange, M. B. (2012). Heated optical fiber for distributed soil-moisture measurements: A lysimeter experiment. *Vadose Zone Journal*, 11(4), 9851. <https://doi.org/10.2136/vzj2011.0199>
- Clauer, C., & Huenges, E. (1995). Thermal conductivity of rocks and minerals. In T. J. Ahrens (Ed.), *Rock physics & phase relations* (pp. 105–126). Washington, DC: American Geophysical Union. <https://doi.org/10.1029/RF003p0105>
- Cobos, D. R., & Baker, J. M. (2003). In situ measurement of soil heat flux with the gradient method. *Vadose Zone Journal*, 2(4), 589–594. <https://doi.org/10.2113/2.4.589>
- Cody, W. J., & Thacher, H. C. J. (1968). Rational Chebyshev approximations for the exponential integral  $E_1(x)$ . *Mathematics of Computation*, 22(103), 641–649. <https://doi.org/10.1090/S0025-5718-1968-0226823-X>
- Colaizzi, P. D., O'Shaughnessy, S. A., Gowda, P. H., Evett, S. R., Howell, T. A., Kustas, W. P., & Anderson, M. C. (2010). Radiometer footprint model to estimate sunlit and shaded components for row crops. *Agronomy Journal*, 102(3), 942–955. <https://doi.org/10.2134/agronj2009.0393>

- Cortes, D. D., Martin, A. J., Yun, T. S., Francisca, F. M., Santamarina, J. C., & Ruppel, C. (2009). Thermal conductivity of hydrate-bearing sediments. *Journal of Geophysical Research*, 114(B11), B11103. <https://doi.org/10.1029/2008JB006235>
- Dalton, F. N., & Van Genuchten, M. T. (1986). The time-domain reflectometry method for measuring soil water content and salinity. *Geoderma*, 38(1–4), 237–250. [https://doi.org/10.1016/0016-7061\(86\)90018-2](https://doi.org/10.1016/0016-7061(86)90018-2)
- Davidson, E. A., Belk, E., & Boone, R. D. (1998). Soil water content and temperature as independent or confounded factors controlling soil respiration in a temperate mixed hardwood forest. *Global Change Biology*, 4(2), 217–227. <https://doi.org/10.1046/j.1365-2486.1998.00128.x>
- de Vries, D. A. (1952). A nonstationary method for determining thermal conductivity of soil in situ. *Soil Science*, 73(2), 83–90. <https://doi.org/10.1097/00010694-195202000-00001>
- de Vries, D. A. (1963). Thermal properties of soil. In W. R. van Dijk (Ed.), *Physics of plant environment* (pp. 210–235). Amsterdam: North Holland Publishing.
- de Vries, D. A., & Peck, A. J. (1958a). On the cylindrical probe method of measuring thermal conductivity with special reference to soils. I: Extension of theory and discussion of probe characteristics. *Australian Journal of Physics*, 11(2), 255–271. <https://doi.org/10.1071/PH580255>
- de Vries, D. A., & Peck, A. J. (1958b). On the cylindrical probe method of measuring thermal conductivity with special reference to soils. II: Analysis of moisture effects. *Australian Journal of Physics*, 11(3), 409–423. <https://doi.org/10.1071/PH580409>
- de Wilde, P., Griffiths, R., & Goodhew, S. (2008). Validation of data analysis routines for a thermal probe apparatus using numerical data sets. *Building Simulation*, 1(1), 36–45. <https://doi.org/10.1007/s12273-008-8105-0>
- Deol, P. K., Heitman, J. L., Amoozegar, A., Ren, T., & Horton, R. (2012). Quantifying non-isothermal sub-surface soil water evaporation. *Water Resources Research*, 48, W11503. <https://doi.org/10.1029/2012WR012516>
- Deol, P. K., Heitman, J. L., Amoozegar, A., Ren, T., & Horton, R. (2014). Inception and magnitude of subsurface evaporation for a bare soil with natural surface boundary conditions. *Soil Science Society of America Journal*, 78(5), 1544–1551. <https://doi.org/10.2136/sssaj2013.12.0520>
- Dong, Y., McCartney, J., & Lu, N. (2015). Critical review of thermal conductivity models for unsaturated soils. *Geotechnical and Geological Engineering*, 33(2), 207–221. <https://doi.org/10.1007/s10706-015-9843-2>
- Endo, A., & Hara, M. (2003). Simultaneous measurement of thermal front advection velocity vector and thermal properties of sandy soil under two-dimensional flow field with quintuple probe heat-pulse technique and its applications. *Transactions of the Society of Instrument and Control Engineers*, 2(12), 88–95.
- Endrizzi, S., Gruber, S., Dall'Amico, M., & Rigan, R. (2014). GEOTop 2.0: Simulating the combined energy and water balance at and below the land surface accounting for soil freezing, snow cover and terrain effects. *Geoscientific Model Development*, 7(6), 2831–2857. <https://doi.org/10.5194/gmd-7-2831-2014>
- Evett, S. R. (2000). Time domain reflectometry (TDR) system manual. USDA-ARS Conservation and Production Research Laboratory. Retrieved from <http://www.cprlars.usda.gov/swmrusw-software-sws.php>
- Ewing, R. P., & Horton, R. (2007). Thermal conductivity of a cubic lattice of spheres with capillary bridges. *Journal of Physics D: Applied Physics*, 40(16), 4959–4965. <https://doi.org/10.1088/0022-3727/40/16/031>
- Farouki, O. T. (1981). *Thermal properties of soils*, CRREL Monograph, (p. 136). Hanover, NH: U.S. Army Corps of Engineers, Cold Regions Research and Engineering Laboratory.
- Forsythe, W. E. (1964). *Smithsonian physical tables*, Smithsonian Institution Publication (Vol. 4169). Washington, DC: American Geophysical Union.
- Fuchs, M., & Tanner, C. B. (1968). Calibration and field test of soil heat flux plates. *Soil Science Society of America Proceedings*, 32(3), 326–328. <https://doi.org/10.2136/sssaj1968.03615995003200030021x>
- Gao, J., Ren, T., & Gong, Y. (2006). Correcting wall flow effect improves the heat-pulse technique for determining water flux in saturated soils. *Soil Science Society of America Journal*, 70(3), 711–717. <https://doi.org/10.2136/sssaj2005.0174>
- Gardner, H. R., & Hanks, R. J. (1966). Evaluation of the evaporation zone in soil by measurement of heat flux. *Soil Science Society of America Proceedings*, 30(4), 425–428. <https://doi.org/10.2136/sssaj1966.03615995003000040010x>
- Gil-Rodríguez, M., Rodríguez-Sinobas, L., Benítez-Buelga, J., & Sánchez-Calvo, R. (2013). Application of active heat pulse method with fiber optic temperature sensing for estimation of wetting bulbs and water distribution in drip emitters. *Agricultural Water Management*, 120, 72–78. <https://doi.org/10.1016/j.agwat.2012.10.012>
- Goodrich, L. E. (1986). Field measurements of soil thermal conductivity. *Canadian Geotechnical Journal*, 23(1), 51–59. <https://doi.org/10.1139/t86-006>
- Granier, A. (1987). Evaluation of transpiration in a Douglas-fir stand by means of sap flow measurements. *Tree Physiology*, 3(4), 309–320. <https://doi.org/10.1093/treephys/3.4.309>
- Green, S., Clothier, B., & Jardine, B. (2003). Theory and practical application of heat pulse to measure sap flow. *Agronomy Journal*, 95(6), 1371–1379. <https://doi.org/10.2134/agronj2003.1371>
- Ham, J. M., & Benson, E. J. (2004). On the construction and calibration of dual-probe heat capacity sensors. *Soil Science Society of America Journal*, 68(4), 1185–1190. <https://doi.org/10.2136/sssaj2004.1185>
- Ham, J. M., & Kluitenberg, G. J. (1993). Positional variation in the soil energy balance beneath a row-crop canopy. *Agricultural and Forest Meteorology*, 63(1–2), 73–92. [https://doi.org/10.1016/0168-1923\(93\)90023-B](https://doi.org/10.1016/0168-1923(93)90023-B)
- Harris, C., Arenson, L. U., Christiansen, H. H., Etzelmüller, B., Frauenfelder, R., Gruber, S., et al. (2009). Permafrost and climate in Europe: Monitoring and modelling thermal, geomorphological and geotechnical responses. *Earth Science Reviews*, 92(3–4), 117–171. <https://doi.org/10.1016/j.earscirev.2008.12.002>
- He, H., & Dyck, M. (2013). Application of multiphase dielectric mixing models for understanding the effective dielectric permittivity of frozen soils. *Vadose Zone Journal*, 12(1). <https://doi.org/10.2136/vzj2012.0060>
- He, H., Dck, M., Horton, R., Li, M., Jin, H. J., & Si, B. C. (2018). Distributed temperature sensing for soil physical measurements and its similarity to heat pulse method. In D. L. Sparks (Ed.), *Advances in agronomy* (Vol. 148, pp. 173–230). Cambridge: Academic Press. <https://doi.org/10.1016/bs.agron.2017.11.003>
- He, H., Dyck, M., Wang, J., & Lv, J. (2015). Evaluation of TDR method for quantifying ice melting caused by heat pulse method for better estimating thermal properties of frozen soils. *Soil Science Society of America Journal*, 79(5), 1275–1288. <https://doi.org/10.2136/sssaj2014.12.0499>
- He, H., Dyck, M., Zhao, Y., Si, B., Jin, H., Zhang, T., et al. (2016). Evaluation of five composite dielectric mixing models for understanding relationships between effective permittivity and unfrozen water content. *Cold Regions Science and Technology*, 130, 33–42. <https://doi.org/10.1016/j.coldregions.2016.07.006>
- He, H., Zhao, Y., Dyck, M., Si, B., Jin, H., Lv, J., & Wang, J. (2017). A modified normalized model for predicting effective soil thermal conductivity. *Acta Geotechnica*, 12(6), 1281–1300. <https://doi.org/10.1007/s11440-017-0563-z>

- Heilman, J. L., McInnes, K., Savage, M., Gesch, R., & Lascano, R. J. (1994). Soil and canopy energy balances in a West Texas vineyard. *Agricultural and Forest Meteorology*, 71(1-2), 99–114. [https://doi.org/10.1016/0168-1923\(94\)90102-3](https://doi.org/10.1016/0168-1923(94)90102-3)
- Heimovaara, T. J. (1993). Design of triple-wire time domain reflectometry probes in practice and theory. *Soil Science Society of America Journal*, 57(6), 1410–1417. <https://doi.org/10.2136/sssaj1993.03615995005700060003x>
- Heitman, J. L., Basinger, J. M., Kluitenberg, G. J., Ham, J. M., Frank, J. M., & Barnes, P. L. (2003). Field evaluation of the dual-probe heat-pulse method for measuring soil water content. *Vadose Zone Journal*, 2(4), 552–560. <https://doi.org/10.2136/vzj2003.5520>
- Heitman, J. L., Horton, R., Ren, T., Nassar, I. N., & Davis, D. D. (2008). A test of coupled soil heat and water transfer prediction under transient boundary temperatures. *Soil Science Society of America Journal*, 72(5), 1197–1207. <https://doi.org/10.2136/sssaj2007.0234>
- Heitman, J. L., Horton, R., Ren, T., & Ochsner, T. E. (2007). An improved approach for measurement of coupled heat and water transfer in soil cells. *Soil Science Society of America Journal*, 71(3), 872–880. <https://doi.org/10.2136/sssaj2006.0327>
- Heitman, J. L., Horton, R., Sauer, T. J., & DeSutter, T. M. (2008). Sensible heat observations reveal soil-water evaporation dynamics. *Journal of Hydrometeorology*, 9(1), 165–171. <https://doi.org/10.1175/2007JHM963.1>
- Heitman, J. L., Xiao, X., Horton, R., & Sauer, T. J. (2008). Sensible heat measurements indicating depth and magnitude of subsurface soil water evaporation. *Water Resources Research*, 44, W00D05. <https://doi.org/10.1029/2008WR006961>
- Heitman, J. L., Zhang, X., Xiao, X., Ren, T., & Horton, R. (2017). Advances in heat-pulse methods: Measuring soil water evaporation with sensible heat balance. *Methods of Soil Analysis*, 2(1). <https://doi.org/10.2136/msa2015.0029>
- Hillel, D. (1998). *Environmental soil physics*. London: Academic Press.
- Hiraiwa, Y., & Kasubuchi, T. (2000). Temperature dependence of thermal conductivity of soil over a wide range of temperature (5–75 °C). *European Journal of Soil Science*, 51(2), 211–218. <https://doi.org/10.1046/j.1365-2389.2000.00301.x>
- Holland, S., Howard, A., Heitman, J. L., Sauer, T. J., Giese, W., Sutton, T. B., et al. (2014). Implications of tall fescue for inter-row water dynamics in a vineyard. *Agronomy Journal*, 106(4), 1267–1274. <https://doi.org/10.2134/agronj13.0488>
- Hooper, F. C., & Lepper, F. R. (1950). Transient heat flow apparatus for the determination of thermal conductivities. *Journal Section of the American Society of Heating and Ventilating Engineers*, 129–140.
- Hopmans, J. W., & Dane, J. H. (1986). Thermal conductivity of two porous media as a function of water content, temperature and density. *Soil Science*, 142(4), 187–195. <https://doi.org/10.1097/00010694-198610000-00001>
- Hopmans, J. W., Simunek, J., & Bristow, K. L. (2002). Indirect estimation of soil thermal properties and water flux using heat pulse probe measurements: Geometry and dispersion effects. *Water Resources Research*, 38(1), 1006. <https://doi.org/10.1029/2000WR000071>
- Horai, K. (1981). The effect of interstitial gaseous pressure on the thermal conductivity of a simulated Apollo 12 lunar soil sample. *Physics of the Earth and Planetary Interiors*, 27(1), 60–71. [https://doi.org/10.1016/0031-9201\(81\)90087-x](https://doi.org/10.1016/0031-9201(81)90087-x)
- Horrocks, J., & McLaughlin, E. (1963). Non-steady-state measurements of the thermal conductivities of liquid polyphenyls. *Proceedings of the Royal Society of London. Series A, Mathematical and Physical Sciences*, 273(1353), 259–274. <https://doi.org/10.1098/rspa.1963.0087>
- Horton, R. (1989). Canopy shading effects on soil heat and water flow. *Soil Science Society of America Journal*, 53(3), 669–679. <https://doi.org/10.2136/sssaj1989.03615995005300030004x>
- Horton, R., Aguirre-Luna, O., & Wierenga, P. J. (1984). Soil temperature in a row crop with incomplete surface cover. *Soil Science Society of America Journal*, 48(6), 1225–1232. <https://doi.org/10.2136/sssaj1984.03615995004800060004x>
- Horton, R., & Wierenga, P. J. (1984). The effect of column wetting on soil thermal conductivity. *Soil Science*, 138(2), 102–108. <https://doi.org/10.1097/00010694-198408000-00002>
- IEEE (1981). IEEE guide for soil thermal resistivity measurements, EEE Std 442-1981, edited, pp. 1–16.
- Jaeger, J. C. (1955). Conduction of heat in a solid in contact with a thin layer of a good conductor. *Quarterly Journal of Mechanics and Applied Mathematics*, 8(1), 101–106. <https://doi.org/10.1093/cjmam/8.1.101>
- Jaeger, J. C. (1956). Conduction of heat in an infinite region bounded internally by a circular cylinder of a perfect conductor. *Australian Journal of Physics*, 9(2), 167–179. <https://doi.org/10.1071/PH560167>
- Johansen, O. (1975). Thermal conductivity of soils, University of Trondheim, Trondheim, Norway, US Army Corps of Engineers, Cold Regions Research and Engineering Laboratory, Hanover, N.H. CRREL Draft English Translation 637.
- Jones, B. W. (1988). Thermal conductivity probe: Development of method and application to a coarse granular medium. *Journal of Physics E: Scientific Instruments*, 21(9), 832–839. <https://doi.org/10.1088/0022-3735/21/9/002>
- Jorapur, N., Palaparthi, V. S., Sarik, S., John, J., Baghini, M. S., & Ananthasuresh, G. K. (2015). A low-power, low-cost soil-moisture sensor using dual-probe heat-pulse technique. *Sensors and Actuators A: Physical*, 233, 108–117. <https://doi.org/10.1016/j.sna.2015.06.026>
- Jury, W., & Bellantuoni, B. (1976). A background temperature correction for thermal conductivity probes. *Soil Science Society of America Journal*, 40(4), 608–610. <https://doi.org/10.2136/sssaj1976.03615995004000040040x>
- Kahan, D. S., Xue, Y., & Allen, S. J. (2006). The impact of vegetation and soil parameters in simulations of surface energy and water balance in the semi-arid Sahel: A case study using SEBEX and HAPEX-Sahel data. *Journal of Hydrology*, 320(1–2), 238–259. <https://doi.org/10.1016/j.jhydrol.2005.07.011>
- Kamai, T. (2013). Development of heat pulse sensors to measure vadose zone thermal properties, water content, and water flux density, (Ph. D. thesis, pp. 197). Davis, Ann Arbor: University of California.
- Kamai, T., & Hopmans, J. W. (2007). Coupled heat and water flow in variably-saturated porous media, Paper presented at Proceedings of the COMSOL Conference 2007, Boston.
- Kamai, T., Hopmans, J. W., Kluitenberg, G. J., & Tuli, A. (2010). Correction to “Soil water flux density measurements near 1 cm d<sup>-1</sup> using an improved heat pulse probe design”. *Water Resources Research*, 44, W07901. <https://doi.org/10.1029/2008WR007036>.
- Kamai, T., Kluitenberg, G., & Hopmans, J. W. (2009). Design and numerical analysis of a button heat pulse probe for soil water content measurement. *Vadose Zone Journal*, 8(1), 167–173. <https://doi.org/10.2136/vzj2008.0106>
- Kamai, T., Kluitenberg, G., & Hopmans, J. W. (2015). A dual-probe heat-pulse sensor with rigid probes for improved soil water content measurement. *Soil Science Society of America Journal*, 79(4), 1059–1072. <https://doi.org/10.2136/sssaj2015.01.0025>
- Kamai, T., Tuli, A., Kluitenberg, G. J., & Hopmans, J. W. (2008). Soil water flux density measurements near 1 cm d<sup>-1</sup> using an improved heat pulse probe design. *Water Resources Research*, 44, W00D14. <https://doi.org/10.1029/2008WR007036>
- Kasubuchi, T. (1977). Twin transient-state cylindrical-probe method for the determination of the thermal conductivity of soil. *Soil Science*, 124(5), 255–258. <https://doi.org/10.1097/00010694-197711000-00001>
- Kersten, M. S. (1949). *Thermal Properties of Soils*, (p. 227). Minneapolis, MN: Minnesota University Institute of Technology.
- Khader, M. S., Crane, R. A., & Vachon, R. I. (1980). Thermal conductivity of granular materials—A review. In A. M. A. Rezk (Ed.), *Heat and fluid flow in power system components* (pp. 111–141). Oxford: Pergamon Press. <https://doi.org/10.1016/B978-0-08-024235-4.50014-1>
- Kirkham, M. B. (2014). Chapter 9 - Dual thermal probes. In M. B. Kirkham (Ed.), *Principles of soil and plant water relations*, (2nd ed. pp. 123–151). Boston: Academic Press. <https://doi.org/10.1016/B978-0-12-420022-7.00009-4>

- Kluitenberg, G. J., Bristow, K. L., & Das, B. S. (1995). Error analysis of heat pulse method for measuring soil heat capacity, diffusivity, and conductivity. *Soil Science Society of America Journal*, 59(3), 719–726. <https://doi.org/10.2136/sssaj1995.03615995005900030013x>
- Kluitenberg, G. J., Ham, J. M., & Bristow, K. L. (1993). Error analysis of the heat pulse method for measuring soil volumetric heat capacity. *Soil Science Society of America Journal*, 57(6), 1444–1451. <https://doi.org/10.2136/sssaj1993.03615995005700060008x>
- Kluitenberg, G. J., Kamai, T., Vrugt, J. A., & Hopmans, J. W. (2010). Effect of probe deflection on dual-probe heat-pulse thermal conductivity measurements. *Soil Science Society of America Journal*, 74(5), 1537–1540. <https://doi.org/10.2136/sssaj2010.0016N>
- Kluitenberg, G. J., Ochsner, T. E., & Horton, R. (2007). Improved analysis of heat pulse signals for soil water flux determination. *Soil Science Society of America Journal*, 71(1), 53–55. <https://doi.org/10.2136/sssaj2006.0073N>
- Kluitenberg, G. J., & Philip, J. R. (1999). Dual thermal probes near plane interfaces. *Soil Science Society of America Journal*, 63(6), 1585–1591. <https://doi.org/10.2136/sssaj1999.6361585x>
- Kluitenberg, G. J., & Warrick, A. W. (2001). Improved evaluation procedure for heat-pulse soil water flux density method. *Soil Science Society of America Journal*, 65(2), 320–323. <https://doi.org/10.2136/sssaj2001.652320x>
- Knight, J. H. (1992). Sensitivity of time domain reflectometry measurements to lateral variations in soil water content. *Water Resources Research*, 28(9), 2345–2352. <https://doi.org/10.1029/92WR00747>
- Knight, J. H., Jin, W., & Kluitenberg, G. J. (2007). Sensitivity of the dual-probe heat-pulse method to spatial variations in heat capacity and water content. *Vadose Zone Journal*, 6(4), 746–758. <https://doi.org/10.2136/vzj2006.0170>
- Knight, J. H., & Kluitenberg, G. J. (2004). Simplified computational approach for dual-probe heat-pulse method. *Soil Science Society of America Journal*, 68(2), 447–449. <https://doi.org/10.2136/sssaj2004.4470>
- Knight, J., & Kluitenberg, G. (2013). Correcting for finite probe diameter in the dual probe heat pulse method of measuring soil water content, 20th International Congress on Modelling and Simulation (Modsim2013), 127–133.
- Knight, J. H., & Kluitenberg, G. J. (2015). A simple rational approximation for heat capacity determination with the dual-probe heat-pulse method. *Soil Science Society of America Journal*, 79(2), 495–498. <https://doi.org/10.2136/sssaj2014.11.0453n>
- Knight, J. H., Kluitenberg, G. J., & Kamai, T. (2016). The dual probe heat pulse method: Interaction between probes of finite radius and finite heat capacity. *Journal of Engineering Mathematics*, 99(1), 79–102. <https://doi.org/10.1007/s10665-015-9822-x>
- Knight, J. H., Kluitenberg, G. J., Kamai, T., & Hopmans, J. W. (2012). Semianalytical solution for dual-probe heat-pulse applications that accounts for probe radius and heat capacity. *Vadose Zone Journal*, 11(2). <https://doi.org/10.2136/vzj2011.0112>
- Kojima, Y. (2015). Sensible heat balance method to determine rates of soil freezing and thawing, (Ph.D. thesis, pp. 136). Iowa State University
- Kojima, Y., Heitman, J. L., Flerchinger, G. N., & Horton, R. (2013). Numerical evaluation of a sensible heat balance method to determine rates of soil freezing and thawing. *Vadose Zone Journal*, 12(1). <https://doi.org/10.2136/Vzj2012.0053>
- Kojima, Y., Heitman, J. L., Flerchinger, G. N., Ren, T., Ewing, R. P., & Horton, R. (2014). Field test and sensitivity analysis of a sensible heat balance method to determine soil ice contents. *Vadose Zone Journal*, 13(9). <https://doi.org/10.2136/vzj2014.04.0036>
- Kojima, Y., Heitman, J. L., Flerchinger, G. N., Ren, T., & Horton, R. (2016). Sensible heat balance estimates of transient soil ice contents. *Vadose Zone Journal*, 15(5). <https://doi.org/10.2136/vzj2015.10.0134>
- Kojima, Y., Heitman, J. L., Noborio, K., Ren, T., & Horton, R. (2018). Sensitivity analysis of temperature changes for determining thermal properties of partially frozen soil with a dual probe heat pulse sensor. *Cold Regions Science and Technology*, 151, 188–195. <https://doi.org/10.1016/j.coldregions.2018.03.022>
- Kolyshkin, A. A., Okoulich-Kazarin, E. G., & Vaillancourt, R. (1990). A combined unsteady method for the determination of thermal conductivity of gases and fluids. *International Communications in Heat and Mass Transfer*, 17(4), 521–526. [https://doi.org/10.1016/0735-1933\(90\)90070-z](https://doi.org/10.1016/0735-1933(90)90070-z)
- Kool, D., Agam, N., Lazarovich, N., Heitman, J. L., Sauer, T. J., & Ben-Gal, A. (2014). A review of approaches for evaporation partitioning. *Agricultural and Forest Meteorology*, 184, 56–70. <https://doi.org/10.1016/j.agrformet.2013.09.003>
- Kozłowski, T. (2012). Modulated Differential Scanning Calorimetry (MDSC) studies on low-temperature freezing of water adsorbed on clays, apparent specific heat of soil water and specific heat of dry soil. *Cold Regions Science and Technology*, 78, 89–96. <https://doi.org/10.1016/j.coldregions.2012.03.001>
- Kristiansen, J. I. (1982). The transient cylindrical probe method for determination of thermal parameters of earth materials, Geolog. Inst., Aarhus University, pp. 154.
- Lapenius, A., Henry, H., Vuille, M., & Mower, J. (2014). Climatic factors controlling plant sensitivity to warming. *Climatic Change*, 122(4), 723–734. <https://doi.org/10.1007/s10584-013-1010-2>
- Li, M., Barbour, S. L., & Si, B. (2015). Measuring solid percentage of oil sands mature fine tailings using the dual probe heat pulse method. *Journal of Environmental Quality*, 44(1), 293–298. <https://doi.org/10.2134/jeq2014.06.0262>
- Li, D., Sun, X., & Khaleel, M. (2012). Comparison of different up-scaling methods for predicting thermal conductivity of complex heterogeneous material system: Application on nuclear waste forms. *Metallurgical and Materials Transactions A-Physical Metallurgy and Material*, 44(S1), 61–69. <https://doi.org/10.1007/s11661-012-1269-3>
- Liang, X., Ge, X., Zhang, Y., & Wang, G. (1991). A convenient method of measuring the thermal conductivity of biological tissue. *Physics in Medicine and Biology*, 36(12), 1599–1605. <https://doi.org/10.1088/0031-9155/36/12/005>
- Liang, X., Lettenmaier, D. P., Wood, E. F., & Burges, S. J. (1994). A simple hydrologically based model of land surface water and energy fluxes for general circulation models. *Journal of Geophysical Research*, 99(D7), 14,415–14,428. <https://doi.org/10.1029/94JD00483>
- Liu, G., Horton, R., Si, B. C., Li, B., & Ren, T. (2008). Analytical solution of heat pulse method in a parallelepiped sample space with inclined needles. *Soil Science Society of America Journal*, 72(5), 1208–1216. <https://doi.org/10.2136/sssaj2007.0260>
- Liu, G., Li, B., Ren, T., & Horton, R. (2007). Analytical solution of the heat pulse method in a parallelepiped sample space. *Soil Science Society of America Journal*, 71(5), 1607–1619. <https://doi.org/10.2136/sssaj2006.0390>
- Liu, X., Lu, S., Horton, R., & Ren, T. (2014). In situ monitoring of soil bulk density with a thermo-TDR sensor. *Soil Science Society of America Journal*, 78(2), 400–407. <https://doi.org/10.2136/sssaj2013.07.0278>
- Liu, G., Lu, Y., Wen, M., Ren, T., & Horton, R. (2017). Advances in the heat-pulse technique: Improvements in measuring soil thermal properties. *Methods of Soil Analysis*, 2(1). <https://doi.org/10.2136/msa2015.0028>
- Liu, X., Ren, T., & Horton, R. (2008). Determination of soil bulk density with thermo-time domain reflectometry sensors. *Soil Science Society of America Journal*, 72(4), 1000–1005. <https://doi.org/10.2136/sssaj2007.0332>
- Liu, G., & Si, B. C. (2008). Dual-probe heat pulse method for snow density and thermal properties measurement. *Geophysical Research Letters*, 35, L16404. <https://doi.org/10.1029/2008GL034897>
- Liu, G., & Si, B. C. (2010). Errors analysis of heat pulse probe methods: Experiments and simulations. *Soil Science Society of America Journal*, 74(3), 797–803. <https://doi.org/10.2136/sssaj2009.0116>

- Liu, G., & Si, B. C. (2011a). Single- and dual-probe heat pulse probe for determining thermal properties of dry soils. *Soil Science Society of America Journal*, 75(3), 787–794. <https://doi.org/10.2136/sssaj2010.0241>
- Liu, G., & Si, B. C. (2011b). Soil ice content measurement using a heat pulse probe method. *Canadian Journal of Soil Science*, 91(2), 235–246. <https://doi.org/10.4141/cjss09120>
- Liu, G., Si, B. C., Jiang, A. X., Li, B. G., Ren, T. S., & Hu, K. L. (2012). Probe body and thermal contact conductivity affect error of heat pulse method based on infinite line source approximation. *Soil Science Society of America Journal*, 76(2), 370–374. <https://doi.org/10.2136/sssaj2011.0228n>
- Liu, G., Wen, M., Chang, X., Ren, T., & Horton, R. (2013). A self-calibrated DPHP sensor for in situ calibrating the probe spacing. *Soil Science Society of America Journal*, 77(2), 417–421. <https://doi.org/10.2136/sssaj2012.0434n>
- Liu, G., Wen, M., Ren, R., Si, B., Horton, R., & Hu, K. (2016). A general in situ probe spacing correction method for dual probe heat pulse sensor. *Agricultural and Forest Meteorology*, 226–227, 50–56. <https://doi.org/10.1016/j.agrformet.2016.05.011>
- Lu, Y., Horton, R., & Ren, T. (2018). Simultaneous determination of soil bulk density and water content: A heat pulse-based method. *European Journal of Soil Science*, 69(5), 947–952. <https://doi.org/10.1111/ejss.12690>
- Lu, Y., Horton, R., Zhang, X., & Ren, T. (2018). Accounting for soil porosity improves a thermal inertia model for estimating surface soil water content. *Remote Sensing of Environment*, 212, 79–89. <https://doi.org/10.1016/j.rse.2018.04.045>
- Lu, S., Ju, Z., Ren, T., & Horton, R. (2009). A general approach to estimate soil water content from thermal inertia. *Agricultural and Forest Meteorology*, 149(10), 1693–1698. <https://doi.org/10.1016/j.agrformet.2009.05.011>
- Lu, Y., Liu, X., Heitman, J., Horton, R., & Ren, T. (2016). Determining soil bulk density with thermo-time domain reflectometry: A thermal conductivity-based approach. *Soil Science Society of America Journal*, 80(1), 48–54. <https://doi.org/10.2136/sssaj2015.08.0315>
- Lu, Y., Liu, X., Zhang, M., Heitman, J., Horton, R., & Ren, T. (2017). Thermo-time domain reflectometry method: Advances in monitoring in situ soil bulk density. *Methods of Soil Analysis*, 2(1). <https://doi.org/10.2136/msa2015.0031>
- Lu, Y., Lu, S., Horton, R., & Ren, T. (2014). An empirical model for estimating soil thermal conductivity from texture, water content, and bulk density. *Soil Science Society of America Journal*, 78(6), 1859–1868. <https://doi.org/10.2136/sssaj2014.05.0218>
- Lu, X., Ren, T., & Gong, Y. (2009). Experimental investigation of thermal dispersion in saturated soils with one-dimensional water flow. *Soil Science Society of America Journal*, 73(6), 1912–1920. <https://doi.org/10.2136/sssaj2008.0251>
- Lu, S., Ren, T., Gong, Y., & Horton, R. (2007). An improved model for predicting soil thermal conductivity from water content at room temperature. *Soil Science Society of America Journal*, 71(1), 8–14. <https://doi.org/10.2136/sssaj2006.0041>
- Lu, Y., Wang, Y., & Ren, T. (2013). Using late time data improves the heat-pulse method for estimating soil thermal properties with the pulsed infinite line source theory. *Vadose Zone Journal*, 12(4). <https://doi.org/10.2136/vzj2013.01.0011>
- Lubimova, H. A., Lusova, L. M., Firsov, F. V., Starikova, G. N., & Shushpanov, A. P. (1961). Determination of surface heat flow in Mazesta (USSR). *Annales de Géophysique*, 14(2), 157–167. <https://doi.org/10.4401/ag-5291>
- Lynch, A. H., McGinnis, D. L., & Bailey, D. A. (1998). Snow-albedo feedback and the spring transition in a regional climate system model: Influence of land surface model. *Journal of Geophysical Research*, 103(D22), 29,037–29,049. <https://doi.org/10.1029/98JD00790>
- Maltese, A., Minacapilli, M., Cammalleri, C., Ciraolo, G., & D'Asaro, F. (2010). A thermal inertia model for soil water content retrieval using thermal and multispectral images, Proceedings of SPIE-The International Society for Optical Engineering. <https://doi.org/10.1117/12.864672>
- Marczewski, W., Schröer, K., Seiferlin, K., Usowicz, B., Banaszkiewicz, M., Hlond, M., et al. (2004). Prelaunch performance evaluation of the cometary experiment MUPUS-TP. *Journal of Geophysical Research*, 109(E7), E07S09. <https://doi.org/10.1029/2003JE002192>
- Marshall, D. C. (1958). Measurement of sap flow in conifers by heat transport. *Plant Physiology*, 33(6), 385–396. <https://doi.org/10.1104/pp.33.6.385>
- Massey, J. D., Steenburgh, W. J., Hoch, S. W., & Knievel, J. C. (2014). Sensitivity of near-surface temperature forecasts to soil properties over a sparsely vegetated dryland region. *Journal of Applied Meteorology and Climatology*, 53(8), 1976–1995. <https://doi.org/10.1175/jamc-d-13-0362.1>
- McCumber, M. C., & Pielke, R. A. (1981). Simulation of the effects of surface fluxes of heat and moisture in a mesoscale numerical model: 1. Soil layer. *Journal of Geophysical Research*, 86(C10), 9929–9938. <https://doi.org/10.1029/JC086JC10p09929>
- Mend (2012). Cold regions cover system design technical guidance document, MEND Report 1.61.5c. Aboriginal Affairs and Northern Development Canada (AANDC) and MEND.
- Merrill, R. B. (1968). Thermal conduction through an evacuated idealized powder over the temperature range of 100 to 500 degrees K, (Ph.D. thesis, pp. 108). Ann Arbor: Brigham Young University.
- Minacapilli, M., Cammalleri, C., Ciraolo, G., D'Asaro, F., Iovino, M., & Maltese, A. (2012). Thermal inertia modeling for soil surface water content estimation: A laboratory experiment. *Soil Science Society of America Journal*, 76(1), 92–100. <https://doi.org/10.2136/sssaj2011.0122>
- Moench, A., & Evans, D. (1970). Thermal conductivity and diffusivity of soil using a cylindrical heat source. *Soil Science Society of America Journal*, 34(3), 377–381. <https://doi.org/10.2136/sssaj1970.03615995003400030012x>
- Morabito, P. (1989). Thermal conductivity and diffusivity measurements by the transient two linear and parallel probe method. *Thermochimica Acta*, 148, 513–520. [https://doi.org/10.1016/0040-6031\(89\)85255-4](https://doi.org/10.1016/0040-6031(89)85255-4)
- Mori, Y., Hopmans, J. W., Mortensen, A. P., & Kluitenberg, G. J. (2003). Multi-functional heat pulse probe for the simultaneous measurement of soil water content, solute concentration, and heat transport parameters. *Vadose Zone Journal*, 2(4), 561–571. <https://doi.org/10.2113/2.4.561>
- Mori, Y., Hopmans, J. W., Mortensen, A. P., & Kluitenberg, G. J. (2005). Estimation of vadose zone water flux from multi-functional heat pulse probe measurements. *Soil Science Society of America Journal*, 69(3), 599–606. <https://doi.org/10.2136/sssaj2004.0174>
- Morin, S., Domine, F., Arnaud, L., & Picard, G. (2010). In-situ monitoring of the time evolution of the effective thermal conductivity of snow, International Snow Science Workshop 2009 Davos. *Cold Regions Science and Technology*, 64(2), 73–80. <https://doi.org/10.1016/j.coldregions.2010.02.008>
- Mortensen, A. P., Hopmans, J. W., Mori, Y., & Simunek, J. (2006). Multi-functional heat pulse probe measurements of coupled vadose zone flow and transport. *Advances in Water Resources*, 29(2), 250–267. <https://doi.org/10.1016/j.advwatres.2005.03.017>
- Nagai, T., & Makino, A. (2011). Differences between rice and wheat in temperature responses of photosynthesis and plant growth. *Plant & Cell Physiology*, 50(4), 744–755. <https://doi.org/10.1093/pcp/pcp029>
- Nagasaka, Y., & Nagashima, A. (1981). Simultaneous measurement of the thermal conductivity and the thermal diffusivity of liquids by the transient hot-wire method. *The Review of Scientific Instruments*, 52(2), 229–232. <https://doi.org/10.1063/1.1136577>
- Nagihara, S., Hedlund, M., Zacny, K., & Taylor, P. T. (2014). Improved data reduction algorithm for the needle probe method applied to in-situ thermal conductivity measurements of lunar and planetary regoliths. *Planetary and Space Science*, 92, 49–56. <https://doi.org/10.1016/j.pss.2013.12.012>

- Nagpal, N., & Boersma, L. (1973). Air entrapment as a possible source of error in the use of a cylindrical heat probe. *Soil Science Society of America Journal*, 37(6), 828–832. <https://doi.org/10.2136/sssaj1973.03615995003700060014x>
- Nassar, I. N., Globus, A. M., & Horton, R. (1992). Simultaneous soil heat and water transfer. *Soil Science*, 154(6), 465–472. <https://doi.org/10.1097/00010694-19921200-00005>
- Nassar, I. N., & Horton, R. (1989). Water transport in unsaturated nonisothermal, salty soil: II. Theoretical development. *Soil Science Society of America Journal*, 53(5), 1330–1337. <https://doi.org/10.2136/sssaj1989.03615995005300050005x>
- Nassar, I. N., & Horton, R. (1992). Simultaneous transfer of heat, water, and solute in porous media: I. Theoretical development. *Soil Science Society of America Journal*, 56(5), 1350–1356. <https://doi.org/10.2136/sssaj1992.03615995005600050004x>
- Nassar, I. N., & Horton, R. (1997). Heat, water, and solute transfer in unsaturated porous media: I. Theory development and transport coefficient evaluation. *Transport in Porous Media*, 27(1), 17–38. <https://doi.org/10.1023/A:1006583918576>
- Nassar, I. N., Horton, R., & Globus, A. M. (1997). Thermally induced water transfer in saline, unsaturated soil. *Soil Science Society of America Journal*, 61(5), 1293–1299. <https://doi.org/10.2136/sssaj1997.03615995006100050002x>
- Nicolas, J., André, P., Rivez, J. F., & Debbaut, V. (1993). Thermal conductivity measurements in soil using an instrument based on the cylindrical probe method. *The Review of Scientific Instruments*, 64(3), 774–780. <https://doi.org/10.1063/1.1144158>
- Niu, G. Y., Yang, Z. L., Mitchell, K. E., Chen, F., Ek, M. B., Barlage, M., et al. (2011). The community Noah land surface model with multiparameterization options (Noah-MP): 1. Model description and evaluation with local-scale measurements. *Journal of Geophysical Research*, 116(D12), D12109. <https://doi.org/10.1029/2010JD015139>
- Niven, C. (1905). On a method of finding the conductivity for heat. *Proceedings of the Royal Society of London. Series A, Containing Papers of a Mathematical and Physical Character*, 76(507), 34–48. <https://doi.org/10.1098/rspa.1905.0003>
- Niven, C., & Geddes, A. E. M. (1912). On a method of finding the conductivity for heat. *Proceedings of the Royal Society of London. Series A, Containing Papers of a Mathematical and Physical Character*, 87(598), 535–539. <https://doi.org/10.1098/rspa.1912.0108>
- Nix, G., Lowery, G., Vachon, R., & Tanger, G. (1967). Direct determination of thermal diffusivity and conductivity with a refined line-source technique. In G. B. Heller (Ed.), *Thermophysics of spacecraft and planetary bodies* (pp. 865–878). Cambridge: Academic Press.
- Noborio, K. (2001). Measurement of soil water content and electrical conductivity by time domain reflectometry: A review. *Computers and Electronics in Agriculture*, 31(3), 213–237. [https://doi.org/10.1016/S0168-1699\(00\)00184-8](https://doi.org/10.1016/S0168-1699(00)00184-8)
- Noborio, K., Horton, R., & Tan, C. S. (1999). Time domain reflectometry probe for simultaneous measurement of soil matric potential and water content. *Soil Science Society of America Journal*, 63(6), 1500–1505. <https://doi.org/10.2136/sssaj1999.6361500x>
- Noborio, K., McInnes, K. J., & Heilman, J. L. (1996a). Two dimensional model for water, heat, and solute transport in furrow-irrigated soil: I. Theory. *Soil Science Society of America Journal*, 60(4), 1010–1021. <https://doi.org/10.2136/sssaj1996.03615995006000040008x>
- Noborio, K., McInnes, K. J., & Heilman, J. L. (1996b). Measurements of soil water content, heat capacity, and thermal conductivity with a single TDR probe. *Soil Science*, 161(1), 22–28. <https://doi.org/10.1097/00010694-199601000-00004>
- Noborio, K., McInnes, K. J., & Heilman, J. L. (2002). On measuring soil thermal properties with a dual-probe heat-pulse technique [in Japanese with English abstract]. *Journal of the Japanese Society of Soil Physics*, 90, 3–9.
- Ochsner, T. E., & Baker, J. M. (2008). In situ monitoring of soil thermal properties and heat flux during freezing and thawing. *Soil Science Society of America Journal*, 72(4), 1025–1032. <https://doi.org/10.2136/sssaj2007.0283>
- Ochsner, T. E., Horton, R., Kluitenberg, G. J., & Wang, Q. (2005). Evaluation of the heat pulse ratio technique for measuring soil water flux. *Soil Science Society of America Journal*, 69(3), 757–765. <https://doi.org/10.2136/sssaj2004.0278>
- Ochsner, T. E., Horton, R., & Ren, T. (2001a). A new perspective on soil thermal properties. *Soil Science Society of America Journal*, 65(6), 1641–1647. <https://doi.org/10.2136/sssaj2001.1641>
- Ochsner, T. E., Horton, R., & Ren, T. (2001b). Simultaneous water content, air-filled porosity, and bulk density measurements with thermo-time domain reflectometry. *Soil Science Society of America Journal*, 65(6), 1618–1622. <https://doi.org/10.2136/sssaj2001.1618>
- Ochsner, T. E., Horton, R., & Ren, T. (2003). Use of the dual-probe heat-pulse technique to monitor soil water content. *Vadose Zone Journal*, 2(4), 572–579. <https://doi.org/10.2136/vzj2003.5720>
- Ochsner, T. E., Horton, R., & Sauer, T. J. (2006). Field tests of the soil heat flux plate method and some alternatives. *Agronomy Journal*, 98(4), 1005–1014. <https://doi.org/10.2134/agronj2005.0249>
- Olmanson, O. K., & Ochsner, T. E. (2006). Comparing ambient temperature effects on heat pulse and time domain reflectometry soil water content measurements. *Vadose Zone Journal*, 5(2), 751–756. <https://doi.org/10.2136/vzj2005.0114>
- Olmanson, O. K., & Ochsner, T. E. (2008). A partial cylindrical thermo-time domain reflectometry sensor. *Soil Science Society of America Journal*, 72(3), 571–577. <https://doi.org/10.2136/sssaj2007.0084>
- Or, D., Lehmann, P., Shahraeeni, E., & Shokri, N. (2013). Advances in soil evaporation physics—A review. *Vadose Zone Journal*, 12(4). <https://doi.org/10.2136/vzj2012.0163>
- Or, D., & Wraith, J. M. (1999). A new soil metric potential sensor based on time domain reflectometry. *Water Resources Research*, 35(11), 3399–3407. <https://doi.org/10.1029/1999WR900226>
- Overduin, P. P., Kane, D. L., & van Loon, W. K. P. (2006). Measuring thermal conductivity in freezing and thawing soil using the soil temperature response to heating. *Cold Regions Science and Technology*, 45(1), 8–22. <https://doi.org/10.1016/j.coldregions.2005.12.003>
- Palaparthi, V. S., Sarik, S., Mehta, A., Singh, K. K., & Baghini, M. S. (2015). An automated, self sustained soil moisture measurement system using low power dual probe heat pulse (DPHP) sensor, Paper presented at SENSORS, 2015 IEEE, 1–4 Nov. 2015.
- Papadakis, G., Glaglaras, P., & Kyritsis, S. (1990). A numerical method for determining thermal conductivity of porous media from in-situ measurements using a cylindrical heat source. *Journal of Agricultural Engineering Research*, 45(4), 281–293. [https://doi.org/10.1016/S0021-8634\(05\)80155-6](https://doi.org/10.1016/S0021-8634(05)80155-6)
- Pedersen, S. H., Liston, G. E., Tamstorf, M. P., Westergaard-Nielsen, A., & Schmidt, N. M. (2015). Quantifying episodic snowmelt events in arctic ecosystems. *Ecosystems*, 18(5), 839–856. <https://doi.org/10.1007/s10021-015-9867-8>
- Peng, X., Heitman, J., Horton, R., & Ren, T. (2015). Field evaluation and improvement of the plate method for measuring soil heat flux density. *Agricultural and Forest Meteorology*, 214–215, 341–349. <https://doi.org/10.1016/j.agrformet.2015.09.001>
- Peng, X., Wang, Y., Heitman, J., Ochsner, T., Horton, R., & Ren, T. (2017). Measurement of soil-surface heat flux with a multi-needle heat-pulse probe. *European Journal of Soil Science*, 68(3), 336–344. <https://doi.org/10.1111/ejss.12421>
- Penner, E. (1970). Thermal conductivity of frozen soils. *Canadian Journal of Earth Sciences*, 7(3), 982–987. <https://doi.org/10.1139/E70-091>
- Peters-Lidard, C. D., Blackburn, E., Liang, X., & Wood, E. F. (1998). The effect of soil thermal conductivity parameterization on surface energy fluxes and temperatures. *Journal of the Atmospheric Sciences*, 55(7), 1209–1224. [https://doi.org/10.1175/1520-0469\(1998\)055<1209:TEOSTC>2.0.CO;2](https://doi.org/10.1175/1520-0469(1998)055<1209:TEOSTC>2.0.CO;2)

- Philip, R. J., & Kluitenberg, G. J. (1999). Errors of dual thermal probes to soil heterogeneity across a plane interface. *Soil Science Society of America Journal*, 63(6), 1579–1585. <https://doi.org/10.2136/sssaj1999.6361579x>
- Pieri, P. (2010). Modelling radiative balance in a row-crop canopy: Row–soil surface net radiation partition. *Ecological Modelling*, 221(5), 791–801. <https://doi.org/10.1016/j.ecolmodel.2009.11.019>
- Pilkington, B., & Grove, S. (2012). Thermal conductivity probe length to radius ratio problem when measuring building insulation materials. *Construction and Building Materials*, 35, 531–546. <https://doi.org/10.1016/j.conbuildmat.2012.04.108>
- Presley, M. A. (1995). Thermal conductivity measurements of particulate materials: Implications for surficial units on Mars, (Ph.D. thesis, pp. 237). Ann Arbor: Arizona State University.
- Presley, M. A., & Christensen, P. R. (1997). Thermal conductivity measurements of particulate materials 1. A review. *Journal of Geophysical Research*, 102(E3), 6535–6549. <https://doi.org/10.1029/96JE03302>
- Price, J. C. (1977). Thermal inertia mapping: A new view of the Earth. *Journal of Geophysical Research*, 82(18), 2582–2590. <https://doi.org/10.1029/JC082i018p02582>
- Progelhof, R. C., Throne, J. L., & Ruetsch, R. R. (1976). Methods for predicting the thermal conductivity of composite systems: A review. *Polymer Engineering and Science*, 16(9), 615–625. <https://doi.org/10.1002/pen.760160905>
- Prowse, T. D., Furgal, C., Chouinard, R., Mellings, H., Milburn, D., & Smith, S. L. (2009). Implications of climate change for economic development in northern Canada: Energy, resource, and transportation sectors. *Ambio*, 38(5), 272–281.
- Pusch, R., Anderson, D. M., & Andersland, O. B. (1978). Physical and thermal properties of frozen ground. In E. Penner (Ed.), *Geotechnical engineering for cold regions* (pp. 37–102). New York: McGraw-Hill Book Company.
- Putkonen, J. (2003). Determination of frozen soil thermal properties by heated needle probe. *Permafrost and Periglacial Processes*, 14(4), 343–347. <https://doi.org/10.1002/ppp.465>
- Quintard, M., & Whitaker, S. (1995). Local thermal equilibrium for transient heat conduction: Theory and comparison with numerical experiments. *International Journal of Heat and Mass Transfer*, 38(15), 2779–2796. [https://doi.org/10.1016/0017-9310\(95\)00028-8](https://doi.org/10.1016/0017-9310(95)00028-8)
- Ranzi, R., Grossi, G., Gitti, A., & Taschner, S. (2010). Energy and mass balance of the Mandrone glacier (Adamello, Central Alps). *Geografia Fisica e Dinamica Quaternaria*, 33(1), 45–60.
- Rau, G. C., Andersen, M. S., McCallum, A. M., Roshan, H., & Acworth, R. I. (2014). Heat as a tracer to quantify water flow in near-surface sediments. *Earth Science Reviews*, 129, 40–58. <https://doi.org/10.1016/j.earscirev.2013.10.015>
- Ren, T., Horton, R., & Noborio, K. (1999). Measuring soil water content, electrical conductivity, and thermal properties with a thermo-time domain reflectometry probe. *Soil Science Society of America Journal*, 63(3), 450–457. <https://doi.org/10.2136/sssaj1999.03615995006300030005x>
- Ren, T., Horton, R., & Ochsner, T. E. (2003). Development of thermo-time domain reflectometry for vadose zone measurements. *Vadose Zone Journal*, 2(4), 544–551. <https://doi.org/10.2136/vzj2003.5440>
- Ren, T., Ju, Z., Gong, Y., & Horton, R. (2005). Comparing heat-pulse and time domain reflectometry soil water contents from thermo-time domain reflectometry probes. *Vadose Zone Journal*, 4(4). <https://doi.org/10.2136/vzj2004.0139>
- Ren, T., Kluitenberg, G. J., & Horton, R. (2000). Determining soil water flux and pore water velocity by a heat pulse technique. *Soil Science Society of America Journal*, 64(2), 552–560. <https://doi.org/10.2136/sssaj2000.642552x>
- Ren, T., Ochsner, T. E., Horton, R., & Ju, Z. (2003). Heat-pulse method for soil water content measurement: Influence of the specific heat of the soil solids. *Soil Science Society of America Journal*, 67(6), 1631–1634. <https://doi.org/10.2136/sssaj2003.1631>
- Riche, F., & Schneebeli, M. (2010). Microstructural change around a needle probe to measure thermal conductivity of snow. *Journal of Glaciology*, 56(199), 871–876. <https://doi.org/10.3189/002214310794457164>
- Robinson, D. A., Jones, S. B., Wraith, J. M., Or, D., & Friedman, S. P. (2003). A review of advances in dielectric and electrical conductivity measurement in soils using time domain reflectometry. *Vadose Zone Journal*, 2(4), 444–475. <https://doi.org/10.2136/vzj2003.4440>
- Roshan, H., Cuthbert, M. O., Andersen, M. S., & Acworth, R. I. (2014). Local thermal non-equilibrium in sediments: Implications for temperature dynamics and the use of heat as a tracer. *Advances in Water Resources*, 73, 176–184. <https://doi.org/10.1016/j.advwatres.2014.08.002>
- Saito, T., Hamamoto, S., Mon, E. E., Takemura, T., Saito, H., Komatsu, T., & Moldrup, P. (2014). Thermal properties of boring core samples from the Kanto area, Japan: Development of predictive models for thermal conductivity and diffusivity. *Soils and Foundations*, 54(2), 116–125. <https://doi.org/10.1016/j.sandf.2014.02.004>
- Saito, H., Šimůnek, J., Hopmans, J. W., & Tuli, A. (2007). Numerical evaluation of alternative heat pulse probe designs and analyses. *Water Resources Research*, 43, W07408. <https://doi.org/10.1029/2006WR005320>
- Sakai, M., Jones, S. B., & Tuller, M. (2011). Numerical evaluation of subsurface soil water evaporation derived from sensible heat balance. *Water Resources Research*, 47, W02547. <https://doi.org/10.1029/2010WR009866>
- Sass, J., Stone, C., & Munroe, R. J. (1984). Thermal conductivity determinations on solid rock—a comparison between a steady-state divided-bar apparatus and a commercial transient line-source device. *Journal of Volcanology and Geothermal Research*, 20(1–2), 145–153. [https://doi.org/10.1016/0377-0273\(84\)90071-4](https://doi.org/10.1016/0377-0273(84)90071-4)
- Sauer, T. J., Ochsner, T. E., & Horton, R. (2007). Soil heat flux plates: Heat flow distortion and thermal contact resistance. *Agronomy Journal*, 99(1), 304–310. <https://doi.org/10.2134/agronj2005.0038s>
- Sayde, C., Buelga, J., Rodriguez-Sinobas, L., Khouri, L., English, M., van de Giesen, N., & Selker, J. S. (2014). Mapping variability of soil water content and flux across 1–1000 m scales using the actively heated fiber optic method. *Water Resources Research*, 50, 7302–7317. <https://doi.org/10.1002/2013WR014983>
- Sayde, C., Gregory, C., Gil-Rodriguez, M., Tufillaro, N., Tyler, S., van de Giesen, N., et al. (2010). Feasibility of soil moisture monitoring with heated fiber optics. *Water Resources Research*, 46, W06201. <https://doi.org/10.1029/2009WR007846>
- Schleiermacher, A. L. E. F. (1888). On the thermal conduction of gas. *Wiedemann's Annalen der Physik*, 34, 623–646.
- Schubert, J., & Schumacher, T. (2005). Construction of three needle heat pulse sensors, edited.
- Selker, J. S., Thévenaz, L., Huwald, H., Mallet, A., Luxemburg, W., van de Giesen, N., et al. (2006). Distributed fiber-optic temperature sensing for hydrologic systems. *Water Resources Research*, 42, W12202. <https://doi.org/10.1029/2006WR005326>
- Sepaskhah, A. R., & Boersma, L. (1979). Thermal conductivity of soils as a function of temperature and water content. *Soil Science Society of America Journal*, 43(3), 439–444. <https://doi.org/10.2136/sssaj1979.03615995004300030003x>
- Sheng, W. Y., Rumana, K., Sakai, M., Silfa, F., & Jones, S. B. (2016). A multi-functional penta-needle thermo-dielectric sensor for porous media sensing. *IEEE Sensors Journal*, 16(10), 3670–3678. <https://doi.org/10.1109/JSEN.2016.2527020>
- Shiozawa, S., & Campbell, G. S. (1990). Soil thermal conductivity. *Remote Sensing Reviews*, 5(1), 301–310. <https://doi.org/10.1080/02757259009532137>
- Si, B., Kachanoski, R. G., Zhang, F., Parkin, G. W., & Elrick, D. E. (1999). Measurement of hydraulic properties during constant flux infiltration field average. *Soil Science Society of America Journal*, 63(4), 793–799. <https://doi.org/10.2136/sssaj1999.634793x>

- Simunek, J., Huang, K., & van Genuchten, M. T. (1997). The HYDRUS-ET software package for simulating the one-dimensional movement of water, heat and multiple solutes in variably-saturated media, version 1.1. Bratislava: Inst. Hydrology Slovak Acad. Sci.
- Song, Y., Ham, J. M., Kirkham, M. B., & Kluitenberg, G. J. (1998). Measuring soil water content under turfgrass using the dual-probe heat-pulse technique. *Journal of the American Society for Horticultural Science*, 123(5), 937–941.
- Song, Y., Kirkham, M. B., Ham, J. M., & Kluitenberg, G. J. (1999). Measurement resolution of the dual-probe heat-pulse technique. In M. T. van Genuchten & F. J. Leij (Eds.), *Characterization and measurement of the hydraulic properties of unsaturated porous media* (pp. 381–386). Riverside, California: University of California.
- Song, Y., Kirkham, M. B., Ham, J. M., & Kluitenberg, G. J. (2000). Root-zone hydraulic lift evaluated with the dual-probe heat-pulse technique. *Soil Research*, 38(5), 927–935. <https://doi.org/10.1071/SR99096>
- Stalhane, B., & Pyk, S. (1931). New method for determining the coefficients of thermal conductivity. *Teknisk Tidsskrift*, 61, 389–393.
- Steele-Dunne, S. C., Ruttan, M. M., Krzeminska, D. M., Hausner, M., Tyler, S. W., Selker, J., et al. (2010). Feasibility of soil moisture estimation using passive distributed temperature sensing. *Water Resources Research*, 46, W03534. <https://doi.org/10.1029/2009WR008272>
- Steinhart, J. S., & Hart, S. R. (1968). Calibration curves for thermistors. *Deep Sea Research*, 15, 497–503.
- Striegl, A. M., & Loehde, S. P. (2012). Heated distributed temperature sensing for field scale soil moisture monitoring. *Ground Water*, 50(3), 340–347. <https://doi.org/10.1111/j.1745-6584.2012.00928.x>
- Sun, H., Liu, S., & Qin, J. (2016). Characterizing subzero-temperature thermal properties of seasonally frozen soil in alpine forest in the western Sichuan Province, China. *Journal of Water Resource and Protection*, 08(05), 583–593. <https://doi.org/10.4236/jwarp.2016.85048>
- Swanson, R. H. (1994). Significant historical developments in thermal methods for measuring sap flow in trees. *Agricultural and Forest Meteorology*, 72(1–2), 113–132. [https://doi.org/10.1016/0168-1923\(94\)90094-9](https://doi.org/10.1016/0168-1923(94)90094-9)
- Tarara, J. M., & Ham, J. M. (1997). Measuring soil water content in the laboratory and field with dual-probe heat-capacity sensors. *Agronomy Journal*, 89(4), 535–542. <https://doi.org/10.2134/agronj1997.00021962008900040001x>
- Tavman, I. H. (1996). Effective thermal conductivity of granular porous materials. *International Communications in Heat and Mass Transfer*, 23(2), 169–176. [https://doi.org/10.1016/0735-1933\(96\)00003-6](https://doi.org/10.1016/0735-1933(96)00003-6)
- Tian, Z., Heitman, J. L., Horton, R., & Ren, T. (2015). Determining soil ice contents during freezing and thawing with thermo-time domain reflectometry. *Vadose Zone Journal*, 14(8). <https://doi.org/10.2136/vzj2014.12.0179>
- Tian, Z., Lu, Y., Ren, T., Horton, R., & Heitman, J. L. (2018). Improved thermo-time domain reflectometry method for continuous in-situ determination of soil bulk density. *Soil and Tillage Research*, 178, 118–129. <https://doi.org/10.1016/j.still.2017.12.021>
- Tian, Z., Ren, T., Kojima, Y., Lu, Y., Horton, R., & Heitman, J. L. (2017). An improved thermo-time domain reflectometry method for determination of ice contents in partially frozen soils. *Journal of Hydrology*, 555, 786–796. <https://doi.org/10.1016/j.jhydrol.2017.10.055>
- Tokumoto, I., Noborio, K., & Koga, K. (2010). Coupled water and heat flow in a grass field with aggregated Andisol during soil-freezing periods. *Cold Regions Science and Technology*, 62(2–3), 98–106. <https://doi.org/10.1016/j.coldregions.2010.03.005>
- Topp, G. C., Annan, A. P., & Davis, J. L. (1980). Electromagnetic determination of soil water content: Measurements in coaxial transmission lines. *Water Resources Research*, 16(3), 574–582. <https://doi.org/10.1029/WR016i003p00574>
- Topp, G. C., Zebchuk, W. D., Davis, J. L., & Bailey, W. G. (1984). The measurement of soil water content using a portable TDR hand probe. *Canadian Journal of Soil Science*, 64(3), 313–321. <https://doi.org/10.4141/cjss84-033>
- Trautz, A. C., Smits, K. M., Schulte, P., & Illangasekare, T. H. (2014). Sensible heat balance and heat-pulse method applicability to in situ soil-water evaporation. *Vadose Zone Journal*, 13(1). <https://doi.org/10.2136/vzj2012.0215>
- Tyler, S. W., Selker, J. S., Hausner, M. B., Hatch, C. E., Torgersen, T., Thodal, C. E., & Schladow, S. G. (2009). Environmental temperature sensing using Raman spectra DTS fiber-optic methods. *Water Resources Research*, 45, W00D23. <https://doi.org/10.1029/2008WR007052>
- Valvano, J., Allen, J., & Bowman, H. (1984). The simultaneous measurement of thermal conductivity, thermal diffusivity, and perfusion in small volumes of tissue. *Journal of Biomechanical Engineering*, 106(3), 192–197.
- van der Held, E. F. M. (1932). Warmte-Technik, 2, 21. In J. Horrocks & E. McLaughlin (1963). Non-steady-state measurements of the thermal conductivities of liquid polyphenyls. *Proceedings of the Royal Society of London. Series A, Mathematical and Physical Sciences*, 273, 259–274.
- Van der Held, E. F. M. (1952). The contribution of radiation to the conduction of heat. *Applied Scientific Research. Series A, Mechanics, Heat, Chemical Engineering, Mathematical Methods*, 3, 237–249.
- Van der Held, E. F. M. (1953). The contribution of radiation to the conduction of heat. *Applied Scientific Research. Series A, Mechanics, Heat, Chemical Engineering, Mathematical Methods*, 4, 77–99.
- Van der Held, E. F. M., & Van Drunen, F. G. (1949). A method of measuring the thermal conductivity of liquids. *Physica*, 15(10), 865–881. [https://doi.org/10.1016/0031-8914\(49\)90129-9](https://doi.org/10.1016/0031-8914(49)90129-9)
- Van Dorssen, J. C. (1949). Nijverheidsorganisatie Toegepast Natuurwetenschap-pelijk Onderzoek. Rap. 7. In de Vries, D. A. (1952), A non-stationary method for determining thermal conductivity of soil in situ. *Soil Science*, 73(2), 83–90.
- Van Haneghem, I. A., Schenk, J., & Boshoven, H. P. A. (1983). An improved non-steady state probe method for measurements in granular materials part II: Experimental results, Paper presented at Proceeding of the 8th European Thermophysical Properties Conference.
- Verma, L. S., Singh, R., & Chaudhary, D. R. (1993). Probe controlled transient method for simultaneous determination of thermal conductivity and thermal diffusivity. *Journal of Physics D: Applied Physics*, 26(2), 259–270. <https://doi.org/10.1088/0022-3727/26/2/014>
- Verstraeten, W. W., Veroustraete, F., van der Sande, C. J., Grootaers, I., & Feyen, J. (2006). Soil moisture retrieval using thermal inertia, determined with visible and thermal spaceborne data, validated for European forests. *Remote Sensing of Environment*, 101(3), 299–314. <https://doi.org/10.1016/j.rse.2005.12.016>
- Waite, W. F., Gilbert, L. Y., Winters, W. J., & Mason, D. H. (2006). Estimating thermal diffusivity and specific heat from needle probe thermal conductivity data. *The Review of Scientific Instruments*, 77(4), 044904. <https://doi.org/10.1063/1.2194481>
- Wang, Z., Kojima, Y., Lu, S., Chen, Y., Horton, R., & Schwartz, R. C. (2014). Time domain reflectometry waveform analysis with second-order bounded mean oscillation. *Soil Science Society of America Journal*, 78(4), 1146–1152. <https://doi.org/10.2136/sssaj2013.11.0497>
- Wang, Z., Lu, Y., Kojima, Y., Lu, S., Zhang, M., Chen, Y., & Horton, R. (2016). Tangent line/second-order bounded mean oscillation waveform analysis for short TDR probe. *Vadose Zone Journal*, 15(1), 15(1). <https://doi.org/10.2136/vzj2015.04.0054>
- Wang, Y., Ochsner, T., Heitman, J., Horton, R., Xue, X., & Ren, T. (2017). Weighing lysimeter data confirm the accuracy and precision of the heat-pulse technique for measuring daily soil evaporation. *Soil Science Society of America Journal*, 81(5). <https://doi.org/10.2136/sssaj2017.02.0049>
- Wang, Q., Ochsner, T. E., & Horton, R. (2002). Mathematical analysis of heat pulse signals for soil water flux determination. *Water Resources Research*, 38(6), 1091. <https://doi.org/10.1029/2001WR001089>

- Wang, X. J., Yang, M. X., Pang, G. J., Wan, G. N., & Chen, X. L. (2015). Simulation and improvement of land surface processes in Nameqie, Central Tibetan Plateau, using the Community Land Model (CLM3.5). *Environment and Earth Science*, 73(11), 7343–7357. <https://doi.org/10.1007/s12665-014-3911-4>
- Wechsler, A. E. (1966). Development of thermal conductivity probes for soils and insulations, (Tech. Rep. 182, p. 83). Hamover, New Hampshire: CRREL.
- Wechsler, A. E., & Glaser, P. E. (1965). Pressure effects on postulated lunar materials. *Icarus*, 4(4), 335–352. [https://doi.org/10.1016/0019-1035\(65\)90038-2](https://doi.org/10.1016/0019-1035(65)90038-2)
- Weishaupt, J. (1940). Nichtstationäres Verfahren zur bestimmung der Wärmeleitzahl von Flüssigkeiten (Non-stationary methods for determination of thermal conductivity of liquids). *Forschung im Ingenieurwesen*, 11(1), 20–34. <https://doi.org/10.1007/BF02584104>
- Weiss, J. D. (2003). Using fiber optics to detect moisture intrusion into a landfill cap consisting of a vegetative soil barrier. *Journal of the Air & Waste Management Association*, 53(9), 1130–1148. <https://doi.org/10.1080/10473289.2003.10466268>
- Welch, S. M., Kluitenberg, G. J., & Bristow, K. L. (1996). Rapid numerical estimation of soil thermal properties for a broad class of heat pulse emitter geometries. *Measurement Science and Technology*, 7(6), 932–938. <https://doi.org/10.1088/0957-0233/7/6/012>
- Wen, M., Liu, G., Li, B., Si, B., & Horton, R. (2015). Evaluation of a self-correcting dual probe heat pulse sensor. *Agricultural and Forest Meteorology*, 200, 203–208. <https://doi.org/10.1016/j.agrformet.2014.09.022>
- White, D. E. (1973). Characteristics of geothermal resources. In P. Kruger & C. Otte (Eds.), *Geothermal energy* (pp. 69–94). Stanford: Stanford University Press.
- Wild, M., Folini, D., Hakuba, M. Z., Schär, C., Seneviratne, S. I., Kato, S., et al. (2014). The energy balance over land and oceans: An assessment based on direct observations and CMIP5 climate models. *Climate Dynamics*, 44(11–12), 3393–3429. <https://doi.org/10.1007/s00382-014-2430-z>
- Wilson, K., Goldstein, A., Falge, E., Aubinet, M., Baldocchi, D., Berbigier, P., et al. (2002). Energy balance closure at FLUXNET sites. *Agricultural and Forest Meteorology*, 113(1–4), 223–243. [https://doi.org/10.1016/S0168-1923\(02\)00109-0](https://doi.org/10.1016/S0168-1923(02)00109-0)
- Woodside, W. (1958). Probe for thermal conductivity measurement of dry and moist materials. *Heating-Piping-Air Conditioning*, 30, 1–10.
- Woodside, W., & Messmer, J. H. (1961a). Thermal conductivity of porous media. I. Unconsolidated sands. *Journal of Applied Physics*, 32(9), 1688–1699. <https://doi.org/10.1063/1.1728419>
- Woodside, W., & Messmer, J. H. (1961b). Thermal conductivity of porous media. II. Consolidated rocks. *Journal of Applied Physics*, 32(9), 1699–1706. <https://doi.org/10.1063/1.1728420>
- Xiao, X., Horton, R., Sauer, T. J., Heitman, J. L., & Ren, T. (2011). Cumulative soil water evaporation as a function of depth and time. *Vadose Zone Journal*, 10(3), 1016–1022. <https://doi.org/10.2136/vzj2010.0070>
- Xiao, X., Horton, R., Sauer, T. J., Heitman, J. L., & Ren, T. (2014). Sensible heat balance measurements of soil water evaporation beneath a maize canopy. *Soil Science Society of America Journal*, 78(2), 361–368. <https://doi.org/10.2136/sssaj2013.08.0371>
- Xiao, X., Zhang, X., Ren, T., Horton, R., & Heitman, J. L. (2015). Thermal property measurement errors with heat-pulse sensors positioned near a soil-air interface. *Soil Science Society of America Journal*, 79(3), 766–771. <https://doi.org/10.2136/sssaj2014.12.0493n>
- Xie, H., & Cheng, S. (2001). A fine needle probe for determining the thermal conductivity of penetrable materials. *Measurement Science and Technology*, 12(1), 58–62. <https://doi.org/10.1088/0957-0233/12/1/307>
- Xu, J., Ma, X., Logsdon, S. D., & Horton, R. (2012). Short, multi-needle frequency domain reflectometry sensor suitable for measuring soil water content. *Soil Science Society of America Journal*, 76(6), 1929–1937. <https://doi.org/10.2136/sssaj2011.0361>
- Yang, C., & Jones, S. B. (2009). INV-WATFLX, a code for simultaneous estimation of soil properties and planar vector water flux from fully or partly functioning needles of a penta-needle heat-pulse probe. *Computational Geosciences*, 35(11), 2250–2258. <https://doi.org/10.1016/j.cageo.2009.04.005>
- Yang, C., Sakai, M., & Jones, S. B. (2013). Inverse method for simultaneous determination of soil water flux density and thermal properties with a penta-needle heat pulse probe. *Water Resources Research*, 49, 5851–5864. <https://doi.org/10.1002/wrcr.20459>
- Yoon, S., Lee, S. R., & Go, G. H. (2014). A numerical and experimental approach to the estimation of borehole thermal resistance in ground heat exchangers. *Energy*, 71, 547–555. <https://doi.org/10.1016/j.energy.2014.04.104>
- Young, M. H., Campbell, G. S., & Yin, J. (2008). Correcting dual-probe heat-pulse readings for changes in ambient temperature. *Vadose Zone Journal*, 7(1), 22–30. <https://doi.org/10.2136/vzj2007.0015>
- Zegelin, S. J., White, I., & Russell, G. F. (1992). A critique of the time domain reflectometry technique for determining field soil-water content. In G. C. Topp, et al. (Eds.), *Advances in measurement of soil physical properties: Bringing theory into practice*, SSSA Spec. Publ., (Vol. 30, pp. 187–208). Madison, WI: SSSA.
- Zent, A. P., Hecht, M. H., Cobos, D. R., Campbell, G. S., Campbell, C. S., Cardell, G., et al. (2009). Thermal and electrical conductivity probe (TECP) for Phoenix. *Journal of Geophysical Research*, 114(E3), E00A27. <https://doi.org/10.1029/2007JE003052>
- Zent, A. P., Hecht, M. H., Cobos, D. R., Wood, S. E., Hudson, T. L., Milkovich, S. M., et al. (2010). Initial results from the thermal and electrical conductivity probe (TECP) on Phoenix. *Journal of Geophysical Research*, 115, E00E14. <https://doi.org/10.1029/2009JE003420>
- Zhang, B., Han, C., & Yu, X. (2015). A non-destructive method to measure the thermal properties of frozen soils during phase transition. *Journal of Rock Mechanics and Geotechnical Engineering*, 7(2), 155–162. <https://doi.org/10.1016/j.jrmge.2015.03.005>
- Zhang, X., Heitman, J., Horton, R., & Ren, T. (2014). Measuring near-surface soil thermal properties with the heat-pulse method: Correction of ambient temperature and soil-air interface effects. *Soil Science Society of America Journal*, 76(3), 1575–1583. <https://doi.org/10.2136/sssaj2011.0052n>
- Zhang, X., Lu, S., Heitman, J., Horton, R., & Ren, T. (2012). Measuring subsurface soil-water evaporation with an improved heat-pulse probe. *Soil Science Society of America Journal*, 78(5), 876–879. <https://doi.org/10.2136/sssaj2014.01.0014>
- Zhang, X., Ren, T., Heitman, J., & Horton, R. (2017). Advances in heat-pulse methods: Measuring near-surface soil water content. *Methods of Soil Analysis*, 2(1). <https://doi.org/10.2136/msa2015.0032>
- Zhang, Y., Treberg, M., & Carey, S. K. (2011). Evaluation of the heat pulse probe method for determining frozen soil moisture content. *Water Resources Research*, 47, W05544. <https://doi.org/10.1029/2010WR010085>
- Zhang, H., Zhao, G., Ye, H., Ge, X., & Cheng, S. (2005). An improved hot probe for measuring thermal conductivity of liquids. *Measurement Science and Technology*, 16(7), 1430–1435. <https://doi.org/10.1088/0957-0233/16/7/004>
- Zheng, D., van der Velde, R., Su, Z., Wang, X., Wen, J., Booij, M. J., & Chen, Y. (2015). Augmentations to the Noah model physics for application to the yellow river source area. Part II: Turbulent heat fluxes and soil heat transport. *Journal of Hydrometeorology*, 16(6), 2677–2694. <https://doi.org/10.1175/JHM-D-14-0199.1>